Modeling the effects of potential management regimes on carbon sequestration in the Tongass National Forest, USA, using spatial analysis

Wayne Waterman Leighty
11 May, 2001

Abstract

Resolution of policy discussions about greenhouse gas emissions trading and allocation of Certified Emissions Reduction credits for land use change require complete understanding of national carbon budgets. Some carbon stock estimates for the United States include Alaska but no estimates of stock changes have been made despite active management of vast areas of productive forests, including the Tongass National Forest in Southeast Alaska. The research presented here was designed to estimate the carbon stock in the Tongass, project carbon flux with different management regimes, and convert flux estimates to monetary units to facilitate comparison of the relative value of forest management for carbon sequestration with other competing forest uses. Spatial Geographic Information System (GIS) data was used to stratify (map) the Tongass according to carbon density. Forest inventory data was used to quantify this stratification, which was then used to estimate carbon stock and fluxes. Carbon flux was estimated with six potential management regimes and converted to monetary units using a value of $20 per metric ton of carbon. The total carbon stock in the Tongass National Forest was estimated to be 2.8 $\pm$ 0.5 Pg, which is 7.7% of the total carbon in forests in the conterminous USA and 0.25% of the total carbon in global forest vegetation and soils. Carbon fluxes ranged from 0.40 Tg annual sequestration to 2.61 Tg annual emission for the period 1995-2095, depending on forest management. For the period 1995-2195, flux estimates ranges from 0.23 Tg annual sequestration to 1.73 Tg annual emission, depending on forest management. Omission of the Tongass National Forest may result in significant inaccuracy in some national carbon budgets for the USA, depending on management of this forest. The net annual value of carbon sequestration during the period 1995-2095 as a result of ceasing all harvest in the Tongass National Forest was estimated to be -$0.7 to $40.6 million dollars, assuming carbon valued at $20/ metric ton. This range results from aggregation of uncertainty; the best estimate of the net annual value of carbon sequestration during the period 1995-2095 as a result of ceasing all harvest in the Tongass is $2.4 to $4.5 million dollars. The net annual value of carbon sequestration during the period 1995-2195 as a result of ceasing all harvest in the Tongass National Forest was estimated to be $0.7 to $33.6 million dollars, assuming

carbon valued at $20/ metric ton. This range results from aggregation of uncertainty; the best estimate of the net annual value of carbon sequestration during the period 1995-2195 as a result of ceasing all harvest in the Tongass is $2.3 to $4.9 million dollars. Estimates of carbon flux were sensitive to projections of the rate of carbon accumulation in secondary growth and to the carbon density left in standing biomass after harvest. The annual value of Tongass management for carbon sequestration is of similar magnitude to the $6.5 million in annual timber sales authorized by the USDA Forest Service timber program.

Introduction

The movement of carbon into and out of the atmosphere in the global carbon cycle is of interest because carbon dioxide is one of the primary heat-trapping gases causing the greenhouse effect and global climate change. Scientific consensus holds that, "The balance of the evidence…suggests a discernible human influence on global climate" as a result of anthropogenic Greenhouse Gas (GHG) emissions (IPCC, 1995). Current global climate models project an increase in global mean surface temperature relative to 1990 of 1 to 3.5 degrees Celsius by 2100, depending on projected GHG emissions and the climate sensitivity to these emissions (ibid.). This projected situation will require expensive action, whether we choose to adapt to climate change or to mitigate the change through reduction of anthropogenic GHG emissions (IPCC, 2001).

Concern over the implications of a changing climate has led to construction of carbon budgets for the forests of the world. The Kyoto Protocol of the UN Framework Convention on Climate Change, signed by 84 countries and ratified by 22 (as of February 2000), represents strong resolve for mitigating global climate change through reduction of GHG emissions (Fletcher, 2000). Furthermore, the Kyoto Protocol provides flexibility mechanisms for meeting GHG emission reduction targets, including a carbon emission trading system. However, the establishment of an active and regulated market has been plagued with controversy over the details of emission reduction crediting and compliance with the Kyoto Protocol. Disagreement about allocation of Certified Emission Reduction Credits (CER) for land-use change persisted at the Conference of the Parties 6 in The Hague, Netherlands in November 2000. Quantifying sources and sinks of carbon and flux resulting from land-use change is essential for accurate and honest functioning of a GHG market that actually achieves GHG emission reduction targets. Although a trading system is not yet in place, carbon may soon become a traded commodity with economic value (some entities have begun speculative carbon trading and hedging activities).

Terrestrial vegetation and soil represent large pools of carbon (IPCC, 2000). Furthermore, carbon flux from these pools to the atmosphere from land-use change accounts for a significant portion of the annual CO_2 budget (ibid). Consequently, the Kyoto Protocol allows for Annex I parties to account for land use, land-use change, and

forestry (LULUCF), including afforestation, reforestation, and deforestation, in meeting their Article 3 GHG reduction targets.

Estimation of the total amount of carbon held in forest ecosystems and how it could change with differing management regimes is central to informing U.S. climate change policy. Furthermore the potential economic value of the carbon currently held in forests may represent an important consideration in developing forest management policies. The Tongass National Forest in Southeast Alaska is the United States' largest national forest and contains the largest intact old-growth temperate rainforest in the world (30% of the unharvested temperate rainforest remaining on the planet) (SEACC, 1999). The management alternatives available for this forest will greatly influence future carbon stocks of this forest. However, few current estimates of carbon pools include Alaska and no estimates of carbon flux include the Tongass National Forest (Turner et al, 1995, Birdsey, 2001). Studies in similar ecosystems in Washington and Oregon confirm the potential for significant carbon flux due to management policy (Harmon et al, 1990), suggesting that the carbon stock in the Tongass may represent a significant economic value (in a carbon emissions and sequestration trading market) that should be considered in developing forest management policies. Conflicts among competing uses of the Tongass, including high quality timber, tourism, and commercial and recreational fisheries (80% of fish caught in SE Alaska were spawned in streams in the Tongass) have increased over the last 30 years. To optimally manage disputes over multiple uses, common metrics of value for each use are needed to facilitate comparison across uses. Registration of the current carbon inventory and management practices in the Tongass will help ensure proper creditation for immediate action to sequester carbon, allowing management to seize a financial opportunity and ease the transition into national compliance with international agreements on GHG emissions (fig. 1).

Commercial timber harvest began in the Tongass in the early 20th century and harvest intensity increased after the granting of 50-year timber contracts to two large pulp mills (Ketchikan Pulp Corporation, KPC and the Alaska Pulp Corporation, APC) in 1954 (fig. 2). Recently, the timber volume harvested from the Tongass has declined with the closure of the APC in 1993 and KPC mill in 1997. The Tongass Timber Reform Act, passed in 1990, supports a shift to Tongass management for multiple uses. It cost the

USDA Forest Service $35.6 million to run the timber program in the Tongass in 1998, with returns of $6.5 million in timber sales (USDA Forest Service, 2001). Management policy for the Tongass is at a crossroads and the value of carbon has not been considered in debates over future forest management.

Understanding carbon in the Tongass National Forest is important on several scales. Global concern about climate change requires complete information on global and national carbon budgets to inform policy debates over mitigation and adaptation action. Regional decisions about the most appropriate combination of multiple-uses of the Tongass National Forest require complete information about all potential uses. With a potentially large pool of carbon available for modification, management policy in the Tongass may affect significant carbon flux. With emerging markets for carbon trading, this flux may be of significant economic value relative to competing uses of the forest. Consequently, this research was designed to assess the magnitude of the carbon stock and potential carbon fluxes from the Tongass relative to national and global carbon budgets and to evaluate the value of forest management for carbon sequestration relative to the value of timber harvest, the primary competing use. Three phases of research were required. The existing carbon stock held in the Tongass National Forest was estimated in the first phase by synthesizing Geographic Information System (GIS) data and forest inventory data. Carbon fluxes over 200 years associated with 6 potential management scenarios were modeled in the second phase, using the model developed in the first phase of research. Finally, the carbon flux associated with each management scenario modeled was converted to monetary units in the third phase, allowing evaluation of whether carbon sequestration could be of significant value relative to competing uses.

Methods

The 17-million-acre Tongass National Forest lies within the Pacific Northwest coastal temperate rainforest biome, with average annual rainfall between 152 and 559 cm, average winter temperature between –1 and 10 degrees C, and average summer temperature between 10 and 21 degrees C. (fig. 3). Stretching 500 miles along the southeast coast of Alaska, it includes 22,000 islands and is a quilt of forested land, muskeg, alpine meadow, rock, water, and ice. Glaciers that covered most of this area only 10,000 years ago during the Little Ice Age have receded but still linger in some mountain valleys (app. C). The temperate rainforest ecosystem in the Tongass is very productive. Lush growth and slow decomposition lead to accumulation of biomass in the forests, soils, and muskegs of Southeast Alaska, suggesting a potentially large carbon stock. Twenty percent of the area of the Tongass is rock and ice, 12% is densely vegetated forestlands, 43% is moderately vegetated forestlands, and 25% is wetlands.

Large tracts of land within the Tongass were returned to Alaska Natives in the form of corporate ownership by the Alaska Native Lands Claim Settlement Act in the 1970's. Many of these areas have been clear-cut. These areas are excluded from this study, which considers only national forest lands within the Tongass National Forest.

Phase one: estimation of existing carbon stock

Step 1: calculation of carbon density at sample locations across the Tongass

Data from the USDA Forest Service 1995 Forest Inventory Assessment (FIA) Southeast Alaska (SEAK) Grid Inventory was used to calculate carbon density at each sample location (app. D). The FIA Grid Inventory utilized a regular grid of more than 2000 sample locations across the Tongass (USDA Forest Service, 1995). Each sampling location was established using a hand-held Global Positioning System (GPS) unit when possible and by navigating from a reference point established with GPS when dense forest cover prevented GPS use at the sampling location (app. E). Four sample points were established at each sample location, including one central point and three other points, each 36.6 meters from the central point, at azimuths of 360^0, 120^0, and 240^0. Data on live and dead vegetation, downed woody debris, and soil data were collected at these

four points using the following sampling scheme. Plots measuring 7.3m in radius for measuring all trees $\geq$ 12.5 cm dbh and 2m radius subplots for measuring all seedling/ saplings were completed at each sample point. Major Vegetation Types (MVT) were defined at each sample location and 5.64m radius horizontal/ vertical (HV) profile plots were measured at two sample points within each MVT identified at the sampling location. Three 11.28m downed-wood transects at each HV plot were arranged to intersect at the center with azimuths of 360^0, 120^0, and 240^0. One soil pit ≤ 50 cm deep was dug at each of the four sample points.

Carbon was divided into 7 pools for carbon inventory: trees, seedlings, standing dead wood, large downed woody debris (average diameter > 7.62 cm), small downed woody debris (average diameter < 7.62 cm), understory vegetation, and soils. Allometric biomass equations (table 1, app. G) were used to convert tree diameter and height data collected in each of the inventory plots at all FIA sample locations into biomass (kg/ ha). Carbon was assumed to account for 50% of total oven-dry tree biomass (Hamburg et al 1997). Root-to-shoot ratios for coniferous forests (with the exception of *Pinus sylvestris*, a European species) range from 15 to 26%, so belowground biomass was conservatively assumed to be 20% of aboveground biomass (Santantonio 1977, Hamburg et al 1997).

To calculate the amount of carbon in standing dead biomass, the biomass estimated using the equations employed to calculate standing live biomass was reduced by a factor to account for the degree of decay (table 3). The same allometric equations were also used for calculating the amount of carbon in seedlings and saplings. See the section on sensitivity analysis for discussion of the implications of biomass equation selection.

The amount of carbon in coarse woody debris (CWD), defined as any dead boles, portions of boles, or primary branches severed from their bases and laying on or above the ground with average diameter greater than 7.62 centimeters, was calculated using the methods described by Waddell (2001). These methods were developed specifically for use with the methods used in the FIA data collection. The cubic volume of each piece of woody debris was calculated as

$$V = [(\pi / 8) \times (D^2{}_S + D^2{}_L) \times l] / 10{,}000$$

where V is the volume in cubic meters; D_S is the small-end diameter in centimeters; D_L is the large-end diameter in centimeters; and l is the debris piece length in meters. The volume (m^3) for each piece of CWD was then converted to a per-hectare value with the equation

$$m^3/ha = (\pi/(2 \times L)) \times (V_m / l) \times 10{,}000 m^2 / ha$$

where L is the total length of the transect line on the plot in meters; V_m is the volume of the individual debris piece in cubic meters; and l is the length of the individual debris piece. Finally, the oven-dry biomass in kilograms per hectare for each piece of CWD was calculated as

$$(\text{cubic meters/ hectare}) \times 1{,}000 \text{ kg/m}^3 \times \text{SpG} \times \text{DCR}$$

where SpG is the specific gravity of the debris piece (which varies by species); DCR is the decay class reduction factor, calculated as 1 – percent decay (recorded to the nearest 5% in FIA data). This result was summed for all pieces of CWD recorded in the FIA data and multiplied by 0.5 to calculate the total carbon density in coarse downed woody debris at each sample point in kilograms per hectare.

The amount of carbon in small woody debris (SWD), defined as for CWD but with average diameter less than 7.62 cm and large-end diameter greater than 2.5 cm, was calculated with the methods described by Brown (1974). For example, total carbon density (kg/ ha) in small woody debris identified as Pacific silver fir was calculated as

$$\{[398.3 \times 11.64 \times \text{freq} \times 2.76 \times 0.4 \times 1.13 \times \sqrt{\ } (1+((\frac{slp}{freq})/100)^2)]/37\} \times 0.5 \times (1-0.008 \times \frac{decay}{freq})$$

where freq is the total number of intersections with Pacific silver fir SWD recorded in the FIA data; slp is the sum of slope estimates for all the records of Pacific silver fir small woody debris in the FIA data; and decay is the sum of decay estimates for all records of Pacific silver fir small woody debris in the FIA data. The quantity (slp/freq) is an estimate of the average slope at the FIA sample point and the quantity (decay/freq) is an estimate of the average amount of decay in Pacific silver fir small woody debris at the FIA sample point. The non-slash, non-horizontal correction factor and "composite" species composition factors described by Brown were used in developing this equation and equations for other species. The specific gravity of hardwood SWD lacking species identification was assumed to be 0.363, the average of all hardwood species found in Southeast Alaska (U.S. Forest Products Laboratory, 1974). Estimates of carbon density in small woody debris calculated with species-specific equations like the one described above were summed across all species to estimate total carbon density (kg/ ha) in small woody debris at each FIA sample point.

Coefficients for calculation of biomass from estimates of percentage foliar cover were developed for many understory species found in Alaska by Yarie and Mead (1988). The understory species described by Yarie and Mead were aggregated into the general taxonomic categories described in the FIA sampling methods. Biomass in understory vegetation for each category was then calculated as a constant (calculated by averaging the constants of all species given by Yarie and Mead in this category) multiplied by the estimated percentage foliar cover in FIA data. Percentage of foliar cover (estimated to the nearest percent) in FIA horizontal-vertical (HV) plot data was estimated for layers recorded to the nearest decimeter. Biomass for each species was scaled by its percent composition in each layer and total biomass estimates for each layer were summed to calculate total understory carbon density (kg/ ha) at the FIA sample point.

Data in the FIA Grid Inventory from soil pits was inadequate for estimation of soil carbon for two reasons. Soil depth in Southeast Alaska ranges from several centimeters to several meters. Limitation of pit depth to a maximum of 50 centimeters left no means for estimating how much carbon was held in soils beneath this limit. Furthermore, location of soil pits in a spatially diverse landscape by ground crews not trained in soil science suggests the potential for failure of the soil pit to accurately

characterize the general soil structure of the sample location area. Consequently, total soil carbon was calculated independently of FIA data using the ten general soil categories developed by Alexander et al based on carbon density. More than 800 USDA Forest Service Soil Management Unit (SMU) codes (USDA 1994, 1992a, b) were classified into these ten categories (app. K, L) (D'Amore, 2001). Some SMU codes fell between two of Alexander et al's categories. When in doubt, judgments were made on the conservative side by categorizing the SMU code in the category with lower carbon density, ensuring that the estimate of total soil carbon is conservative (app. J). Furthermore, soils described as "moderately deep" were generally categorized into the appropriate "shallow" category rather than "deep" category (no "moderately deep" categories were described by Alexander et al but many SMU codes describe moderately deep soil complexes). SMU codes define "shallow" as less than 50cm, "deep" as more than 100 cm, and "moderately deep" as the middle ground (50-100 cm) (U.S. Department of Agriculture, Soil Survey Division Staff, 1993). Sample locations were identified according to these ten soil categories and data on soil carbon density from the literature (Alexander et al, 1990) was used to calculate the total soil carbon in each category. Forest floor litter and humus was included in soil carbon, small and coarse woody debris in was included in the woody debris carbon pool, and living ground-level vegetation was included in understory carbon. Soil type has not been mapped in some areas of the Tongass, mostly wilderness areas. Soil carbon density for these areas was assumed to be a weighted average of all known soil types. See the section on sensitivity analysis for discussion of the implications of these methods.

Estimates of carbon density (kg/ ha) in each of the seven carbon pools at each of the sample points at an FIA Grid Inventory sample location were aggregated by sample location.

Step 2: creation of spatial projections of carbon density

A Geographic Information System (GIS) polygon coverage for carbon density was created using existing USDA Forest Service GIS coverages (spatial data), as an extension of the work by Caouette et al (2000) (figs. 4, 5, app. F, N). GIS coverages specified in figure 4 were "unioned" using ArcInfo to create a complete coverage of the

Tongass with polygons containing the data from all unioned coverages. The union process in Arc overlays GIS coverages to create new polygons containing all the data of both original coverages. This coverage, called "timclapu" contained all the attributes used for creation of the carbon density coverage (fig. 4b, app O). A SAS program was used to create an attribute for carbon-density polygon identification (called "fingroup") from the coverage timclapu based on the flow chart shown in figure 4. This attribute was joined with the original data table for the coverage timclapu, which was then "dissolved" based on the attribute fingroup to create the coverage of carbon density for the Tongass. The dissolve process in Arc removes boundaries between polygons with the same value of the specified attribute, fingroup in this case. The independence of the soil carbon calculation from FIA Grid Inventory data allowed condensing of the 373 polygon types established by the logic in figure 4 to just 43 "aboveground" polygon types. Polygon slivers, defined as polygons with area < 1 acre and $\frac{perimeter}{area}$ ratio > 1, created through the iterative "union" process were merged with neighboring polygons with the largest area with the "eliminate" command in ArcInfo (app. P).

Step 3: combination of spatial data with carbon density estimates

Each FIA Grid Inventory sample location was assigned to one of the 43 "aboveground" polygon types in the carbon density map by running an Arc Macro Language (AML) program to determine the polygon type within which each FIA sample location was positioned (app. Q). Distinction of soil type was dropped from polygon type delineation in "aboveground" polygon types for calculation of carbon density from FIA data to reduce the number of polygon types, thereby increasing the number of sample locations representing each polygon type. The independence of soil carbon (calculated with figures from Alexander et al) and aboveground carbon (calculated with FIA data) allowed this simplification. All of the carbon density (kg/ ha) data from the FIA Grid Inventory sample locations in each polygon type was averaged to provide a representative carbon density for each polygon type (app. R_1). The total carbon stock in the Tongass was calculated by multiplying the average carbon density for each polygon type times the land area occupied by each polygon type and summing all polygon types.

Phase 2: Projection of Carbon Flux

The chronosequence data from permanent plots located throughout the Tongass that have been measured with FIA data collection methods repeatedly over varying time periods (DeMars, 2000) was used in conjunction with the SAS programs used in phase 1 to calculate biomass accretion in standing aboveground vegetation over the first 100 years after harvest (app. S). Carbon accretion curves were established by combining these curves with estimates of carbon density in standing aboveground vegetation in virgin forest from FIA inventory data (fig. 6). The value of carbon density for old-growth forests used in creation of the carbon accretion models was calculated as a weighted average of old-growth commercial forest polygon types from the carbon map and it was assumed that secondary growth reached old-growth status in 350 years. See the section on sensitivity analyses for methods used to evaluate the implications of the carbon accretion curves used.

Carbon flux was modeled for six management scenarios (app. R_3). The scenario modeling cessation of all timber harvest assumed re-growth of secondary forest and equilibrium in unharvested areas. Carbon flux since 1900 was estimated based on historical harvest volumes (fig 2). Carbon flux was also modeled for management of all forested lands on 100- and 200-year rotations and for management of all lands currently available for harvest on 100- and 200-year rotations. Lands currently available for harvest were mapped using the GIS coverage LUD99 (app. T) and the 1997 Tongass National Forest Land and Resource Management Plan (CD 6).

In the scenarios modeling cessation of harvest, re-growth on harvested polygon lands was assumed to follow the carbon accretion curve relative to the precut carbon density. For modeling past carbon flux, the total carbon stock in 1900 was calculated by assuming a carbon density for all harvested polygon types equal to equivalent unharvested polygon types. The difference between the carbon stock in 1900 and 1995 represents carbon flux from the Tongass over the 95 years. The total flux was proportioned between the early 1900's, when there was relatively little cutting, and the later half of the century when cutting was significantly higher based on percent of the total harvest (1900-1995) in each period and then annualized (fig. 2). Finally, this

estimate of carbon flux from the forest was modified to reflect storage of carbon in the products flowing from the Southeast Alaska timber industry to estimate carbon flux from the Tongass to the atmosphere (fig. 7). Starting with 100 arbitrary units of carbon harvested, 60% becomes merchantable volume while the remaining 40% is left on site as slash and stumps (Sampson & Hair, 1996). Roughly half of the merchantable volume enters the sawtimber production process and the other half enters the pulpwood production process (Warren, 1999). Once in the sawtimber production process, 43.5% of the carbon becomes product (long term storage), 13% is lost to the atmosphere, and 43.5% enters the pulpwood production process (Sampson & Hair, 1996). In the pulpwood production process, 62% of the carbon becomes product (short-term storage) and 38% is lost to the atmosphere. See the section on sensitivity analyses for further elaboration of the methods used to decompose various carbon pools in calculation of carbon flux between the Tongass and the atmosphere (app I).

The same model of forest carbon was used for all scenarios involving harvest rotations (fig. 8). Three equations approximating annual carbon flux were applied to all forested areas of the Tongass in the scenarios modeling harvest of all forested lands, with r equal to 100 yr. and 200 yr. respectively.

Annual carbon flux into the forest product production process (FP) = $0.6 \times (B - C) \times \frac{A}{r}$

Annual carbon flux into slash and stumps left on site (S) = $0.4 \times (B - C) \times \frac{A}{r}$

Annual carbon sequestration in secondary growth (SG) = $((\frac{C + F}{2}) - C) \times \frac{A}{r}$

These equations use the total area of each polygon type (A), carbon density in 1995 (B), carbon density after harvest (C), carbon density after r years of regrowth (F) and the rotation length (r) as data inputs. See the section on sensitivity analyses for evaluation of the implications of the value of carbon density after harvest (C).

Most of the carbon entering the forest product production process is quickly emitted to the atmosphere, but 21.7% becomes long-term product, which was decomposed linearly starting at 100 years and extending 50 years, resulting in an average

lifespan of 125 years (fig 8). Carbon in slash and stumps left on site after harvest was decomposed linearly over 50 years. The downed woody debris carbon pool existing prior to harvest was decomposed after harvest linearly for the first 50 years to a density equal to 0.5 of the original density to account for decreased input to this pool in the early stages of secondary growth. This carbon pool was then increased back to the original density over the next 200 years.

The net annual carbon flux from the Tongass was calculated by synthesizing these fluxes:

Net annual carbon flux from the Tongass = FP + (b × S) + (c × DWD) +(d × PS)– SG

where FP is the annual carbon flux into the forest product production process, b is a variable coefficient determined by the state of decomposition in slash and stumps left after harvest, S is the annual carbon flux into slash and stumps left on site after harvest, c is a variable coefficient determined by the state of decomposition or re-accumulation in the downed woody debris pool existing before harvest, DWD is the downed woody debris pool existing before harvest in the area harvested each year, d is a variable coefficient determined by the state of decomposition slash and stumps left after harvest prior to 1995, PS is the annual carbon flux into slash and stumps left after harvest prior to 1995, and SG is the annual carbon sequestration in secondary growth.

Similarly, the net annual carbon flux to the atmosphere was calculated as:

Net annual carbon flux = (0.783 × FP) + (a × 0.217 × FP) + (b × S) + (c × DWD) + (d × PS) – SG

where FP is the annual carbon flux into the forest product production process, a is a variable coefficient determined by the state of decomposition in long-term forest products, b is a variable coefficient determined by the state of decomposition in slash and stumps left after harvest, S is the annual carbon flux into slash and stumps left on site after harvest, c is a variable coefficient determined by the state of decomposition or re-accumulation in the downed woody debris pool existing before harvest, DWD is the

downed woody debris pool existing before harvest in the area harvested each year, d is a variable coefficient determined by the state of decomposition slash and stumps left after harvest prior to 1995, PS is the annual carbon flux into slash and stumps left after harvest prior to 1995, and SG is the annual carbon sequestration in secondary growth.

The area of forested polygons to which these equations were applied in scenarios modeling harvest of forested lands available for harvest was found by overlaying a map of land use designations on the carbon map. This allowed identification of the areas available for harvest and those areas off-limits due to land use designation as defined in the 1997 Tongass National Forest Land and Resource Management Plan (e.g. roadless areas, national monument) (app. T) (USDA Forest Service, 1997). Areas available for harvest were treated as in the scenarios modeling rotational harvest of all forested lands and areas not available for harvest were treated as in the scenario modeling cessation of all harvest, with harvested areas re-growing according to either the polynomial or asymptotic accretion curve.

The variable B is the initial carbon density of each polygon type. All scenarios use 1995 as the base year because FIA data collection began in 1995 and because spatial data in the GIS coverages used to create the carbon map were created using data that predates this inventory. Therefor, the assumption was made that estimates of the existing carbon stock most closely represents that present in 1995. The carbon density after r years of re-growth (F) was estimated by using carbon accretion curves to predict the percent of original carbon density that would be present after r years. The flux projections were completed using both polynomial and asymptotic accretion curves for calculation of the carbon density after r years of re-growth (F). See the section on sensitivity analyses for evaluation of the implications of the value used for carbon density after harvest (C).

Phase 3: conversion of carbon flux to monetary units

Estimates of the value of carbon in potential emissions trading markets vary widely, from $5 per metric ton to $125 (Weyant, 2000). Estimates of carbon flux to the atmosphere from the Tongass were multiplied by $20 per metric ton to estimate the economic value of Certified Emissions Reduction credits (CERs) associated with these

fluxes. The value in the speculative markets of today is less; the value in a regulated emissions trading markets may be significantly more. Consideration of leakage should be included in estimates of the number of CERs associated with projected carbon fluxes although this is necessarily speculative because it depends on international agreements yet to be framed.

Statistics

All manipulation of FIA Grid Inventory data described was done with the SAS system, version 6.12 (app. F). All flux calculations were done with the Microsoft Excel files indexed in appendix N, and plotted with the files indexed in appendix S. The forest structure models (GIS coverages) were created and manipulated with the GIS programs Arc and ArcInfo. Both Microsoft Excel and SAS were used to calculate mean, standard error, and confidence interval statistics.

Sensitivity analyses

Two estimations of total carbon were made in order to account for the uncertainty introduced by selection of biomass equations (table 2). One estimate was made using equations resulting in the lowest biomass estimates for all species with more than one equation available and a second estimate was made using equations for these species that resulted in the highest biomass (table 1, app. H). Equations for paper birch and willow were unavailable so one estimate was made omitting these species and one was made using the equation for black cottonwood for Paper Birch and the equation for quaking aspen for willow (table 1). The FIA data included very few of either species.

The total amount of carbon accounted for in trees outside the diameter-at-breast-height (dbh) range for which each allometric equation used had been verified was determined in order to estimate the potential uncertainty associated with the use of these equations for large trees and small seedlings (table 2). Three-dimensional surface plots were created to examine the behavior of all allometric equations over the whole range of dbh and height to which they were applied (app. H). The equations were used as a

reasonable estimate of tree biomass outside the dbh range for which they have been verified because the surface plots all maintained their general shape beyond these limits.

Total soil carbon was calculated from FIA soil pit data as well as the methods described above using the work by Alexander et al. This was done using data on soil carbon density in each soil horizon from the literature (Alexander et al, 1990) and confirmed the inadequacy of the FIA soil pit data. Consequently, the approach to soil carbon estimation based on the categories described by Alexander et al was used for all total carbon stock estimation and flux projections. The total amount of carbon accounted for in soils subject to methodological assumptions was calculated for an indication of the potential influence of these assumptions on estimates of the total carbon stock in the Tongass.

It was not possible to resolve from the available data whether asymptotic or polynomial curves best describe the pattern of carbon accretion following harvest. Therefor, carbon flux scenarios were modeled using both asymptotic and polynomial accretion curves to test the sensitivity of the results to this uncertainty. Flux scenarios were also calculated using the mean carbon density for each polygon type as well as with the upper and lower 95% confidence interval.

For modeling carbon flux with cessation of harvest, the equivalent unharvested polygon type most appropriate for indication of the carbon density expected in currently cut-over lands once at old-growth status was not clear in some cases. For example, the question of whether polygon type **7 will eventually reach the carbon density of polygon type **8 or **10 was unresolvable (fig. 4). For such lands, the sensitivity of flux projections to the assumed pre-cut carbon density was tested by running the model once with the assumption of re-growth in each polygon type to a carbon density of the most similar polygon type and running the model once with the assumption of re-growth in each polygon type to a carbon density of a similar polygon type with highest timber volume. For modeling past carbon flux, sensitivity analysis of the choice of equivalent unharvested polygon types, similar to that completed for the scenario modeling cessation of harvest, was performed.

The carbon accretion curves used for flux modeling are based on standing aboveground biomass (aboveground biomass excluding downed woody debris) and all

flux calculations are based on this pool, with changes in belowground biomass calculated as 20% of the change in aboveground standing biomass and changes in downed woody debris calculated as 40% of the aboveground standing biomass harvested (left on site as slash and stumps after harvest). The carbon density in aboveground standing biomass of polygon type **23 was used as an estimate of the amount of carbon present immediately after harvest (C) for all polygon types in one model run because it is the polygon type that most closely approximates this value. However, this polygon type is defined as containing forest composed of seedlings and saplings, which identifies it as areas in which somewhere between 5 and 15 years have elapsed since harvest. Although the closest approximation available in the polygon types quantified with FIA data, the carbon density in this polygon type is not an accurate estimate of the carbon density immediately following harvest. The density of carbon in standing aboveground biomass following clear-cutting should be closer to zero than the density found in polygon type **23 (86 Mg/ ha). Consequently, flux projections were performed a second time using zero as the value for carbon density in aboveground standing biomass (C).

Two models were created to test the sensitivity of flux projections to assumptions about the release of carbon to the atmosphere from decomposition. The results of these models are presented in the sections "Flux Model One" and "Flux Model Two." In Flux Model One, carbon in long-term storage in sawtimber products was decomposed linearly over 50 years starting 100 years after harvest, resulting in an average product lifespan of 125 years. Material left on site (slash and stumps) was decomposed linearly over 50 years. Carbon in pulpwood products was assumed to be released to the atmosphere quickly enough that no decomposition factor was needed. The net result of these assumptions is that 47% of carbon impacted by harvest leaves the Tongass and enters the atmosphere as CO_2 within a short time after harvest. Forty percent of the carbon impacted by harvest is left on site and moves from the forest to the atmosphere over the 50 years after harvest. The remaining 13% of carbon impacted by harvest leaves the Tongass immediately after harvest as sawtimber products, begins moving to the atmosphere 100 years after harvest, and continues to do so for 50 years. The carbon in downed woody debris on the site prior to harvest was decomposed linearly over 50 years to ½ the original amount to account for reduced input of material to this carbon pool

following harvest. This carbon pool was increased back to the original pre-harvest amount linearly over 200 years starting 50 years after harvest.

Calculations in Flux Model Two assume linear decomposition of carbon in long-term storage in sawtimber products over 50 years starting 50 years after harvest, resulting in an average product lifespan of 75 years. Material left on site (slash and stumps) was decomposed linearly over 100 years. Carbon in pulpwood products was decomposed linearly over 50 years. The net result of these assumptions is that 20% of carbon impacted by harvest leaves the Tongass and enters the atmosphere as CO_2 within a short time after harvest. The carbon impacted by harvest and left on site as slash (40%) moves from the Tongass to the atmosphere over a span of 100 years after harvest. The carbon in pulpwood products (27%) moves to the atmosphere over a span of 50 years after harvest. The remaining 13% of carbon impacted by harvest leaves the Tongass immediately after harvest as sawtimber products, begins moving to the atmosphere 50 years after harvest, and continues to do so for 50 years. Carbon in downed woody debris on the site prior to harvest was decomposed and accreted as in Flux Model One.

Results

Evaluation of the carbon density GIS coverage on several levels indicates successful creation and accurate representation of forest structure. Arc reported no label errors, meaning all polygons retained their data through all the "union" and "dissolve" manipulations. Visual comparison with sample areas demonstrates correlation with observable transitions in forest structure. For example, the carbon density GIS coverage corresponds with visual borders in forest structure at John Caouette's study site in Crab Bay (fig. 9). The carbon densities of each polygon type in the GIS coverage, calculated from carbon density estimates for FIA sample locations identified as being representative of each polygon type, show quantitative differences in carbon density between polygon types (fig. 10a). Twelve polygon types account for over 90% of the area of the Tongass and ten of these account for 86% of the total carbon (tables 4, 5). Redrawing figure 10 with only these ten polygon types further demonstrates the quantitative success of spatial modeling of the carbon stock in the Tongass (fig. 10b). Polygon types with few FIA sample locations have consequently large uncertainty in carbon density estimates but also represent very small land areas and therefor contribute very little to the total carbon stock in the Tongass (fig. 11). Polygon types with fewer than 5 representative FIA sample locations (17 types) represent 2% of the total area of the Tongass and 1% of the total carbon.

Quantified aboveground carbon density in each polygon type in the GIS coverage corresponds with the qualitative descriptions dictated by the logic used in creation of the map (table 6). For example, polygon types with high volume forest are clustered near higher aboveground carbon density while non-forested polygon types are clustered near lower aboveground carbon density. The influence of soil carbon causes some deviation from this pattern in total carbon density because soils are not directly tied to the description of aboveground forest structure. However, a relationship between aboveground carbon density and soil carbon density was found despite the independence of soil carbon from the "aboveground" polygon types that reflect only aboveground forest structure. This finding demonstrates the connection between aboveground forest structure and soil type (fig. 12). Very high carbon density in muskeg and deep saprist soils correlates with the moderate aboveground carbon density associated with sparse

aboveground biomass in forested muskegs. As soil carbon density declines from the high concentrations found in muskeg areas, aboveground carbon density increases because soil moisture and acidity become less limiting. Soil carbon density stays relatively constant in the mineral soils of a variety of locations while aboveground carbon density covers a range due to the other factors included in the carbon mapping process (fig. 4). Finally, the extremely low density of soil carbon in rock and ice areas correlates with low aboveground carbon densities found in the sparse vegetation that can grow in these harsh conditions.

Total carbon in the Tongass (soil, aboveground biomass, and roots) was estimated to be 2.8 $\pm$ 0.5 Pg (table 3). Sixty-six percent of the total carbon is in the soils, 30% is in aboveground biomass (15.0% in live trees, 5.6% in seedlings and saplings, 3.0% in standing dead wood, 5.6% in CWD, 0.0% in SWD, and 0.7% in understory vegetation), and 4% is in roots. Less than 0.1% of the total carbon was influenced by assumptions about aboveground polygon types (app. J) and only 0.7% was found to be in understory vegetation, estimation of which was subject to several assumptions. However, 22% of the total carbon is in the soils of polygon types positioned in areas where soil types have not been mapped (mostly wilderness areas). The results from application of soil carbon density estimates from Alexander et al (total soil carbon = 1.86 Pg) were compared with total soil carbon given by calculations using FIA Grid Inventory soil pit data (total soil carbon = 0.49 Pg) to confirm the assumption that the later method would underestimate total soil carbon in the Tongass (app. M). The uncertainty in carbon density estimates used to calculate the total carbon stock (+- 0.5 Pg 95% confidence interval) is accounted for by: 42% from uncertainty in aboveground carbon density estimates from FIA sample location data; 6% from root carbon estimates; 52% from the confidence intervals for soil carbon estimates given by Alexander et al (1990).

Projections of carbon flux to or from the atmosphere over the next 200 years for the 6 management scenarios modeled differ from projections of flux to or from the forest because of the delayed release of carbon in slash, long-term forest products, and short-term forest products (fig. 13). The assumption of whether polynomial or asymptotic carbon accretion rates in secondary growth more accurately describe the Tongass alters the shape of flux projections (except estimation of historical flux) (fig. 13). Total carbon

in the Tongass increases to a lower maximum with cessation of all harvest under the assumption of asymptotic carbon accretion (2.85 Pg) as opposed to the assumption of polynomial carbon accretion (2.87 Pg). Furthermore, active carbon accretion continues for a much shorter period of time (55 yr.) under the assumption of asymptotic carbon accretion than under the assumption of polynomial carbon accretion (175 yr.). Projections of flux for management scenarios involving harvest on 200-year rotations are more profoundly altered by carbon accretion assumptions than projections of carbon flux involving 100-year harvest rotations because the 200-year rotations allow sufficient time for secondary growth to increase carbon density to the peak in the polynomial accretion curve. Annual rates of carbon flux vary for each permutation of the management scenarios modeled (tables 7, 8).

FIA data were used to calculate the confidence interval (95%) for estimates of carbon density in each polygon type in the carbon density GIS coverage. The estimated range in total carbon stock in the Tongass was calculated with this confidence interval. The ranges in projections of carbon flux associated with forest management policies result from aggregation of the confidence interval for total carbon stock as well as the ranges in certainty given by all of the sensitivity analyses performed in flux projection calculations. These include evaluation of the influence on flux projections of assumptions regarding re-growth patterns (polynomial or asymptotic carbon accretion, ultimate carbon density in secondary growth stands), carbon density immediately after harvest, and carbon release to the atmosphere from decomposition of slash, short-term forest products, and long-term forest products.

Average annual carbon flux from the Tongass during the period from 1900 to 1954 was between 31 and 85 thousand metric tons (76,500 best estimate) and the average annual flux for the period from 1954 to 1995 was between 160 and 420 thousand metric tons (380,000 best estimate) (app. U). Estimates of average annual carbon sequestration with cessation of all harvest vary from 107 to 404 thousand metric tons over the period 1995-2095 and 53 to 232 thousand metric tons over the period 2195 as a result of the accretion curve used and the confidence intervals for carbon density in each polygon type. Similarly, estimates of average annual carbon flux from the Tongass to the atmosphere with management of all forested lands on a 100-year rotation vary from -260

to 1,738 thousand metric tons over the period 1995-2095 and vary from 126 to 1683 thousand metric tons over the period 1995-2195 (table 8). Estimates of average annual carbon flux from the Tongass to the atmosphere with management of forested lands available for harvest on a 100-year rotation vary from -207 to 414 thousand metric tons over the period 1995-2095 and vary from -80 to 436 thousand metric tons over the period 1995-2195 (table 8). Estimates of average annual carbon flux from the Tongass to the atmosphere with management of all forested lands on a 200-year rotation vary from -499 to 876 thousand metric tons for the period 1995-2095 and vary from -258 to 1,207 thousand metric tons for the period 1995-2195 (table 8). Estimates of average annual carbon flux from the Tongass to the atmosphere with management of forested lands available for harvest on a 200-year rotation vary from -205 to 207 thousand metric tons for the period 1995-2095 and vary from -192 to 291 thousand metric tons for the period 1995-2195 (table 8).

Multiplying these flux estimates by the monetary value of $20 per metric ton yielded estimates of the monetary value of these carbon fluxes (table 9). Positive numbers represent potential revenue from the sale of carbon emission permits made possible by the carbon sequestration associated with the management policy modeled while negative numbers represent the cost of emission permit purchase for carbon emissions associated with these management policies. The monetary values of projected annual carbon fluxes, assuming $20 per metric ton, range from $8.1 million annual revenue for the period 1995-2095 and $4.6 million annual revenue for the period 1995-2195 from carbon sequestration associated with cessation of timber harvest to $34.8 million annual cost for the period 1995-2095 and $33.7 million annual cost for the period 1995-2195 from carbon loss associated with harvest of all forested lands on a 100-year rotation (table 9). Between $1.9 and $8.1 million worth of carbon would be sequestered each year for 100 years and between $0.9 and $4.6 million worth of carbon would be sequestered each year for 200 years with cessation of all harvest. Between $1.3 and $3.9 million worth of carbon has been emitted annually from the Tongass since 1900. Management of all forested lands on a 100-year rotation would result in -$5.2 to $34.8 million worth of carbon emissions annually over 100 years and $2.5 to $33.7 million worth of carbon emissions annually over 200 years. Management of forested lands

available for harvest on a 100-year rotation would result in -$4.1 to $8.3 million worth of carbon emissions annually over 100 years and -$1.6 to $8.7 million worth of carbon emissions annually over 200 years. Management of all forested lands on a 200-year rotation would result in -$10.0 to $17.5 million worth of carbon emissions annually over 100 years and -$5.2 to $24.1 million worth of carbon emissions annually over 200 years. Management of forested lands available for harvest on a 200-year rotation would result in -$4.1 to $4.1 million worth of carbon emissions annually over 100 years and -$3.8 to $5.8 million worth of carbon emissions annually over 200 years.

Discussion

The novel method used in this study of spatially modeling carbon density with available GIS data to calculate existing carbon stock and to project carbon flux produced robust results. The carbon density coverage corresponds with visual borders in forest structure at John Caouette's study site in Crab Bay. Polygon types represent quantitative differences in carbon density, which correspond to what one would expect from the qualitative description of each polygon type. Although the estimates of carbon density for some polygon types contain significant uncertainty, these tend to be rare polygon types with very small aggregate area, which therefor contribute very little to the total amount of carbon in the Tongass. Twelve polygon types account for over 90% of the area in the Tongass; ten of these polygon types account for 86% of the total carbon in the Tongass. The estimate of 2.8 Pg total carbon in the Tongass is subject to a relatively tight 95% confidence interval (0.5 Pg) and is robust to all major assumptions employed in the process of creating this model.

Furthermore, the computer programs and methods developed for this study could be applied to a new study area with relatively simple modifications, suggesting that this is a method for carbon inventory and flux projection with possibilities for further applications. One advantage of the approach of spatially modeling carbon density is that the spatial aspect of the data is retained, allowing calculation of the total carbon stock and carbon flux for any specific area of land. However, this methodology also makes use of aggregated data and will break down if the analysis is employed on a scale too small.

Although existing data was successfully used in this research to create a spatial model of carbon density for the Tongass, the process could be simplified to produce more accurate results with revision of GIS data collection goals to better meet the needs of forest structure modeling. This possibility is being researched as forest management shifts from a focus on timber production to multiple-use management goals (Caouette et al, 2000, 2001).

The distribution of carbon between soils (66%), aboveground (30%) and roots (4%) is reasonable in comparison with carbon inventories completed in other ecosystems (Turner et al, 1995). The large contribution of soil carbon likely results from the significant areas of muskeg and deep organic saprists in Southeast Alaska. Uncertainty in

the soil component of total carbon contributes a large portion to the overall confidence interval of carbon stock estimates in this study, 52% of the confidence intervals for carbon density in each polygon type, as is true with much other forestry research. However, this uncertainty had no impact on estimates of carbon flux with management scenarios because the soil carbon pool was assumed to remain in equilibrium for all flux models. GIS soil data for Southeast Alaska is linked to forest cover and not directly measured from soil characteristics because it is based on interpretation of aerial photos with some ground-truthing. Furthermore, some have questioned the accuracy of the soil categorization presented by Alexander et al (D'Amore and Lynn, unpublished). Specifically, D'Amore and Lynn suggest that many areas mapped as saprists may really be hemists, with higher carbon density. Hence, estimates of soil carbon in this study are conservative. Finally, classification of Soil Management Unit (SMU) codes into the ten categories presented by Alexander et al was done conservatively, further ensuring that the estimate of total soil carbon is conservative.

The carbon stock in the Tongass represents a significant portion of estimates of the total amount of carbon in forests of the Unites States and a significant portion of estimates of carbon in global forest vegetation and soils. The carbon stock in the Tongass (2.8 Pg) is 7.7% of the carbon in forests of the conterminous United States (36.7 Pg) (Turner et al, 1995) and 0.25% of the carbon in global forest vegetation and soils (1146 Pg) (Dixon et al, 1994).

The sensitivity of carbon stock and carbon flux estimates to major assumptions was tested with repeated model runs. However, one set of carbon flux projections can be identified as the most realistic estimate. The rates of decomposition assumed in "Flux Model Two" for slash and stumps left on site after harvest, pulpwood products, and sawtimber products most closely approximate extant conditions in the Tongass forest and the life-cycles of forest products in the United States. A value of zero more closely approximates carbon density in standing aboveground biomass after clearcutting than does the carbon density in seedlings and saplings present in polygon type **23. Reduction of carbon sequestration associated with cessation of harvest in the Tongass by 13% to account for reduced carbon storage in long-term forest products yields a

conservative approximation of the allocation of CERs for land use management change in the Tongass. Current management of the timber harvest in the Tongass equates to management on a 200-year rotation, suggesting this management scenario as the "business as usual" upon which CER allocation may be based. The 0.15×10^6 hectares of forest that has been harvested over the past 40 years (1955-1995) is 22% of the 0.68×10^6 hectares of commercially viable forest initially present in the Tongass and available for harvest under current land use designations. Thus, continuation of harvest volumes of the past 40 years would result in complete harvest of the available timber stock in just over 180 years of harvesting. This logic identifies the projections for carbon flux in "Flux Model Two", with the carbon density in standing aboveground biomass after harvest equal to zero and carbon sequestration associated with cessation of harvest reduced 13% as the most realistic estimates of carbon flux associated with management policies modeled. Furthermore, CER allocation could be based on the difference between the values in this model run for carbon sequestration resulting from cessation of harvest and carbon emission associated with management of available forested lands on a 200-year rotation. Therefor, the best estimate of the net annual value of carbon sequestration as a result of ceasing all harvest in the Tongass is $2.4 to $4.5 million dollars for the 100-year period 1995-2095 and $2.3 to $4.9 million dollars for the 200-year period 1995-2195.

Some additional factors left out of the sensitivity analyses performed in this research deserve mention. The increasing atmospheric CO_2 concentration and changing regional climates predicted for the future may change some characteristics of the Tongass, including carbon stock and flux. However, recent studies suggest the magnitude of the changes in carbon stock associated with climate change are small compared to changes caused by land use (Caspersen et al, 2000, Houghton et al, 1999).

The assumption of unchanging carbon stock in old-growth forests is ubiquitous despite a dearth of data available to either confirm or disprove it, for Alaska or elsewhere (McClellan, 2001). Furthermore, this problem is confounded in Alaska by the relative youth (on a geologic scale) of the landscape and consequent likelihood of carbon sequestration on many sites that now support forests. In fact, the glacial history of Southeast Alaska suggests that the ecosystem is not in steady state. Most of the Tongass

was covered ice 10,000 years ago during the Little Ice Age and most glaciers are still receding. However, with no way to model this long-term change, the carbon density in unharvested polygon types was assumed to remain constant for the next 200 years despite the likelihood of carbon accretion in these areas due to primary succession as glaciers recede and continuing carbon accretion in deepening muskeg.

The independence of soil carbon calculations from FIA grid data forced the assumption of constant soil carbon density in flux projections. Recent research shows that forest harvest has little effect on soil carbon on average but that specific harvest techniques can cause increases or decreases in soil carbon (Johnson and Curtis, 2001).

Young-growth forests generally have lower levels of defect from decay than do old-growth forests (McClellan, 2001). Consequently, the proportion of harvested material left as slash on site may decrease with conversion of forested lands in the Tongass from old-growth to managed young-growth stands.

Many options exist for making timber harvesting more conducive to carbon sequestration (McClellan, 2001), none of which could be included in the models of carbon flux presented here because they depend on unpredictable future forestry management decisions. For example, increased efficiency in conversion of timber to durable products could reduce carbon emission during harvest and production operations. Use of durable wood products as substitutes for building materials with high energy costs for their production (e.g. concrete, aluminum, and steel), could also result in net reduction of carbon emission to the atmosphere. Use of marginal quality wood in engineered wood products could reduce logging residues currently left on site after harvest and burning logging residues for power generation could replace the fossil fuels currently used in the generators of many southeast Alaska communities, offsetting these carbon emissions.

The uncertainty in flux estimates resulted largely from uncertainty over which accretion curve, asymptotic or polynomial (fig. 6a, b), most accurately describes secondary growth in the Tongass. The rapidity with which carbon accretion progresses to equilibrium predicted by the asymptotic model may be unrealistic and the magnitude of carbon density above that found in old-growth forests predicted by the polynomial model may also be unrealistic. However, limited chronosequence data and the resulting lack of

resolution in carbon accretion during the transition period from early secondary growth to old-growth required use of these two models to frame carbon flux projections. The value of carbon density for old-growth forests used in creation of the carbon accretion models was calculated as a weighted average of old-growth commercial forest polygon types from the carbon map and it was assumed that secondary growth reached old-growth status in 350 years. Sufficient specificity for more detailed estimation of old-growth carbon density, for example with changes in site productivity, was not available in the data. Furthermore, estimates of old-growth carbon density include the influence of roads, lakes, and other anomalies encountered in the FIA sample locations used to calculate carbon density for each mapped polygon type whereas chronosequence data from permanent plots reflect carbon density in completely forested areas. This may be part of the reason for higher carbon density calculated from permanent plot data than estimated for old-growth polygon types. The peak in the polynomial carbon accretion curve at about 200 years of re-growth (absent in asymptotic carbon accretion) causes projections of carbon sequestration with cessation of harvest modeled with the polynomial accretion curve to peak around the year 2180 (fig 13). The total carbon stock in the Tongass begins to decline prior to the year 2200 and will continue to decline in this model scenario until all harvested areas reach equilibrium old-growth carbon density and the total carbon stock equals 2.85 Pg. Projections of carbon flux with management scenarios involving 200-year rotations differ dramatically with the carbon accretion curve selection because harvested areas are allowed to re-grow to the peak carbon density in the polynomial accretion curve, well above old-growth carbon density. Thus, the forest is essentially managed at a peak carbon density that is above the carbon density of old-growth forests in 200-year-rotation management scenarios modeled with polynomial carbon accretion. Selection of carbon accretion curve causes less difference in management scenarios involving 100-year rotations because forested lands are harvested before carbon accretion extends very far into the peak in the polynomial accretion curve. More complete determination of the rate of carbon accretion during secondary growth in the Tongass will lead to more precise estimates of the carbon flux associated with each management policy modeled.

The rate of carbon loss caused by wood decomposition varies with the proportion of "white" and "brown" rots. The proportions of each cause of decomposition varies with species, with 98% of decay in Western redcedar, 62% of decay in Western hemlock, and 16% of decay in Sitka Spruce caused by white rot (Kimmey, 1956). Carbon loss from standing wood and the large amount of slash left on-site after harvest in the Tongass (fig. 7) may be reduced by altering species composition of the forest toward more decomposition-resistant Western redcedar. However, decomposition of this material is accounted for in flux projections by linear decay over a period of 50 or 100 years. Consequently, the specificity of this method is not sufficient for examination of the difference between white-rot and brown-rot in releasing carbon from downed woody debris. Similarly, the amount of carbon in standing dead wood was reduced by decay factors but no distinction between white- and brown-rot was possible. Therefor, the model developed here lacks the specificity required to model whether altering species composition in Southeast Alaska could be an effective strategy for increased carbon sequestration due to reduced decomposition.

Carbon flux into or out of the Tongass could be small but significant for national level carbon budgets and could be very important for the economics of Tongass management, depending on management policy. Ceasing all harvest in the Tongass results in annual sequestration of 107 – 404 thousand metric tons of carbon (0.10 – 0.40 Tg). For comparison, the Conservation Reserve Program (CRP) presents the opportunity for 1 – 16 Tg carbon sequestration per year (Barker et al, 1995) and the forests of the conterminous United States are sequestering 79 Tg carbon per year, mostly in secondary-growth forests in the northeast (Turner et al, 1995). In 1996 the CRP consisted of 16.2×10^6 ha cropland converted to 14.7×10^6 ha grassland and of 1.5×10^6 ha forestland. The area of the Tongass is 7.0×10^6 ha, less than half the area involved in the CRP. Past harvest caused the loss of 0.8 – 2.2 Tg carbon from the Tongass from 1900 to 1954 (app. P), while land use in the conterminous United States caused the loss of 27,000 $\pm$ 6,000 Tg carbon from 1900 to 1945 (Houghton et al, 1999). Harvest in the Tongass from 1954 to 1995 caused the loss of 6.6 – 17.8 Tg carbon while land use in the conterminous Unites States caused 2,000 $\pm$ 2,000 Tg carbon sequestration, mostly in the northeast

(ibid.). Most of the carbon sequestration during this period was due to passive abandonment (Hamburg, 2001). The Tongass contains 0.2×10^6 hectares of harvested area and 2.1×10^6 hectares of unharvested land with potentially commercial forest volume. Of this unharvested area, 0.5×10^6 hectares are available for harvest under current land use designations. Research in similar forests in Washington and Oregon determined that conversion of 6×10^6 hectares of old-growth to young plantations resulted in loss of 1,500 – 1,800 Tg carbon to the atmosphere (Harmon et al, 1990). Timber harvest in the Tongass has caused only a small fraction of the potential carbon emissions from conversion of unharvested lands to young plantations.

The economic value of carbon sequestration associated with ceasing harvest in the Tongass may be significant relative to the value of timber harvest (table 10). Timber sales in the Tongass are worth $6.5 million annually (USDA Forest Service, 2001). The net value of switching management from timber harvest to no harvest depends on what is deemed "business-as-usual" in the allocation of Certified Emission Reduction Credits (CER) under article 3 of the Kyoto Protocol. Allocation of CERs for land-use change is controversial, depending mostly on the details of exactly how business as usual is defined and thus, how many CERs one gets for a certain management change.

Some argue that carbon sequestration from land-use change may not mitigate climate change as effectively as reduction of GHG emissions from fossil fuel use, citing the possibility for leakage in the quantification of emissions reduction from land-use change. How this issue of leakage is dealt with in the allocation of CERs for land-use change depends on future policy negotiations but one can speculate about some implications for the research presented here. Reducing harvest in the Tongass requires increased harvest elsewhere to keep product supply constant. Consequently, carbon flux estimates for the Tongass do carry the estimated monetary values for Tongass management in a carbon emissions market (this forest gets the CERs and can sell them to some other forest for increased production), but these values are not accurate measures of the net social benefit or benefit to the USDA Forest Service because another national forest must buy CERs from the Tongass to keep the total product stream from national forest lands constant by increasing its harvest. However, increased harvest elsewhere to

compensate for decreased harvest in the Tongass will likely still result in net reductions in GHG emissions because of greater efficiency in road building, transportation, harvest, secondary growth, and the forest products industry in other managed forests. Finally, existing monetary inefficiency in the form of what amounts to an annual subsidy of $29 million to run the Tongass timber program indicates further net social benefit from moving timber production to another area. This demonstrates added financial benefit to ceasing harvest in the Tongass permanently and indicates the unique status of the Tongass as a place where ceasing harvest could have permanent annual financial benefits from subsidy savings. This fiscal motivation could ensure a permanent increase in the carbon stock in the Tongass from a permanent end to harvest, thereby justifying the validity of allocation of CERs for this land-use change. Furthermore, allocation of CERs for reduced harvest in the Tongass remains justified in a regulated system of carbon emissions trading even with the possibility of future increases in harvest (due, for example, to changes in wood product supply or demand that make the economics of harvest in the Tongass advantageous) because forest managers would have to buy back CERs to begin harvest.

The forest industry in Alaska employs 2,000 - 2,500 people (Warren, 1999). The recent closures of the Alaska Pulp Corporation mill in Sitka and Ketchikan Pulp Corporation mill in Ketchikan have demonstrated the impact of reducing harvest from the Tongass on the local economies in Sitka and Ketchikan. These closures have also initiated a process of downsizing that could be continued or reversed. Many people previously employed in the forestry industry have begun to transition to new occupations as a result of these two mill closures. Although the annual monetary value of carbon sequestration from cessation of harvest in the Tongass is equivalent to the annual monetary value of timber sales in the Tongass, elimination of the $29 million annual subsidy for the Tongass Timber program with cessation of harvest could impact local economies. Further study of this subsidy is necessary to evaluation this potential consequence of forest management.

The range in estimates of the net monetary value of carbon sequestration from ceasing timber harvest in the Tongass results from the cumulative effect of the sensitivity analyses and confidence intervals established in the several phases of this research. The 95% confidence interval in carbon density estimates for each polygon type, sensitivity analyses of allometric biomass equation selection, assumptions of standing aboveground carbon density after harvest and of ultimate carbon density achieved by secondary growth, and the carbon accretion model used as well as uncertainty in the allocation of CERs and carbon release to the atmosphere from decomposition of slash, short-term forest products, and long-term forest products are all incorporated into the estimated range of net economic value. Therefor, this range represents a generous confidence interval for the actual value.

The net value of carbon sequestration associated with switching management to no harvest in the Tongass clearly depends on the value of CERs. This value was assumed to be $20 per metric ton in this analysis but estimates of the value of CERs in a regulated marketplace range from $5 to $125 (Weyant, 2000). Deviation in the value of CERs from $20 per metric ton was not included in the estimated range of net monetary value from carbon sequestration associated with cessation of timber harvest in the Tongass, although the range given can easily be scaled to do so.

International climate change mitigation negotiations must move forward and lead to the creation of treaties, similar to the Kyoto Protocol, that enforce GHG emission reductions and allow for emissions trading as a mechanism for achieving these reductions for land use management for carbon sequestration to attain economic value. In the meantime, registry of current management policy and existing carbon stock is important to establish a baseline of "business-as-usual" and allow management to begin climate change mitigation with the security that they will get credit for this action in the framework of eventual international treaties.

The Tongass must be included in national carbon budgets. Management of the Tongass for carbon sequestration may be of equivalent economic value to timber harvest. Furthermore, valuation of potential carbon sequestration in the Tongass from ceasing harvest is amplified by indirect benefits of not harvesting, like maintenance of the

Southeast Alaska fisheries and tourism industries and reduced subsidy payments for the Tongass timber program. Nationally, this subsidy may be better spent developing an alternative energy market in Southeast Alaska, which could employ an equal number of people and multiply the carbon benefits from cessation of timber harvest. The emerging economic value of carbon sequestration requires consideration of carbon flux in the development of future Tongass management plans.

References Cited

Alexander, E.B., E. Kissinger, R.H. Huecker, P. Cullen. 1990. Soils of Southeast Alaska as Sinks for Organic Carbon Fixed from Atmospheric Carbon-Dioxide. USDA Forest Service, Juneau, AK.

Barker, Jerry R., Greg A. Baumgardner, David P. Turner and Jeffrey J. Lee. 1995. Potential carbon benefits of the Conservation Reserve Program in the United States. *Journal of Biogeography* 22, 743-751.

Birdsey, Richard A. 2001. Personal Communication. Program Manager, Global Change Research, USDA Forest Service. 11 Campus Blvd. Ste. 200, Newtown Square, PA 19073, rbirdsey@fs.fed.us

Brown, James K. 1974. Handbook for Intventorying Downed Woody Material. Gen. Tech. Rep. INT-GTR-16. Ogden, UT: U.S. Department of Agriculture, Forest Service, Intermountain Forest and Range Experiment Station. 24 p.

Caouette, John P. 2001. Personal communication, USDA Forest Service GTR "Modeling Forest Structure in Southeast Alaska" currently under peer review.

Caouette, John P., Marc G. Kramer, Gregory J. Nowacki. 2000. Deconstructing the Timber Volume Paradigm in the Management of the Tongass National Forest. United States Department of Agriculture Forest Service, Pacific Northwest Research Station, General Technical Report PNW-GTR-482.

Caspersen, J.P., S.W. Pacala, J.C. Jenkins, G.C. Hurtt, P.R. Moorcraft, and R.A. Birdsey. 2000. Contributions of Land-Use History to Carbon Accumulation in U.S. Forests. *Science*, 290, 1148-1151

D'Amore, David V. 2001. Personal communication. USDA Forest Service, Pacific Northwest Research Station, 2770 Sherwood Lane, Suite 2A, Juneau, AK, USA 99801-8545

D'Amore, David V. and Warren C. Lynn. Classification of Forested Histosols in Southeast Alaska. USDA Forest Service, Pacific Northwest Research Station, unpublished

DeMars, Donald J. 2000. Stand-Density Study of Spruce-Hemlock Stands in Southeastern Alaska. United States Department of Agriculture Forest Service, Pacific Northwest Research Station, General Technical Report PNW-GTR-496.

Dixon, R.K., S. Brown, R.A. Houghton, A.M. Solomon, M.C. Trexler, J. Wisniewski. 1994. Carbon Pools and Flux of Global Forest Ecosystems. *Science* vol 263, 14 January 1994, p. 185.

Fletcher, Susan R. 2000. Global Climate Change Treaty: The Kyoto Protocol. Congressional Research Service Report for Congress 98-2, The National Council for Science and the Environment, Washington D.C. http://www.cnie.org/nle/clim-3.html (18 December, 2000).

Hamburg, Steven P. 2001. Personal Communication. Brown University Box 1943, Providence,RI 02912-1943

Hamburg, Steven P., Dmitri G. Zamolodchikov, George N. Korovin, Viktor V. Nefedjev, Anatoly I. Utkin, Jakov I. Gulbe, Tatjana A Gulbe. 1997. Estimating the Carbon Content of Russian Forests: A Comparison of Phytomass/Volume and Allometric Projections. *Mitigation and Adaptation Strategies for Global Change* 2:247-265.

Harmon, M. E. 2001. Carbon cycling in forests: simple simulation models. H. J. Andrews Research Report Number 2 (http://www.fsl.orst.edu/lter/pubs/res_rpts/CcycleForest.htm)

Harmon, Mark E., William K. Ferrell, Jerry F. Franklin. 1990. Effects on Carbon Storage of Conversion of Old-Growth Forests to Young Forests. *Science*, vol. 247: 699-702.

Houghton, R.A., J.L. Hackler, K.T. Lawrence. 1999. The U.S. Carbon Budget: Contributions from Land-Use Change. *Science* 285, 574-577.

Intergovernmental Panel on Climate Change (IPCC), Working Group II. 2001. Summary for Policymakers, Climate Change 2001: Impacts, Adaptation, and Vulnerability. http://www.usgcrp.gov/ipcc/ (4-15-01).

Intergovernmental Panel on Climate Change (IPCC) (Robert T. Watson, Ian R. Noble, Bert Bolin, N.H. Ravindranath, David J. Verardo and David J. Dokken eds.). 2000. Land Use, Land-Use Change, and Forestry, Cambridge University Press.

Johnson, Dale W., Peter S. Curtis. 2001. Effects of forest management on soil C and N storage: meta analysis. *Forest Ecology and management* 140, 227-238.

Kimmey, James W. 1956. Cull Factors for Sitka Spruce, Western Hemlock and Western Redcedar in Southeast Alaska. United States Department of Agriculture Forest Service, Alaska Forest Research Center, Station Paper No. 6.

McClellan, Michael H. 2001. Personal Communication. Supervisory Research Ecologist, Team Leader, Silviculture & Ecology of Southeast Alaska. USDA Forest Service, Pacific Northwest Research Station, 2770 Sherwood Lane, Suite 2A, Juneau, AK, USA 99801-8545

Sampson, R. Neil and Dwight Hair. 1996. Forest and Global Change, Vol 2: forest management opportunities for mitigating carbon emissions. American Forests.

Santantonio, D., R.K. Hermann, W.S. Overton 1977. Root biomass studies in forest ecosystems. *Pedobiologia*, Bd. 17, S. 1-31. Paper 957. Forest Research Laboratory, School of Forestry Oregon State University, Corvallis, Oregon.

Schimel, et al. 1995. CO2 and the carbon cycle. Climate Change 1994. Cambridge University Press: Cambridge, UK.

Turner, D.P., G.J. Koerper, M.E. Harmon, and J.J. Lee. 1995. A carbon budget for forests of the conterminous United States. *Ecological Applications*, 5(2):421-436.

U.S. Forest Products Laboratory 1974. Wood Handbook: Wood as an engineering material. USDA Forest Service Agr. Handb. 72. pp. 3-6, 3-12, 3-13, 4-7.

USDA Forest Service, National Headquarters, 2001. Timber Sale Program Information Reporting System (TSPIRS), FY 1998 TSPIRS documents. www.fs.fed.us/land/fm/tspirs/1998tspirs/

USDA Forest Service, Alaska Region. 1997. Tongass National Forest Land and Resource Management Plan 1997. R10-MB 338-CD.

USDA Forest Service, Alaska Region. 1995. Timber Supply and Demand. Alaska National Interest Lands Conservation Act, Section 706(a) Report to Congress number 15.

USDA Forest Service, PNW Station – Forestry Sciences Lab & Region 10 – Alaska. 1995. Field Procedures for the Southeast Alaska Inventory 1995.

U.S. Department of Agriculture Soil Conservation Service, 1994. Classification and Correlation of the Soils of the Ketchikan Area, Alaska. SSSA-644, Anchorage, Alaska.

U.S. Department of Agriculture Soil Conservation Service, 1992a. Classification and Correlation of the Soils of the Stikine Area, Alaska. SSSA-645, Anchorage, Alaska.

U.S. Department of Agriculture Soil Conservation Service, 1992b. Classification and Correlation of the Soils of the Chatham Area, Alaska. SSSA-646, Anchorage, Alaska.

Waddell, Karen L. Draft. An application of line intersect sampling to estimate attributes of coarse woody debris in resource inventories. USDA Forest Service, Pacific Northwest Research Station, Forest Sciences Laboratory.

Warren, Debra D. 1999. Production, Prices, Employment, a Trade in Northwest Forest Industries, Fourth Quarter 1997. United States Department of Agriculture Forest Service, Pacific Northwest Research Station Resource Bulletin, PNW-RB-230.

Weyant, John P. 2000. An Introduction to the Economics of Climate Change Policy. Prepared for the Pew Center on Global Climate Change.

Yarie, John and Bert R. Mead 1988. Twig and foliar biomass estimation equations for major plant species in the Tanana River Basin of interior Alaska. Res. Pap. PNW-RP-401. Portland, OR: U.S. Department of Agriculture, Forest Service, Pacific Northwest Research Station. 20 p.

Additional Reference Information

Alaback, P.B. 1989. Logging of Temperate Rainforests and the Greenhouse Effect: Ecological Factors to Consider. *Watershed '89*, USDA Forest Service Pacific Northwest Research Station, Juneau, AK.

Alemdag, I.S. 1984. Total tree and merchantable stem biomass equations for Ontario hardwoods. Inf. Rep. PI-X-46. Chalk River, Ontario: Canadian Forestry Service, Patawawa National Forestry Institute. 54p.

Barker, Jerry R., G.A. Baumgardner, D.P. Turner, and J.J. Lee. 1995. Potential carbon benefits of the Conservation Reserve Program in the United States. *Journal of Biogeography*, 22: 743-751.

Bobbe, T., D. Reed, J. Schramek. 1993. Georeferenced airborne video imagery – natural-resource applications on the Tongass. *Journal of Forestry*, 91: (8) 34-37.

Elias, Thomas S. 1987. The Complete Trees of North America. Gramercy Publishing Company, New York.

Farr, Wilbur A, Vernon J. LaBau and Thomas H. Laurent 1976. Estimation of Decay in Old-growth Western Hemlock and Sitka Spruce in Southeast Alaska. Res. Pap. PNW-204. Portland, OR: U.S. Department of Agricluture, Forest Service, Pacific Northwest Forest and Range Experiment Station. 24 p.

Forest Inventory Division. 1976. Whole stem cubic metre volume equations and tables: centimeter diameter class merchantable volume factors. B.C. For. Serv. Victoria, B.C.

IPCC [Intergovernmental Panel on Climate Change]. 1990. Scientific assessment of climate change. World Meteorological Organization/ United Nations Environmental Program. Cambridge University Press, Cambridge, England.

----------. 1992. Climate Change 1992. World Meteorological Organization/ United Nations Environmental Program. Cambridge University Press, Cambridge, England.

----------. 1995. Climate Change 1995. World Meteorological Organization / United Nations Environmental Program. Cambridge University Press, Cambridge, England.

Johnson, D. W. 1992. Effects of forest management on soil carbon storage. Water, Air, and Soil Pollution 64: 83-120.

Julin, Kent R. and Shaw, Charles, G. 1999. Science Matters: Information for Managing the Tongass National Forest. U.S. Department of Agriculture Forest Service, Pacific Northwest Research Station, Portland, Oregon, Miscellaneous Publication, April 1999.

Krumlik, G.J. 1974. Biomass and Nutrient Distribution in Two Old Growth Forest Ecosystems in South Coastal British Columbia. Masters thesis, University of British Columbia.

Krumlik, G.J. and J.P. Kimmins. Studies of Biomass distribution and tree form in old virgin forests in the mountains of south coastal British Columbia, Canada.

Kurz, Werner A., Sarah J. Beukema, and Michael J. Apps. 1996. Estimation of root biomass and dynamics for the carbon budget model of the Canadian forest sector. *Can. J. For. Res.* 26: 1973-1979.

Larson, Frederic R 1992. Downed Woody Material in Southeast Alaska Forest Stands. Res. Pap. PNW-RP-452. Portland, OR: U.S. Department of Agriculture, Forest Service, Pacific Northwest Research Station. 12 p.

Manning, G.H, M.R.C. Massie and J. Rudd. Metric single-tree weight tables for the Yukon Territory. Inf. Rep. BC-X-250. Vancouver B.C.: Canadian Forestry Service, Pacific Forest Research Centre. 60 p.

Mead, Bert R. 1998. Phytomass in Southeast Alaska. Res. Pap. PNW-RP-505. Portland, OR: U.S. Department of Agriculture, Forest Service, Pacific Northwest Research Station. 48 p.

Nordhaus, William D. 1992. An optimal transition path for controlling greenhouse gases. *Science* 258: 1315-1319.

Pastor, J.; Post, W.M. 1986. Influence of climate, soil moisture, and succession on forest carbon and nitrogen cycles. Biochemistry 2: 3-27.

Post, W.M., T-H. Peng, W.R. Emanuel, A.W. King, V.H. Date, and D.L. DeAngelis. 1990. The global carbon cycle. *American Scientist* 78:310-326.

Schimel, D.S. 1995. Terrestrial Ecosystems and the Carbon-Cycle. *Global Change Biology* 1: (1) 77-91.

Southeast Alaska Conservation Council. 1999. http:\\www.seacc.org, Southeast Alaska Conservation Council, Jan. 20, 1999.

Servid, Carolyn and Donald Snow. 1999. The Book of the Tongass. Milkweed Editions, Minneapolis, Minnesota.

Singh, T. 1984. Biomass equations for six major tree species of the Northwest Territories. Inf. Rep. NOR-X-257. Edmonton, Alberta: Environ. Can., Can. For. Serv., North. For. Res. Cent. 22 p.

Singh, T 1983. Weight Tables for Important Tree Species in the Northwest Territories. NOR FMN-27. Edmonton, Alberta: Canadian Forestry Service, Northern Forest Research Centre.

Standish, J.T, G.H. Manning and J.P. Demaerschalk. Inf. Rep. BC-X-264. Vancouver, B.C.: Canadian Forestry Service, Pacific Forest Research Centre. 48p.

Turner, David P., J.K. Winjum, T.P. Kolchugina, and M.A. Cairns. 1997. Accounting for biological and anthropogenic factors in national land-base carbon budgets. *Ambio*, 26: (4) 220-226.

U.S. Department of Agriculture, Soil Survey Division Staff, 1993. Soil Survey Manual. USDA Handbook No. 18. U.S. Government Printing Office, Washington, DC.

U.S.D.A. Forest Service, 1991. Tongass Soil Handbook, Tongass National Forest, Alaska Region.

USDA Forest Service, Alaska Region. 1996. Timber Supply and Demand 1995. Alaska National Interest Lands Conservation Act Section 706(a) Report to Congress, report number 15.

Woodwell, G. M.l, Hobbie, J. E.; Houghton, R.A.; Melillo, J. M.; Moore, B.; Park, A.B.; Peterson, B.J.;Shaver, G.R. 1984. Measurement of changes in the vegetation of the earth by satellite imagery. In: Woodwell, G.W.,ed. The role of terrestrial vegetation in the global carbon cycle: measurement by remote sensing, Scope 23.[Place of publication unknown]: John Wiley and Sons. p 272.

Wurtz TL, Gasbarro AF. 1996. A brief history of wood use and forest management in Alaska. *Forestry Chronicle*, 72: (1) 47-50.

Yarie, John and Delbert R. Mead 1982. Aboveground Tree Biomass on Productive Forest Land in Alaska. Res. Pap. PNW-298. Portland, OR: U.S. Department of

Agriculture, Forest Service, Pacific Northwest Forest and Range Experiment Station. 16p.

Figures

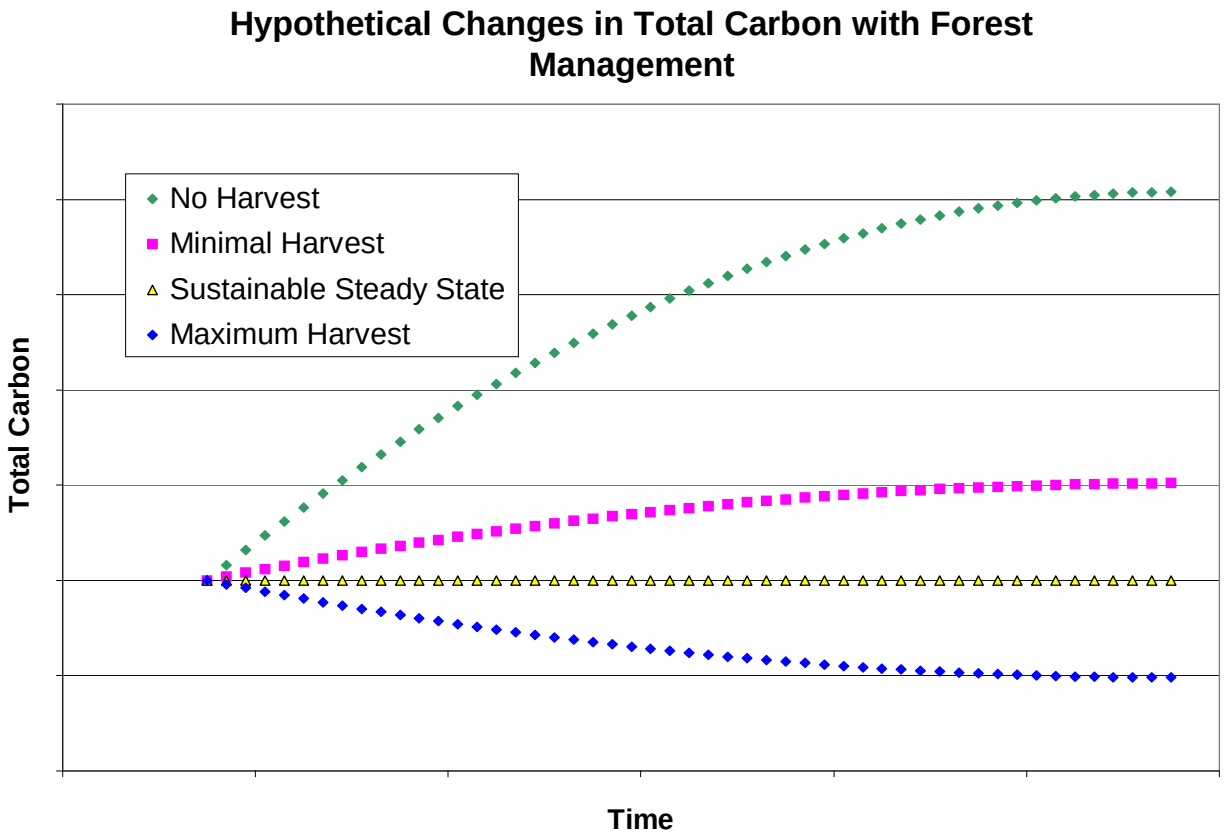

Figure 1: (demochart on CD one)

The total carbon stock in a forest can change with different management. This figure shows projections of changes in total carbon stock for a hypothetical forest under four hypothetical management scenarios. Certified Emissions Reduction credits (CERs), proposed under article 3 of the Kyoto protocol, may be allocated based on the difference in total carbon stock between how the forest was being used ("business as usual") and how the forest is now used. Thus, quantifying carbon flux under the new management is important for appropriate allocation of CERs as well as establishing a definition of business as usual. The question of whether forest managers who switch to no harvest should be credited the difference between this carbon stock and that projected under minimal harvest, sustainable steady state, or maximum harvest remains unresolved in international climate change policy debates.

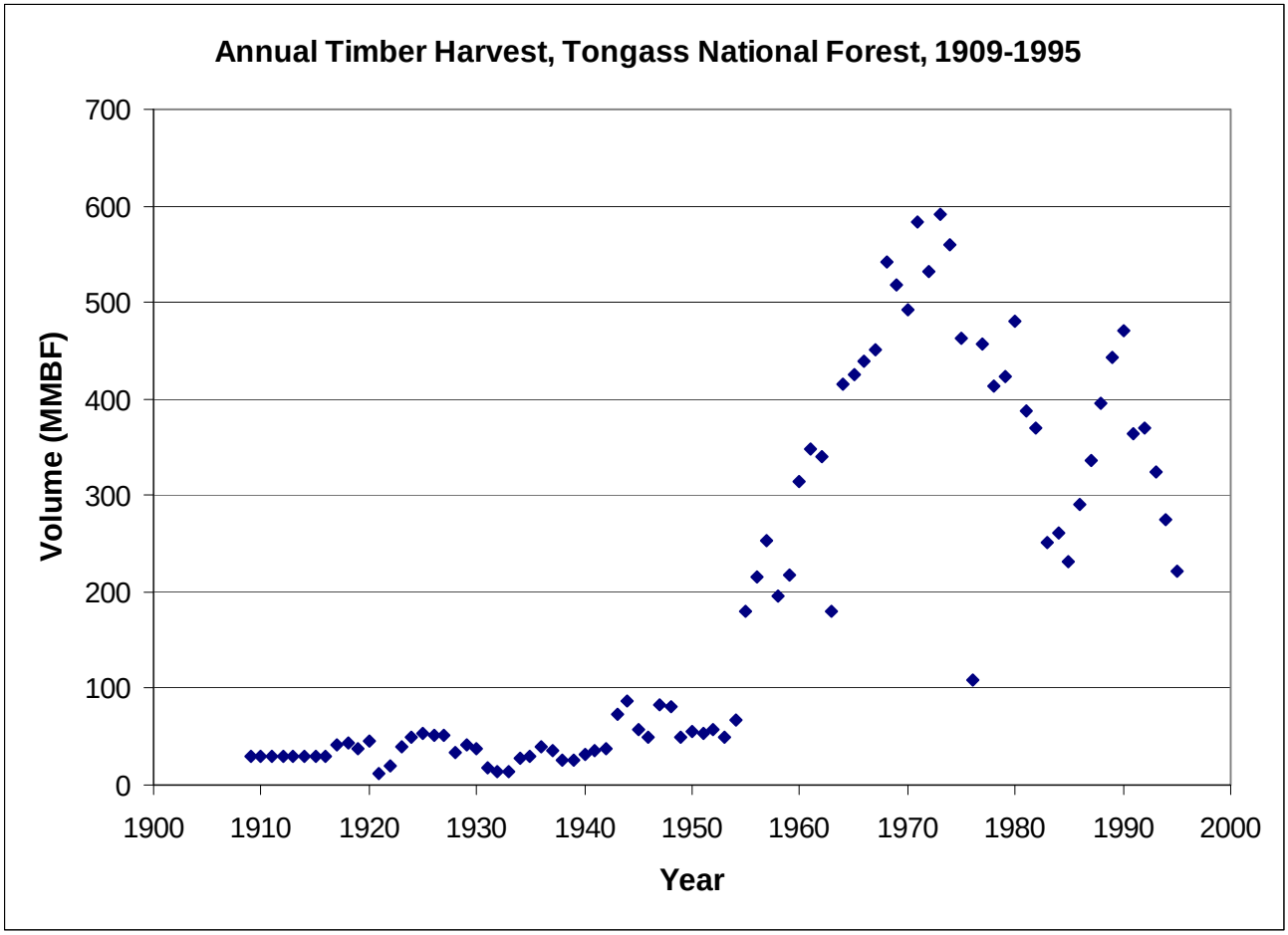

Figure 2: (past timber harvest on CD one)

The harvest history in the Tongass National Forest was split into two time periods, 1900 – 1954 and 1955 – 1995, based on historical annual timber harvest volumes shown here. The rate of timber harvest increased dramatically in 1954 with the initiation of two long-term timber contracts with the Alaska Pulp Corporation (APC) and Ketchikan Pulp Corporation (KPC). Data was reported for calendar years prior to 1951 and for fiscal years after 1952. The outlier in 1976 results from a change in fiscal year. Data is from USDA Forest Service Alaska Region, 1995.

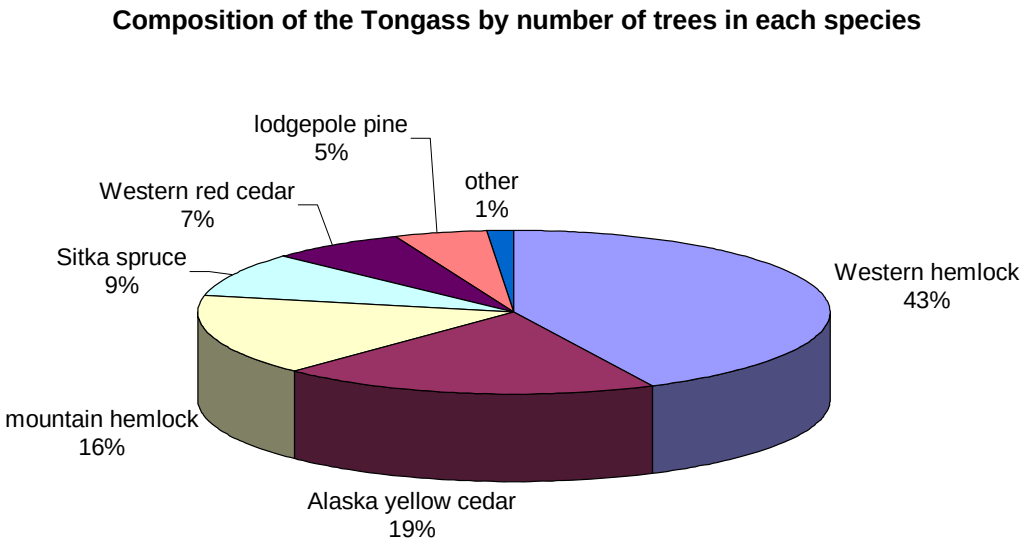

Figure 3: (%composition on CD one)

Contributions of major tree species to the forests of the Tongass National Forest were calculated based on the number of records (trees) for each species in the 1995 FIA forest inventory data used for carbon density calculations. A high latitude temperate rainforest, conifers dominate the forest with the prevalence of cedars decreasing with increasing latitude.

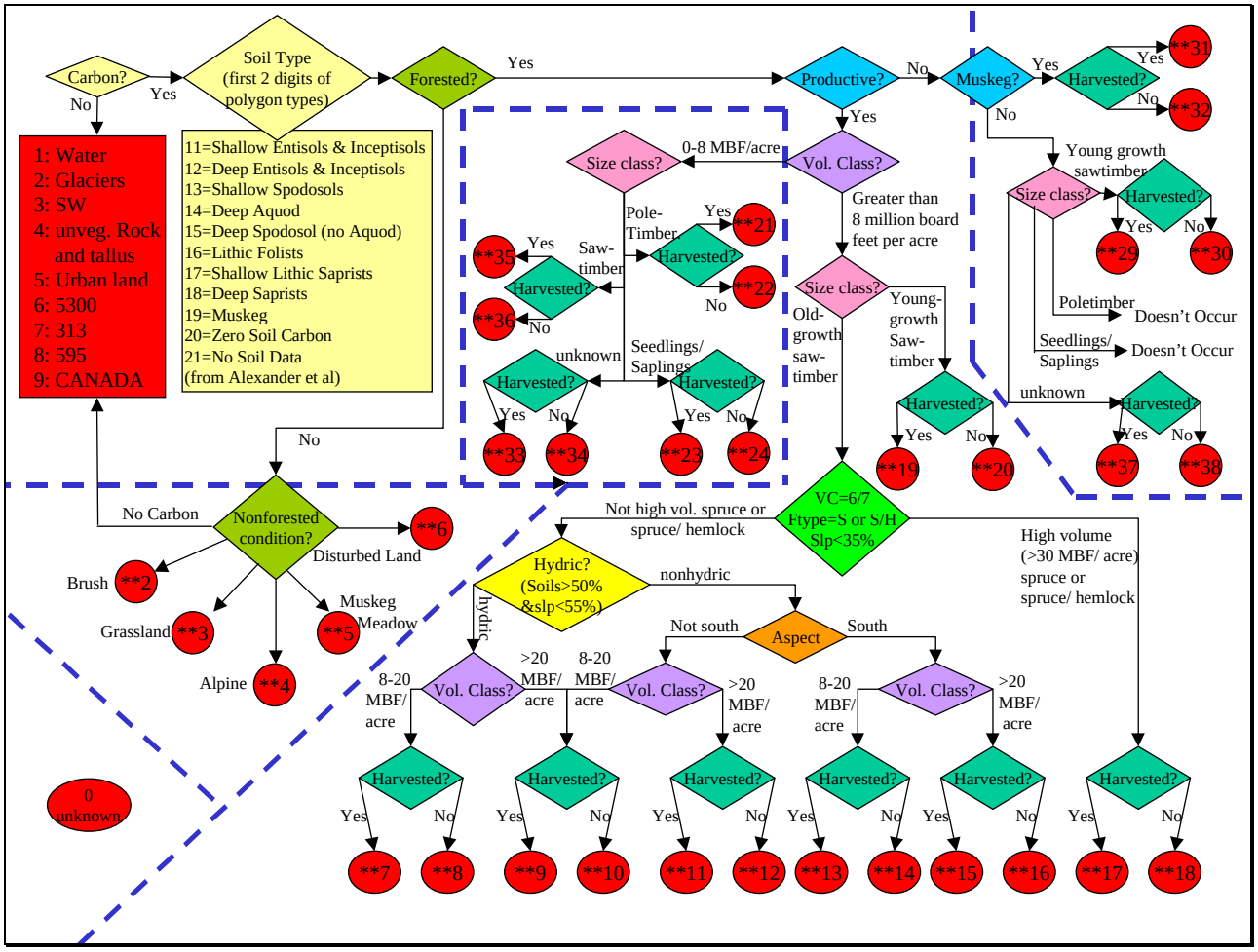

Figure 4: (new flow chart on CD one)

The flow chart shows how existing GIS attributes were used to delineate polygon areas expected to contain differing carbon density. Red ovals correspond to carbon density polygon types and diamonds are color-coded based on the source of data used for that decision (fig. 4b). After areas with no carbon were removed from consideration, the first stage of delineation was by the soil categories described by Alexander et al. These categories were coded as the first two numbers of a four-digit code system for carbon density polygon types, represented as ** in the red ovals in this diagram. Delineation of polygon types by soil category was left out for aboveground carbon density calculation to reduce the number of polygons to the 43 types shown in this figure. Polygon types were simplified in this same manner for most of the analysis because of the independence of soil carbon from FIA data and the need for aggregation of polygon types to achieve sample sizes sufficient for calculation of aboveground carbon density for each one from FIA data.

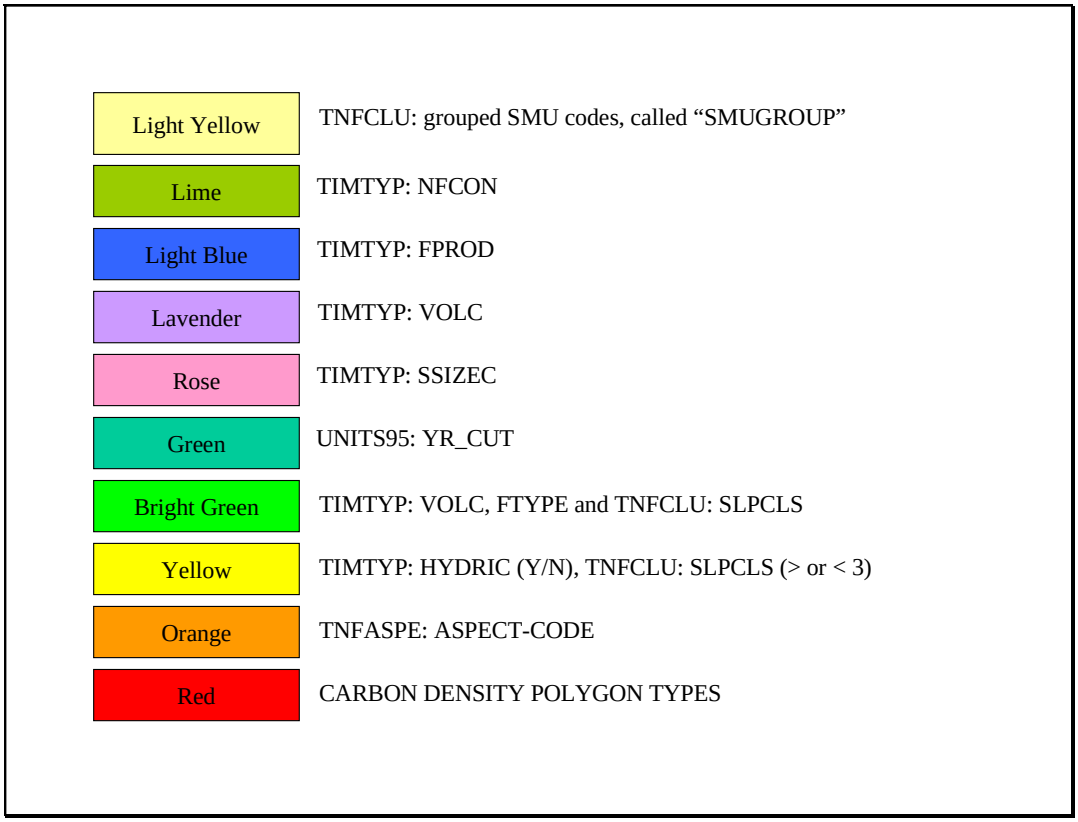

Figure 4b:

The sources of data for the flow of logic used to map carbon density in the Tongass are shown. Colors correspond to the flowchart in figure 4. The letters preceding the colon indicate the name of the forest service GIS coverage containing the attribute(s) specified after the colon. SMU codes describe over 800 soil associations and complexes; NFCON indicates several nonforested conditions; FPROD classifies an area according to the expected annual volume of growth; VOLC class describes areas based on timber volume; SSIZEC describes areas based on the dominant timber size; YR_CUT record whether an area has been harvested by recording the year of harvest; FTYPE describes the general forest type; SLPCLS indicates the slope gradient; HYDRIC records hydric and nonhydric soil conditions; ASPECT-CODE indicates slope aspect.

Figure 5:

The carbon density GIS coverage (Leighty9) was condensed into 13 major categories of polygon types to simplify the visual complexity. The table below explains this simplification. This coverage is saved as "figure5" on CD 3b and can be found in printed form on the back cover.

Legend:

polygon number (figure 5)	"Aboveground" polygon types represented	Description
1	**16, **18, **8, **14, **12, **10	unharvested high-volume timber
2	**34, **38	unknown size class, low volume, productive & unproductive
3	**32	forested muskeg
4	**23	harvested, seedlings & saplings
5	**6, **5, **2, **4	Nonforested
6	**7, **9, **11, **13, **15, **17, **19, **21, **29, **31, **33, **35, **37	Harvested
7	**3	Grasslands
8	**20, **22, **24, **30, **36	unharvested low-volume forest
9	0	Unknown
10	1, 3, 10	Water
11	2, 9	glacier, Canada
12	4, 6, 8	rock and tallus
13	5	urban land

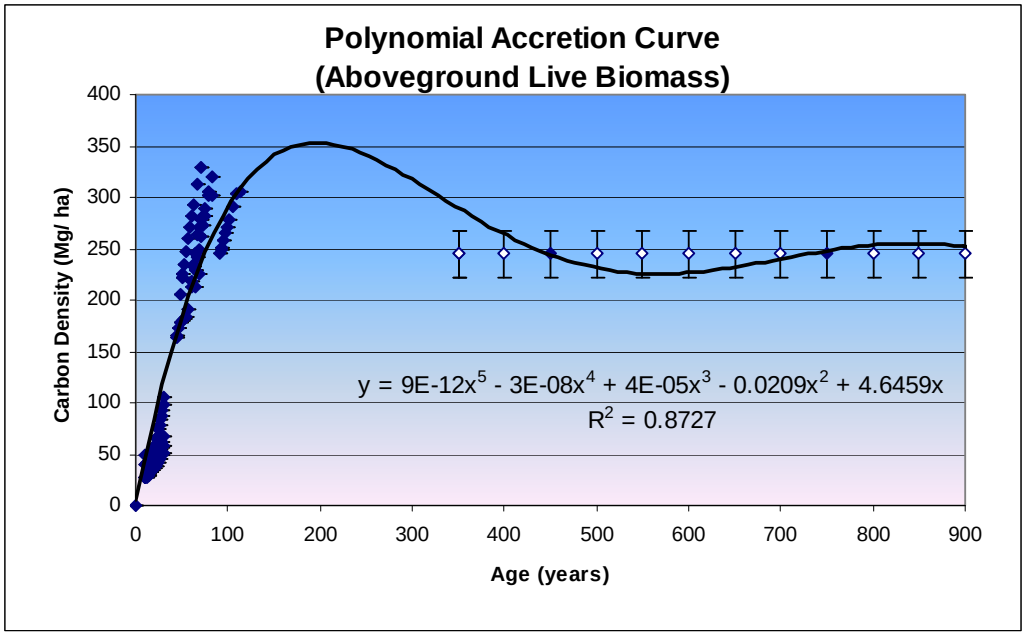

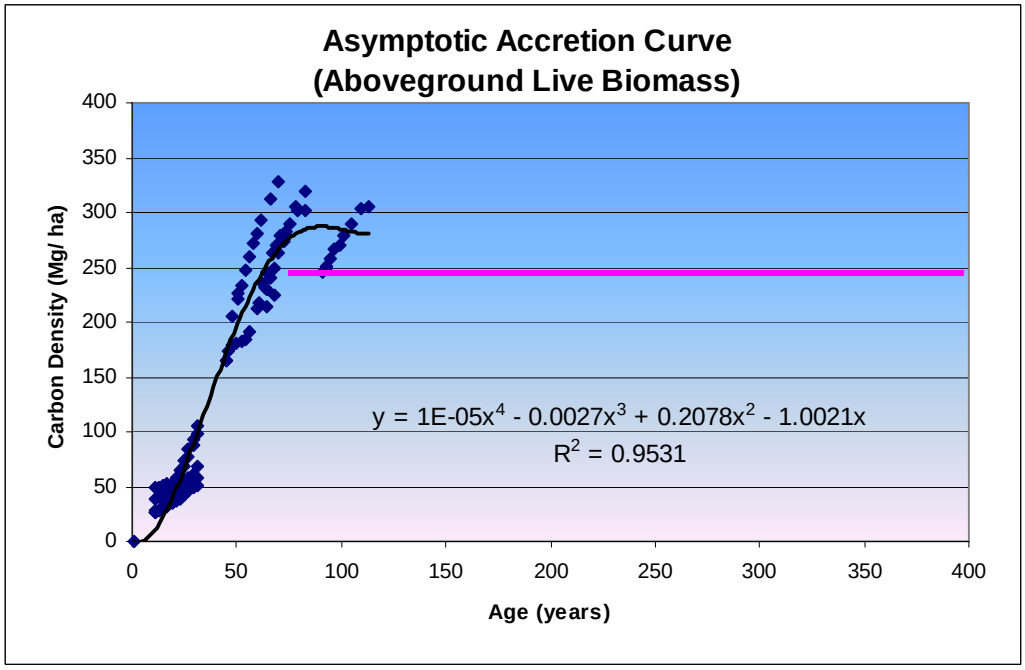

Figure 6a (top) and 6b (bottom): (stand density accretion curves3 on CD one)

Carbon accretion curves were developed by synthesizing permanent plot data (filled diamonds) and carbon density estimates for unharvested, old-growth carbon density polygon types (open diamonds, pink line). The curves model change in carbon density in live aboveground biomass with time. Carbon density was calculated from permanent plot data with the same allometric equations and SAS programs that were used for calculation of carbon density from FIA data. Lack of data for forest stands between 100 and 350 years old prevented resolution of whether polynomial accretion or asymptotic accretion more accurately describes secondary growth in Southeast Alaska. Consequently, both accretion curves were used in carbon flux modeling to test the sensitivity of flux estimates to the shape of this curve. Divergence in permanent plot data

over time results from differences in site quality, as indicated by the site index recorded in permanent plot data. Data from sample locations representing a full range of site indexes was used in creation of these carbon accretion curves. Local spatial heterogeneity may have been greater at FIA sample locations than permanent plots. If so, this could partially explain why carbon density in standing aboveground biomass in oldgrowth polygon types is less than that at older permanent plots.

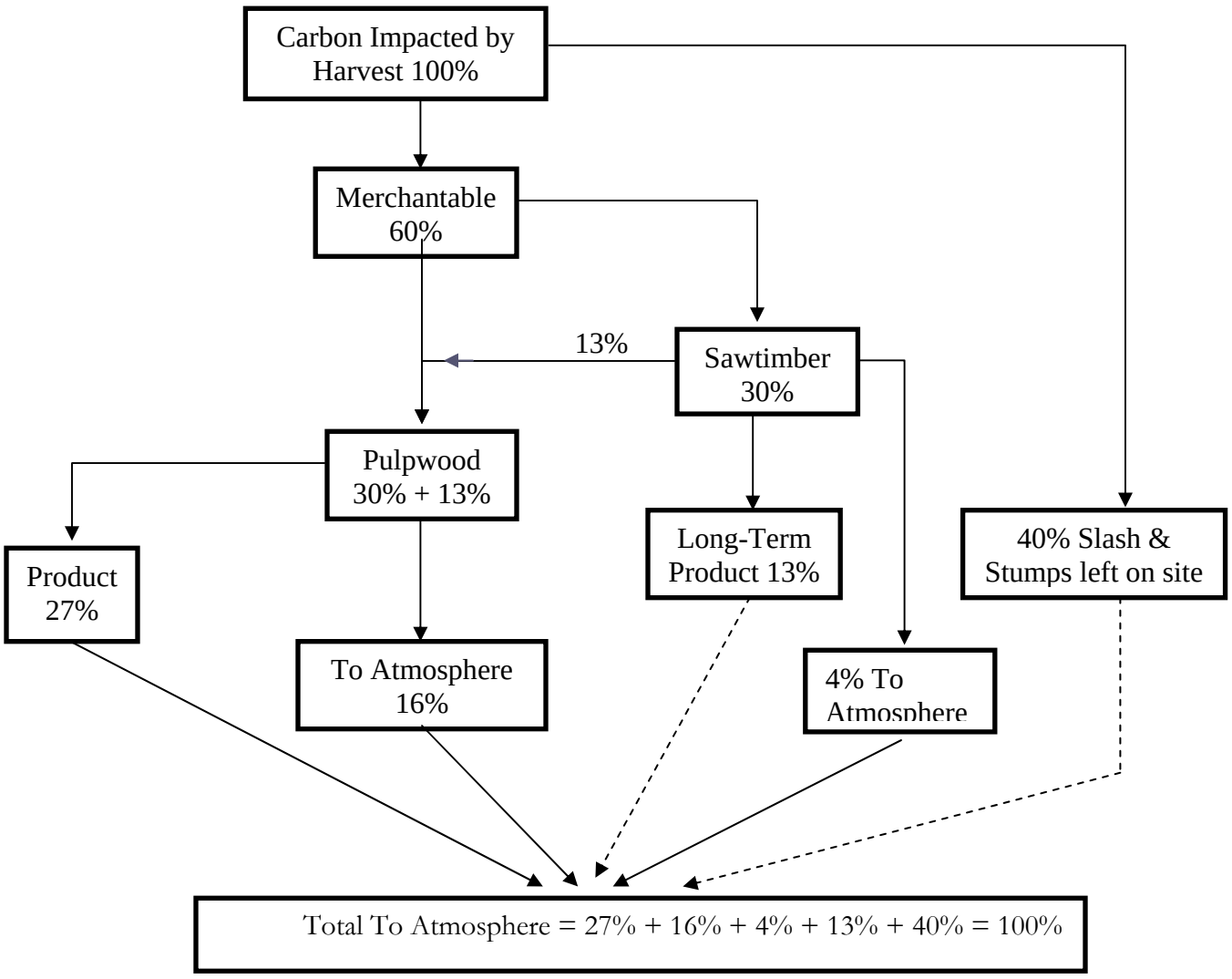

Figure 7:

Product flow for Southeast Alaska timber industry is shown. Starting with 100 arbitrary units of carbon harvested, 60% becomes merchantable volume while the remaining 40% remains on site after harvest as slash and stumps and is lost to the atmosphere over time as it decomposes (Sampson & Hair, 1996, Harmon, 2001). Roughly half of the merchantable volume enters the sawtimber production process and the other half enters the pulpwood production process (Warren, 1999). Once in the sawtimber production process, 43.5% of the carbon becomes product (long term storage), 13% is lost to the atmosphere, and 43.5% enters the pulpwood production process (Sampson & Hair, 1996). In the pulpwood production process, 62% of the carbon becomes product (short-term storage) and 38% is lost to the atmosphere. See the section on sensitivity analyses for discussion of how decomposition of forest products and slash was included in flux projections.

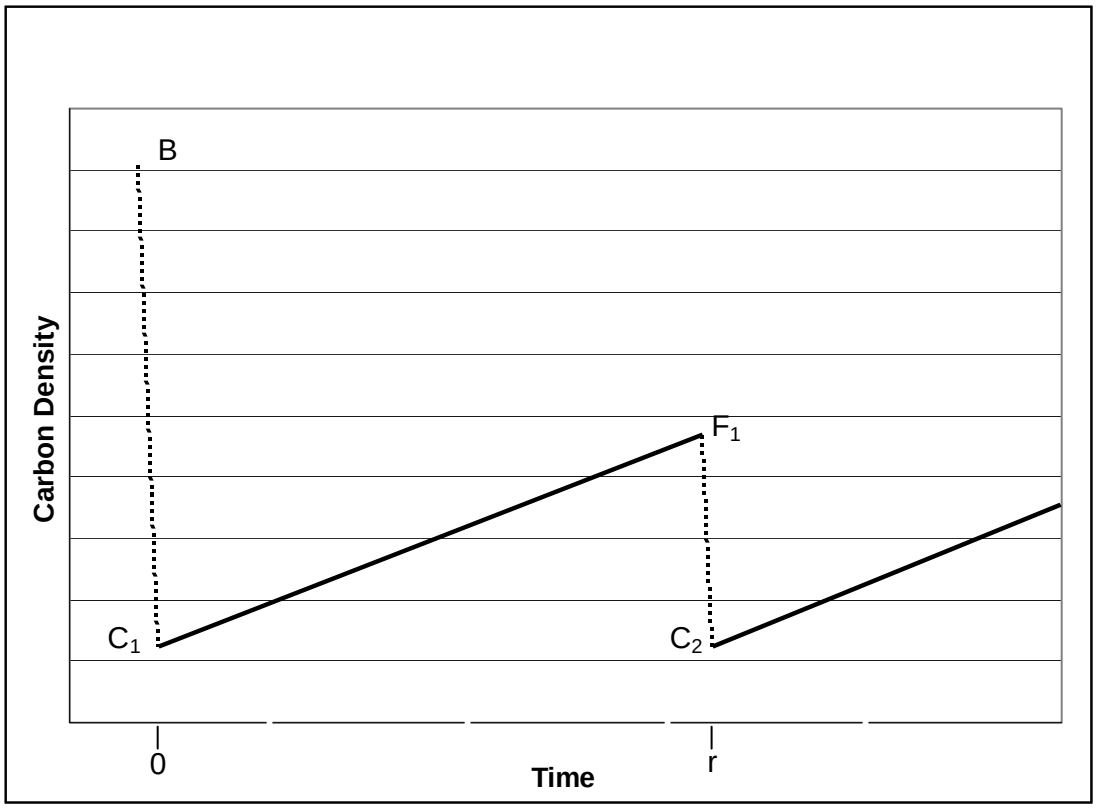

Figure 8:

This model of changes in carbon density with harvest was used to project carbon flux in management scenarios involving 100- and 200-year rotations. For each polygon type, the total area (A), carbon density in 1995 (B), carbon density after harvest (C), carbon density after r years of re-growth (F) and the rotation length (r) were used to calculate annual carbon flux.

$$Annualflux = \frac{A \times (B - (0.5 \times (F - C) + C))}{r} = \frac{A \times (B - 0.5 \times (F + C))}{r}$$

A first approximation of net annual carbon flux based on this equation was used in initial flux models. The equation was then broken into 3 component parts, given by the following equations, for more accurate modeling of decomposition of slash, downed woody debris, and sawtimber products. Net carbon flux was calculated as the sum of these equations.

Annual carbon flux into the forest product production process (FP) = $0.6 \times (B - C) \times \frac{A}{r}$

Annual carbon flux into slash and stumps left on site (S) = $0.4 \times (B - C) \times \frac{A}{r}$

Annual carbon sequestration in secondary growth (SG) = $((\frac{C + F}{2}) - C) \times \frac{A}{r}$

Carbon density after harvest (C) was assumed to equal the density in polygon type **23 for all polygon types in one set of model runs and was assumed to equal zero in another set of model runs. The carbon density after r years of re-growth (F) was calculated as a percentage of the original carbon density in 1995 (B) based on the carbon accretion curve used in each model run. Two methods were used for estimation of the length of re-growth since harvest for harvested polygon types to test the sensitivity of flux projections to assumptions about the progression of

re-growth. One method (denoted as scenario “a”) assumed an ultimate carbon density after re-growth of harvested polygon types equal to the most similar unharvested polygon type. The other method (denoted as scenario “b”) assumed an ultimate carbon density after re-growth of harvested polygon types equal to the similar unharvested polygon type with largest volume.

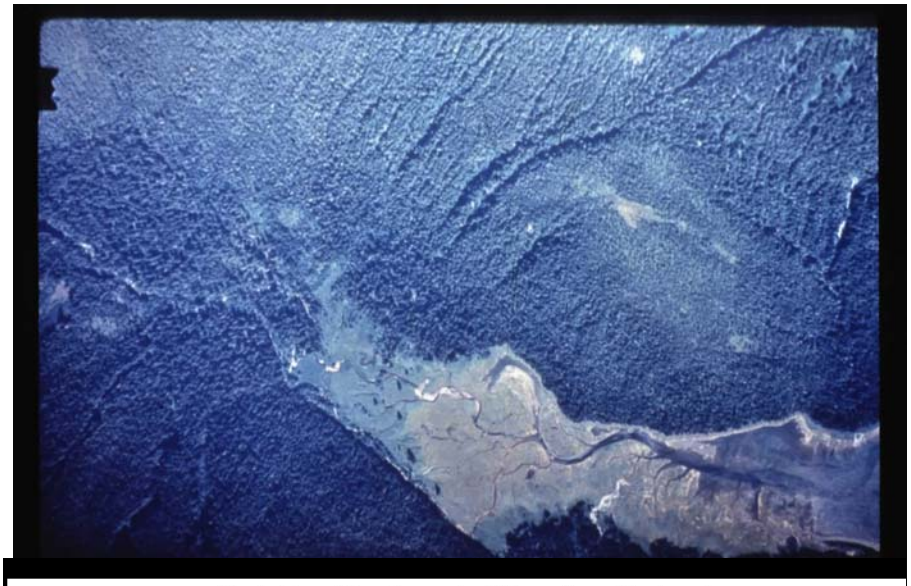

Aerial photo of Crab Bay

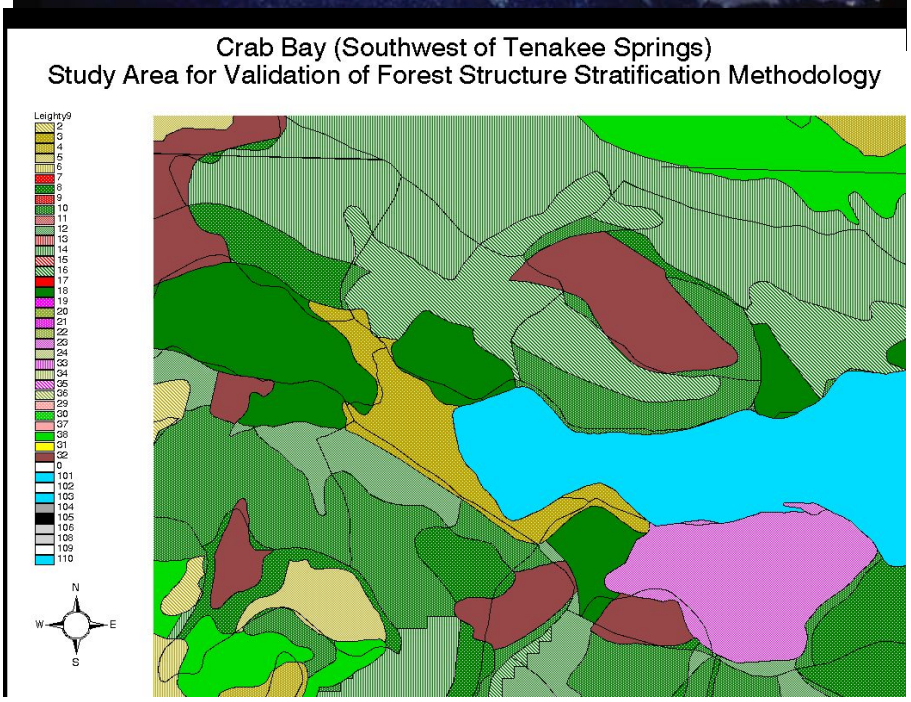

Carbon density map for Crab Bay

Figure 9:

Comparisons of aerial photos with the carbon density map confirm correlation with observable transitions in forest structure. The brown area in the aerial photo of Crab Bay corresponds with the extent of water shown in the carbon density map. Moving northwest, we see intertidal grasslands in the aerial photo corresponding to the brown "nonforested" area in the carbon density map. Dark greens in the carbon density map indicate high volume forest, visible in the aerial photo as rough texture. Lighter greens indicate lower-volume forest, visible in the photo as smoother textures. The maroon areas are muskeg areas, visible as patches of brown within the forest. Notice especially the large area of upland muskeg north of the Bay separated from the water by rough-textured high volume forest. The pink area in the carbon density map indicates a harvested alluvial fan, not visible in the aerial photo.

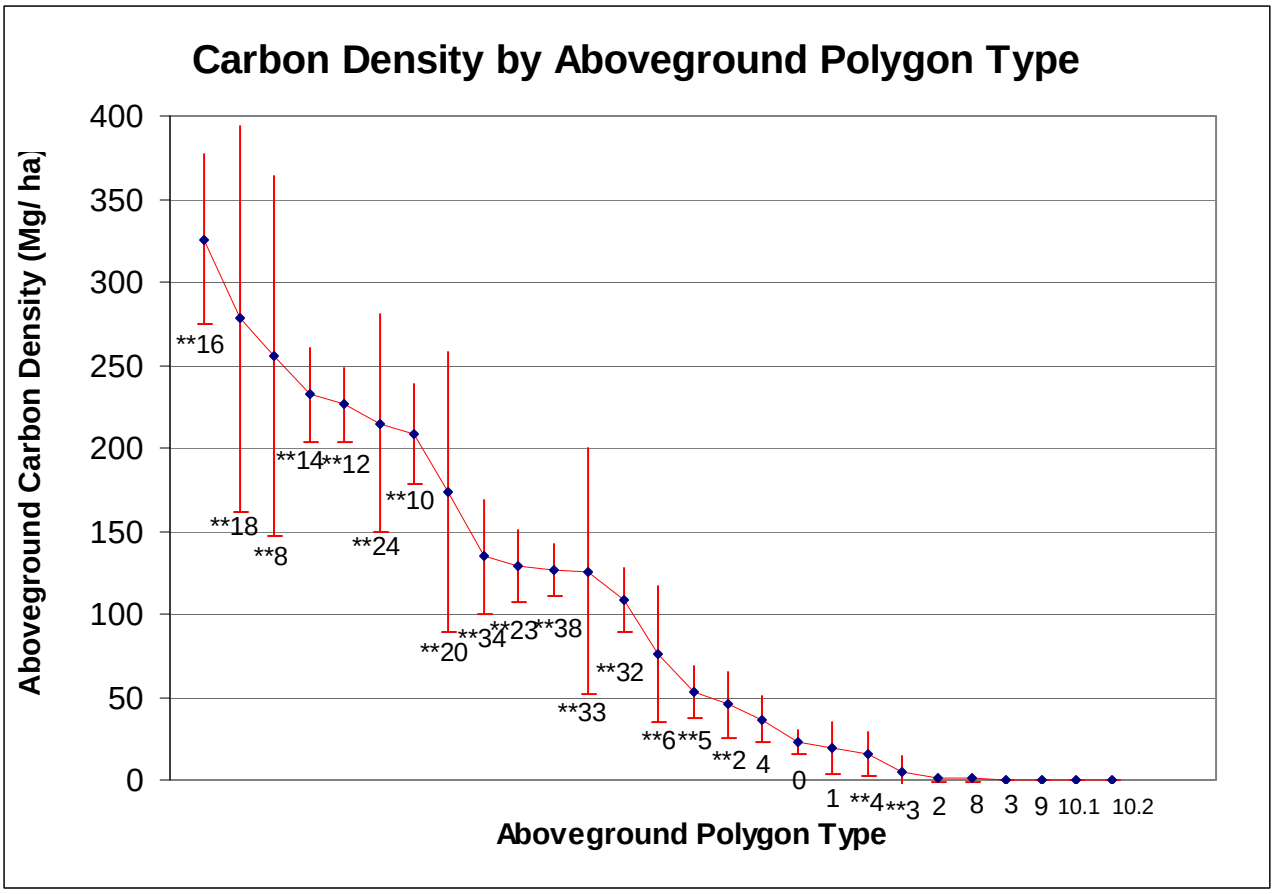

Figure 10a:

Polygon types in the carbon density map were simplified to create "aboveground polygon types" by dropping soil type delineation for calculation of aboveground carbon density from FIA data. Simplified polygon types with n<=4 are omitted (table 6, fig.11). Quantitative estimation of carbon density in each polygon type confirms the theoretical prediction of differing carbon density by polygon type, indicating successful mapping of carbon density in the Tongass. Error bars represent 95% confidence in carbon density. The confidence interval is especially large for polygon type **34 because all nonproductive, low volume (0-8 MBF/ acre) areas lacking size class data were lumped into this category (fig 4).

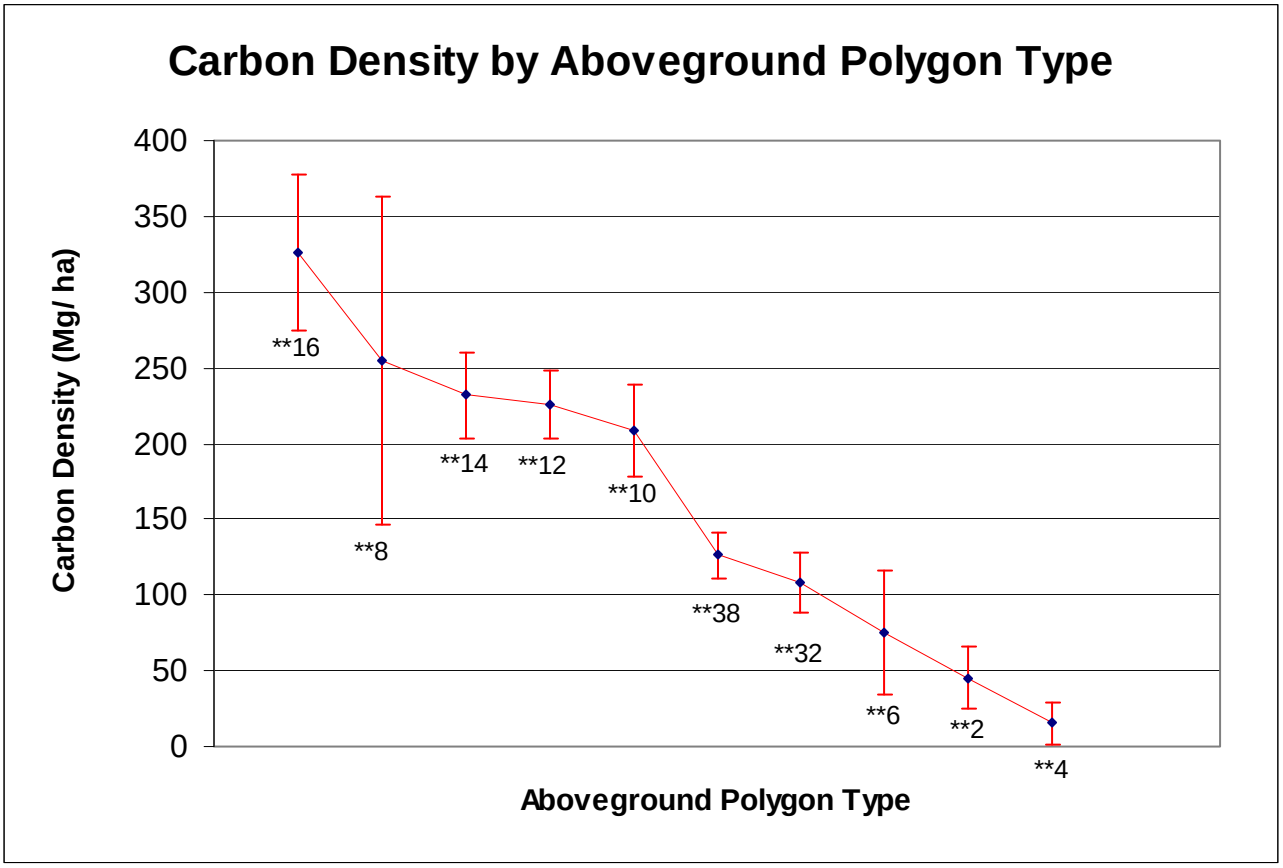

Figure 10b:

Carbon density for the 10 polygon types contributing 86% of total carbon in the Tongass is shown. Error bars indicate 95% confidence in carbon density. This continued simplification of polygon types further demonstrates the success of carbon density mapping in the Tongass and suggests the robustness of this technique for estimation of existing carbon stock.

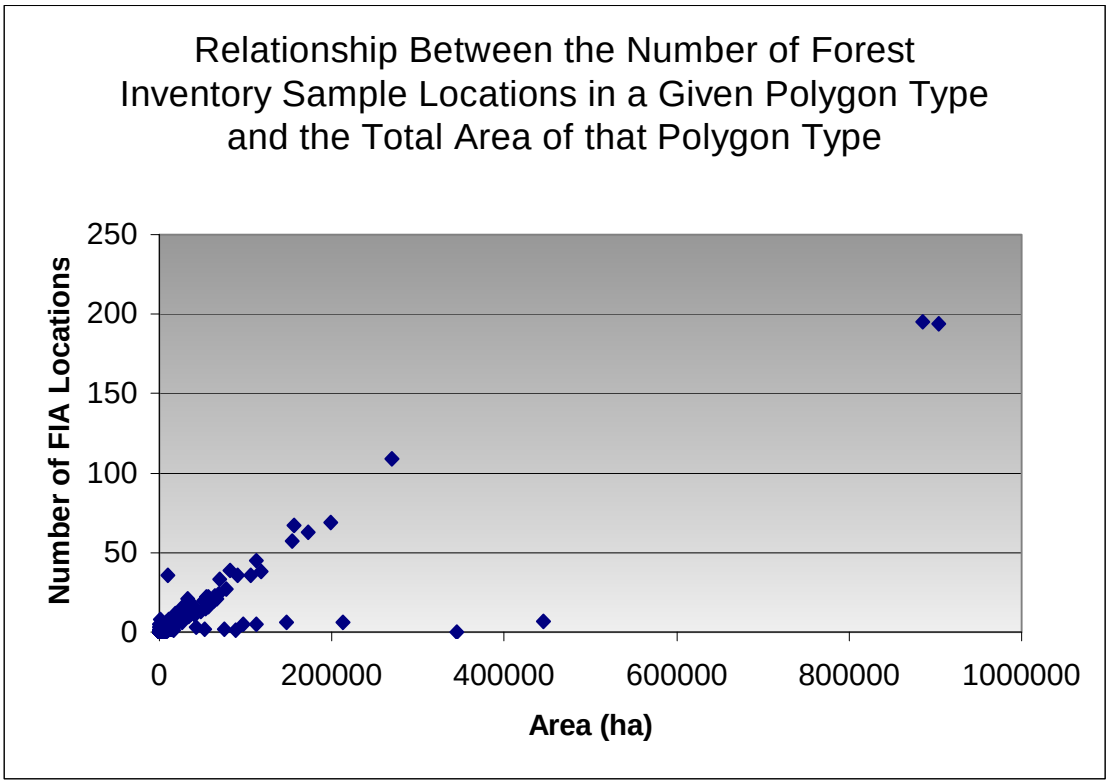

Figure 11:

Insufficient FIA data for some polygon types resulted in large uncertainty in carbon density due to very small sample sizes. However, the number of FIA sample locations representing a polygon type generally correlates with the total area of that polygon type. Consequently, those polygons with large uncertainty in carbon density estimates were also the polygon types with very little total area in the Tongass, thereby reducing the significance of uncertainty in carbon density. The polygon types with large area represented by very few FIA locations include land cover like glaciers, rock, and water, where FIA sampling was determined unnecessary from the air.

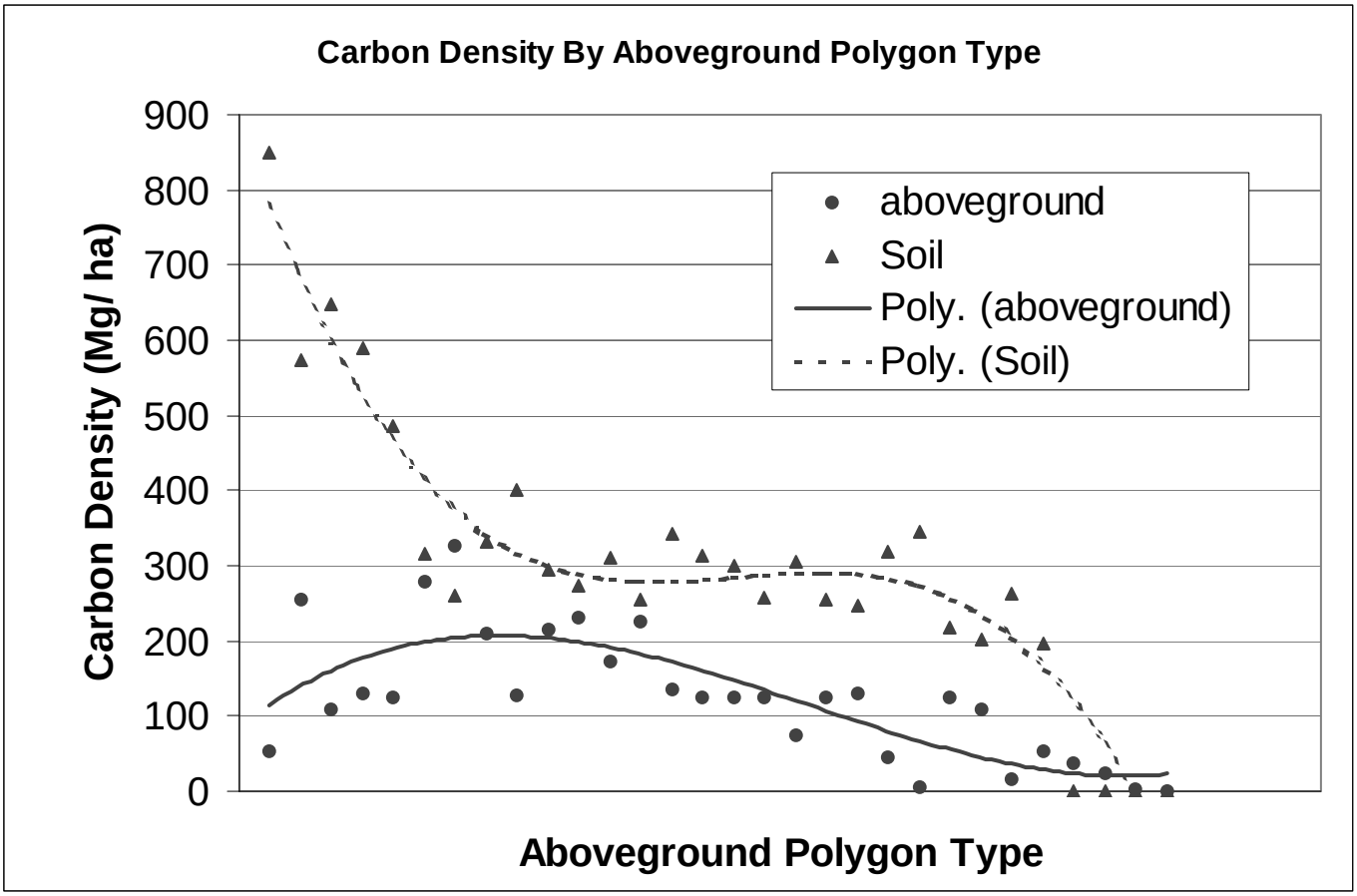

Figure 12:

A relationship between aboveground and soil carbon density corresponding to what is observed in the Tongass indicates the success of carbon mapping for the Tongass. Carbon density in aboveground biomass and soil is plotted by aboveground-carbon-density polygon type and a polynomial regression line is drawn for each. The left side of the graph represents muskeg areas, with very high soil carbon density and relatively low aboveground carbon density. In the center of the graph, soil carbon density stays relatively constant in the mineral soils of a variety of locations while aboveground carbon density covers a range due to the other factors included in the carbon mapping process (fig. 4). The right side of the graph represents rocky, icy, and otherwise harsh locations that have very little soil and aboveground carbon density. Regression lines were calculated with polynomial equations using Microsoft Excel.

Figures 13A – 13H are in the sections “Flux Model One” and “Flux Model Two”

Tables

Species	"Low-end" Equation	Source	"High-end" Equation	Source
Pacific silver fir *(Abies amabilis)*	(12.8+183.6*D^2*H)	Standish, 1983	N/A	N/A
subalpine fir *(Abies lasiocarpa)*	(14.3+186.2*D^2*H)	Standish, 1983	N/A	N/A
Alaska yellow cedar *(Chamaecyparis nootkatensis)*	(9.2+191.6*D^2*H)	Standish, 1983	N/A	N/A
tamarack *(Larix laricina)*	(6.32169+.01728*D^2*H)	Singh, 1983	N/A	N/A
white spruce *(Picea glauca)*	(32.2+146.9*D^2*H)	Standish, 1983	N/A	N/A
black spruce *(Picea mariana)*	(22.4+159.5*D^2*H)	Standish, 1983	N/A	N/A
Sitka spruce *(Picea sitchensis)*	(17.6+172.1*D^2*H)	Standish, 1983	N/A	N/A
Lodgepole pine *(Pinus contorta)*	(10.7+205.7*D^2*H)	Standish, 1983	N/A	N/A
Pacific yew *(Taxus brevifolia)*	N/A	N/A	N/A	N/A
western red cedar *(Thuja plicata)*	(40.4+96.9*D^2*H)	Standish, 1983	(1.270 + 0.01501*(d^2H))	Shaw, 1977
western hemlock *(Tsuga heterophylla)*	(29.8+155.8*D^2*H)	Standish, 1983	(0.497 + 0.02113*(d^2H))	Shaw, 1977
mountain hemlock *(Tsuga mertensiana)*	(14.6+198.9*D^2*H)	Standish, 1983	(386.715 + 117.631*(d^2H))	Krumlik, 1974
red alder *(Alnus rubra)*	(4.8+206.5*D^2*H)	Standish, 1983	N/A	N/A
paper birch *(Betula papyrifera)*	(7.4+156.4*D^2*H)	Standish, 1983	N/A	N/A
balsam poplar *(Populus balsamifera)*	(.018505*d^2*H)	Alemdag, 1984	(-1.29892+0.01472*d^2*H)	Singh, 1984
quaking aspen *(Populus tremuloides)*	(4.1+195.5*D^2*H)	Standish, 1983	N/A	N/A
black cottonwood *(Populus trichocarpa)*	(7.4+156.4*D^2*H)	Standish, 1983	N/A	N/A
willow *(Salix)*	(4.1+195.5*D^2*H)	Standish, 1983	N/A	N/A

Table 1:

Biomass equations used to convert FIA grid data to estimates of carbon density are shown. Measurements of diameter at breast height in meters (D) and centimeters (d), and measurements of height (H) in meters from FIA data were used in the equations. See appendix G for detailed discussion of equation selection.

	Model Runs*					
Carbon Pools (Pg)	1	1-2	2	2b	3	5
Total	**2.85**	**2.83**	**2.83**	**2.83**	**2.80**	**2.28**
95% C.I. (+/-)	**0.51**	**0.48**	**0.48**	**0.48**	**0.51**	**0.40**
Total above-ground	0.87	0.85	0.85	0.85	0.82	0.38
Roots	0.12	0.12	0.12	0.12	0.12	0.04
Soil	1.86	1.86	1.86	1.86	1.86	1.86
Trees	0.42	0.42	0.42	0.42	0.53	0.18
Seedlings/ saplings	0.16	0.16	0.16	0.16	0.05	0.03
Dead Snags	0.09	0.09	0.09	0.09	0.10	0.04
Large DWD	0.18	0.16	0.16	0.16	0.12	0.12
Small DWD	0.00	0.00	0.00	0.00	0.00	0.00
Understory	0.02	0.02	0.02	0.02	0.02	0.02

Model Run	*Description
1	low-end equations, no willow or birch, DWD outlier included
1-2	low-end equations, no willow or birch, DWD outlier removed
2	low-end equations, willow and birch included, DWD outlier removed
2b	low-end equations, willow and birch included, DWD outlier removed, weighted
	averages for unknown confidence intervals
3	high-end equations, willow and birch included, DWD outlier removed
5	low-end equations, willow and birch included, DWD outlier removed, only trees
	within specified allometric equation range included

Table 2:

Estimates of the total carbon stock in various pools in the Tongass were made to test the sensitivity of the model to several assumptions (app. J). These estimates and brief descriptions of the assumptions made in each model run are presented. Assumptions about the allometric biomass equation used for willow and birch, the exclusion of an outlying downed woody debris (DWD) data point, and estimation of confidence intervals for carbon density in polygon types lacking sufficient data for this calculation all do not significantly change the estimate of total carbon or the confidence interval for this estimate. Trees outside the size range for which allometric equations had been verified account for 19.4% of the total carbon estimate.

		Percent of original Carbon					
Time Since Death	Log/Snag Stage	Foliage	Bark	Sm. Branches	Med. Branches	Lrg. Branches	Wood
less than 5 years	1	20%	100%	90%	100%	100%	100%
Greater than 5 years	2	0%	70%	50%	100%	100%	100%
Greater than 5 years	3	0%	40%	30%	80%	90%	100%
Greater than 5 years	4	0%	20%	10%	50%	75%	90%
Greater than 5 years	5	0%	0%	0%	0%	20%	70%

Log/ Snag Stage	Description
1	bark tight and intact; branches and twigs present; cross section retains original shape; bole is ridged.
2	<= 50% of bark loose/ missing; primary branches missing; cross-section original shape; if down, bole may sag unless supported.
3	up to 75% bark missing or decayed; primary and secondary branches missing or broken; cross-section may be distorted from original shape; if down, bole is sagging or fully supported by ground.
4	more than 75% bark missing or decayed; most primary branches absent or broken; cross-section partially eroded and top may be broken; if down, bole is sagging or fully supported by the ground.
5	bark and all limbs absent or decayed; cross-section severely distorted or eroded from original shape; top possibly broken; if down, fully supported by the ground or merging with the soil layer (must be >50% sound).

Table 3:

The decay reduction factors for calculation of carbon in standing dead wood are shown. Carbon in standing dead wood was calculated with the same allometric equations used for live trees, then reduced by the appropriate percentage in this table (app. F, G). Descriptions of the visual cues used by FIA crews to determine the stage of decay are given in the second table.

		SORTED BY TOTAL CARBON			aggregate % of
Polygon Type	Total Carbon (Tg)	Aboveground Carbon (Tg)	Soil Carbon (Tg)	Total Area (ha)	total Tongass carbon
**38	679	163	516	1289432	23.8%
**32	335	48	287	441831	35.5%
**16	306	170	135	523046	46.2%
**14	274	126	148	543382	55.8%
**10	208	80	128	385205	63.1%
**2	194	24	170	532617	69.9%
**8	178	55	123	215790	76.1%
**12	146	69	78	303665	81.2%
**5	96	6	91	106557	84.6%
**18	80	37	42	134738	87.4%
**6	78	15	62	203628	90.1%
**4	60	3	56	212834	92.2%
**34	59	17	42	123554	94.3%
**23	46	16	30	122013	95.9%
4	33	33	0	904046	97.0%
**20	25	9	16	52443	97.9%
**24	12	5	7	21097	98.3%
**22	10	3	7	22724	98.7%
**3	6	0	6	18579	98.9%
**33	6	2	4	14598	99.1%
**36	5	2	3	9963	99.3%
**15	3	1	2	9980	99.4%
**21	2	1	1	5115	99.5%
5	2	2	0	9285	99.5%
**11	2	0	1	6716	99.6%
**7	2	0	1	2504	99.7%
**13	2	1	1	3689	99.7%
**9	2	1	1	3906	99.8%
1	1	1	0	70338	99.8%
**19	1	1	1	2560	99.9%
2	1	1	0	733844	99.9%
**37	1	0	1	1883	99.9%
**17	1	0	1	1604	100.0%
**31	1	0	1	902	100.0%
**35	0	0	0	721	100.0%
8	0	0	0	23346	100.0%
6	0	0	0	2616	100.0%
0	0	0	0	852	100.0%
**29	0	0	0	38	100.0%
**30	0	0	0	10	100.0%
3	0	0	0	4317906	100.0%
9	0	0	0	824421	100.0%
10.1	0	0	0	105711	100.0%
10.2	0	0	0	6360	100.0%
Sums	2855	892	1963	12316050	

Table 4:

Polygon types after simplification through elimination of delineation by soil category ("aboveground" polygon types), listed in order of decreasing total carbon stores. Ten polygon types (**38, **14, **2, **16, **32, **10, **12, **8, **4, **6) account for 86% of the total carbon stock in the Tongass. These polygon types represent large areas in the Tongass (table 5) and contain relatively high carbon concentrations (table 6).

SORTED BY TOTAL AREA					aggregate % of	Aggregate
Polygon Type	Total Carbon (Tg)	Aboveground Carbon (Tg)	Soil Carbon (Tg)	Total Area (ha)	total Tongass land area	percent of total area
3	0	0	0	4317906	Salt Water	35.1%
**38	679	163	516	1289432	18.5%	45.5%
4	33	33	0	904046	31.4%	52.9%
9	0	0	0	824421	Canada	59.6%
2	1	1	0	733844	41.9%	65.5%
**14	274	126	148	543382	49.7%	69.9%
**2	194	24	170	532617	57.3%	74.3%
**16	306	170	135	523046	64.8%	78.5%
**32	335	48	287	441831	71.2%	82.1%
**10	208	80	128	385205	76.7%	85.2%
**12	146	69	78	303665	81.0%	87.7%
**8	178	55	123	215790	84.1%	89.4%
**4	60	3	56	212834	87.2%	91.2%
**6	78	15	62	203628	90.1%	92.8%
**18	80	37	42	134738	92.0%	93.9%
**34	59	17	42	123554	93.8%	94.9%
**23	46	16	30	122013	95.5%	95.9%
**5	96	6	91	106557	97.1%	96.8%
10.1	0	0	0	105711	Water	97.6%
1	1	1	0	70338	Water	98.2%
**20	25	9	16	52443	97.8%	98.6%
8	0	0	0	23346	98.1%	98.8%
**22	10	3	7	22724	98.5%	99.0%
**24	12	5	7	21097	98.8%	99.2%
**3	6	0	6	18579	99.0%	99.3%
**33	6	2	4	14598	99.2%	99.4%
**15	3	1	2	9980	99.4%	99.5%
**36	5	2	3	9963	99.5%	99.6%
5	2	2	0	9285	Urban Land	99.7%
**11	2	0	1	6716	99.6%	99.7%
10.2	0	0	0	6360	Water	99.8%
**21	2	1	1	5115	99.7%	99.8%
**9	2	1	1	3906	99.8%	99.9%
**13	2	1	1	3689	99.8%	99.9%
6	0	0	0	2616	99.8%	99.9%
**19	1	1	1	2560	99.9%	99.9%
**7	2	0	1	2504	99.9%	100.0%
**37	1	0	1	1883	99.9%	100.0%
**17	1	0	1	1604	100.0%	100.0%
**31	1	0	1	902	100.0%	100.0%
0	0	0	0	852	100.0%	100.0%
**35	0	0	0	721	100.0%	100.0%
**29	0	0	0	38	100.0%	100.0%
**30	0	0	0	10	100.0%	100.0%
Sums	2855	892	1963	12316050		
		Total Tongass land area:		6982028	Hectares	
				17252969	Acres	

Table 5:

Polygon types after simplification through elimination of delineation by soil category ("aboveground" polygon types), listed in order of decreasing total area. Twelve polygon types (**38, 4, 2, **14, **2, **16, **32, **10, **12, **8, **4, **6) account for

over 90% of the total area in the Tongass. Two of these polygon types, 4 (un-vegitated rock and tallus) and 2 (glaciers), contain very little or no carbon. The remaining ten polygon types represent large percentages of the total carbon in the Tongass (table 4) and contain relatively high carbon concentrations (table 6). The total area of the Tongass is just less than 6 million hectares, or slightly more than 17 million acres.

Carbon density (Mg/ ha) by aboveground polygon type			
Sorted by aboveground carbon density			
Polygon type	Total (A.G. + Soil)	aboveground	Soil
**16	584	325	259
**18	593	278	315
**8	829	254	574
**14	505	232	273
**12	481	225	255
(**19)	(451)	(225)	(225)
(**36)	(548)	(219)	(328)
**24	509	215	294
(**13)	(427)	(211)	(215)
**10	540	208	331
(5)	(183)	(183)	(0)
**20	482	173	309
(**7)	(666)	(150)	(515)
**34	477	134	343
(**9)	(577)	(132)	(444)
**23	375	128	247
(**31)	(719)	(128)	(590)
**38	526	126	399
(**21)	(381)	(125)	(255)
**29	382	125	256
**33	425	125	299
(**35)	(344)	(125)	(218)
(**37)	(611)	(125)	(485)
**22	436	123	312
**30	310	108	202
**32	757	108	649
**6	381	75	306
(**15)	(261)	(62)	(199)
(**17)	(425)	(53)	(371)
**5	903	53	849
(**11)	(250)	(53)	(197)
**2	363	45	318
4	36	36	0
0	22	22	0
1	19	19	0
**4	279	15	263
(6)	(7)	(7)	(0)
**3	349	4	344
2	1	1	0
8	1	1	0
(3)	(0)	(0)	(0)
(9)	(0)	(0)	(0)
(10.1)	(0)	(0)	(0)
(10.2)	(0)	(0)	(0)

Table 6:

Polygon types after simplification through elimination of delineation by soil category ("aboveground" polygon types), listed in order of decreasing aboveground carbon density. Parentheses indicate that fewer than 4 FIA sample locations represent the polygon type. These polygon types tend to represent relatively small areas in the Tongass (table 5). The ten polygon types (**38, **14, **2, **16, **32, **10, **12, **8,

**4, **6) identified as representing both large areas (table 5) and large percentages of the total carbon stock in the Tongass (table 4) tend to contain relatively high carbon concentrations.

Tables 7 – 12 are in the sections “Flux Model One” and “Flux Model Two”

Flux Model One

Unique Assumptions:

1.) Carbon in pulpwood products is released to the atmosphere rapidly, either through decomposition or combustion
2.) Carbon in sawtimber products is released to the atmosphere through decomposition linearly over 50 years, beginning 100 years after harvest (average product lifespan = 125 years)
3.) Carbon in slash and stumps left on site after harvest is released to the atmosphere through decomposition linearly over 50 years
4.) Carbon in the extant downed woody debris pool prior to harvest decomposes to ½ of the original amount linearly over 50 years due to decreased input of material after harvest. This pool then increases to the original amount linearly over 200 years, beginning 50 years after harvest.

Figure 13:

Projections of carbon flux to and from the Tongass National Forest under siz potential management scenarios are shown. The total carbon stock in the Tongass in 1995 was estimated to be 2.83 Pg. Carbon flux from decomposing slash and stumps left on site after harvest and from decomposition of sawtimber products from previous harvests are included to convert estimates of changes in the carbon stock in the Tongass to estimates of the change in Tongass carbon stock that is exchanged with the atmosphere. The assumption of whether polynomial or asymptotic secondary growth rates more accureately describe the Tongass significantly influences the carbon flux projections, as does the value for standing aboveground carbon density after harvest used in the model. Panels A, B, E, and F show the results of model runs assuming polynomial carbon accretion in secondary growth. Panels C, D, G, and H show the results of model runs assuming asymptotic carbon accretion in secondary growth. Panels A-D show the results of model runs assuming carbon density in standing aboveground biomass after harvest equal to that in polygon type **23 (seedlings and saplings). Panels E-H show the results of model runs assuming carbon density in standing aboveground biomass after harvest equal to zero.

A (CD 1\excel models 5-5-01\final versions 1\flux graph poly B2)

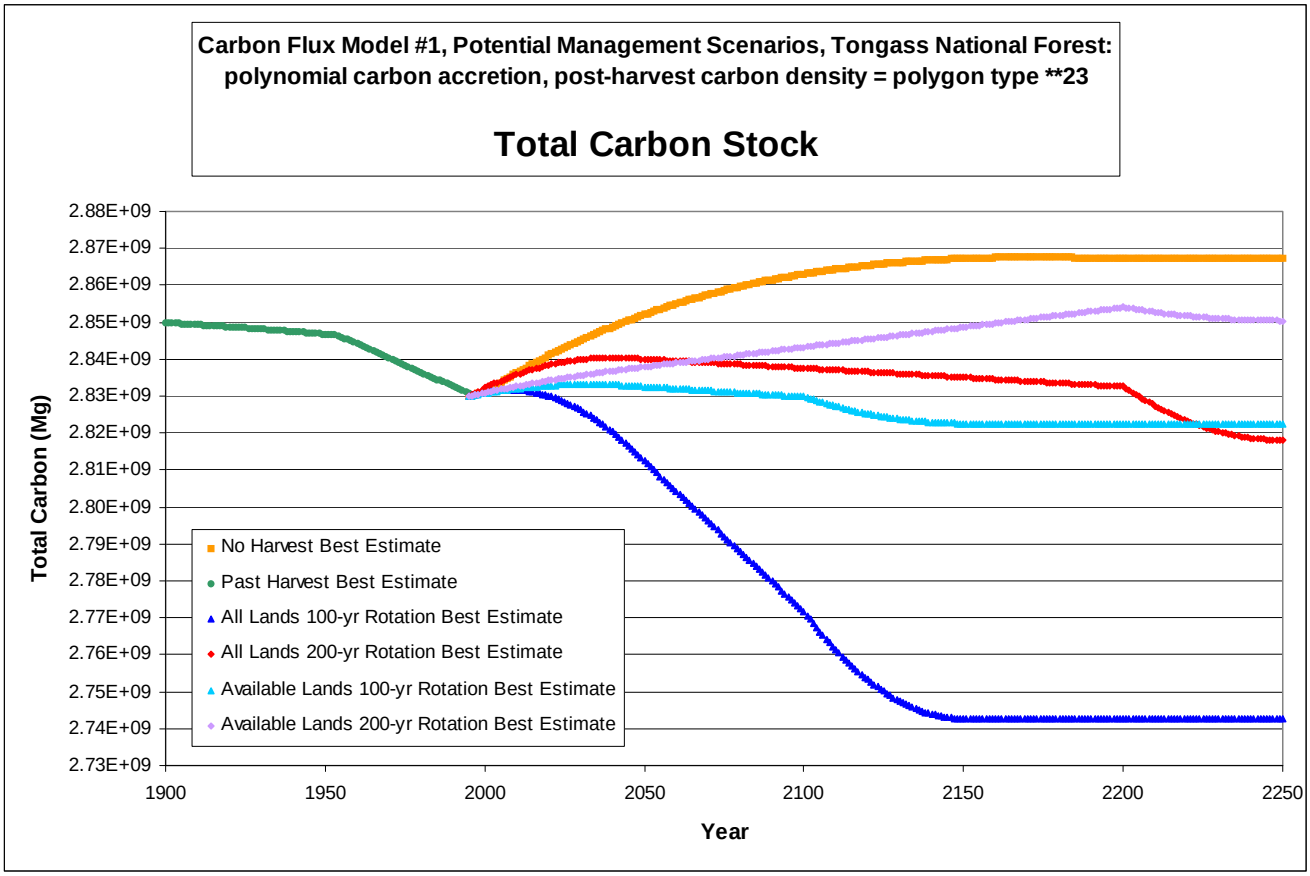

B (CD 1\excel models 5-5-01\final versions 1\flux graph poly B2)

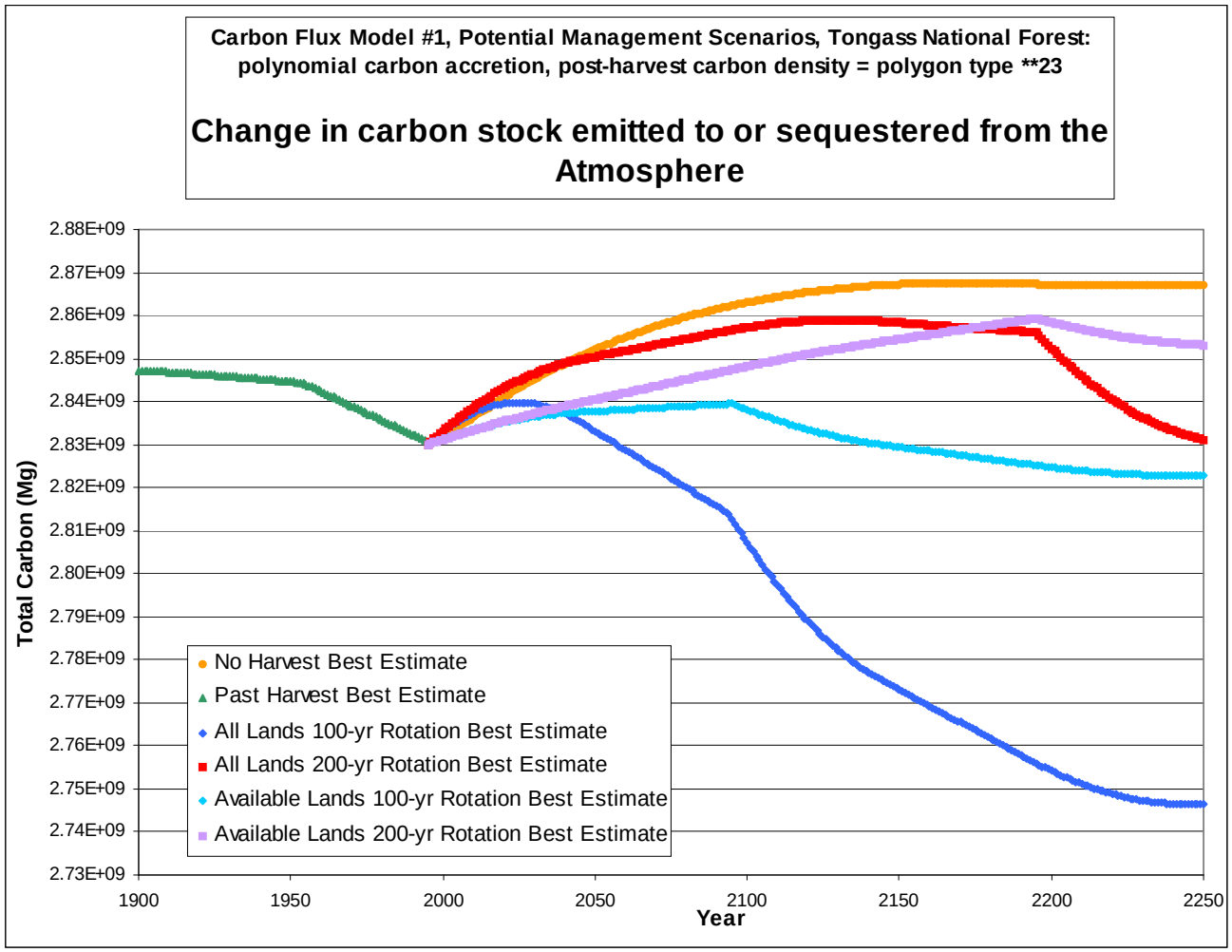

C (CD 1\excel models 5-5-01\final versions 1\ flux graph asym B2)

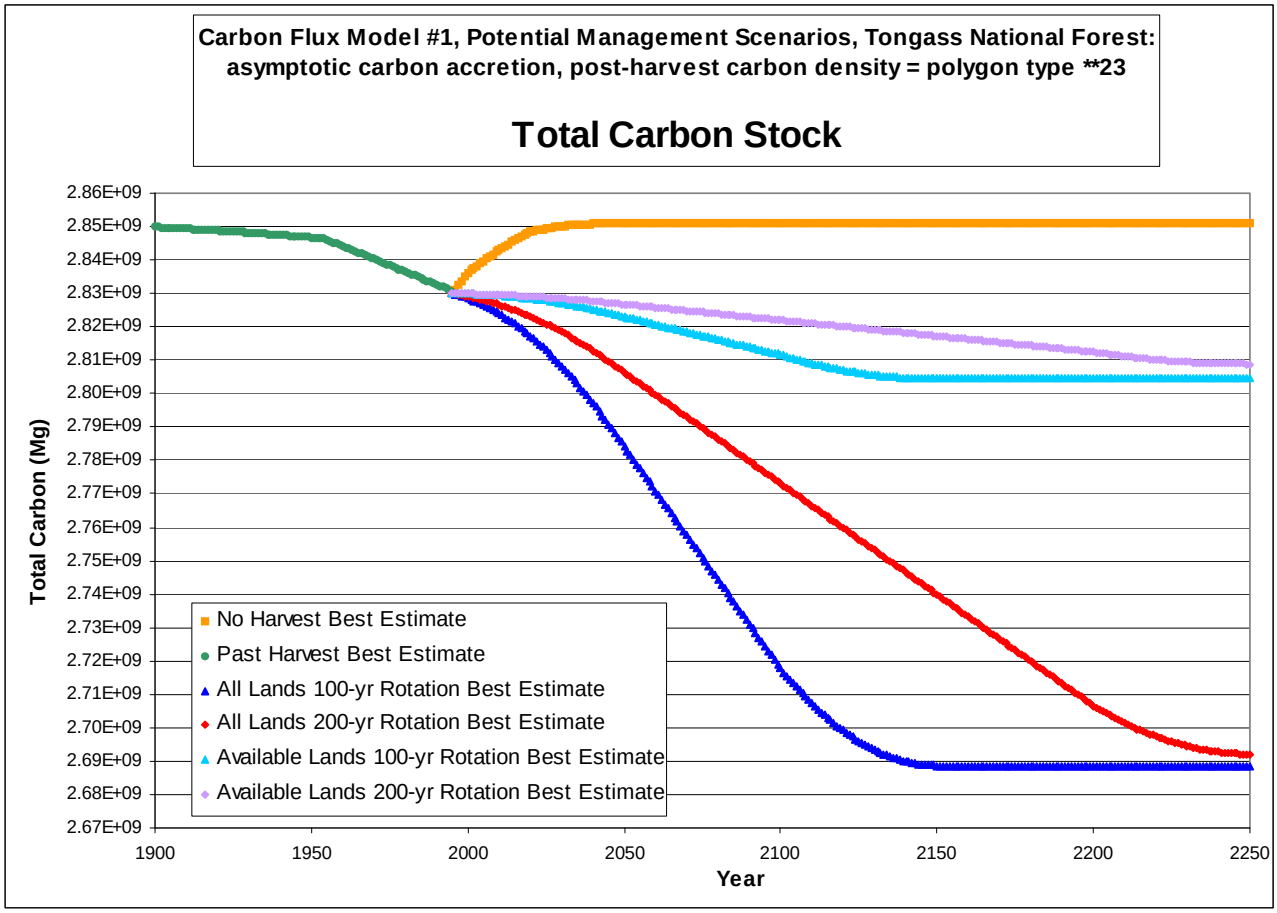

D (CD 1\excel models 5-5-01\final versions 1\ flux graph asym B2)

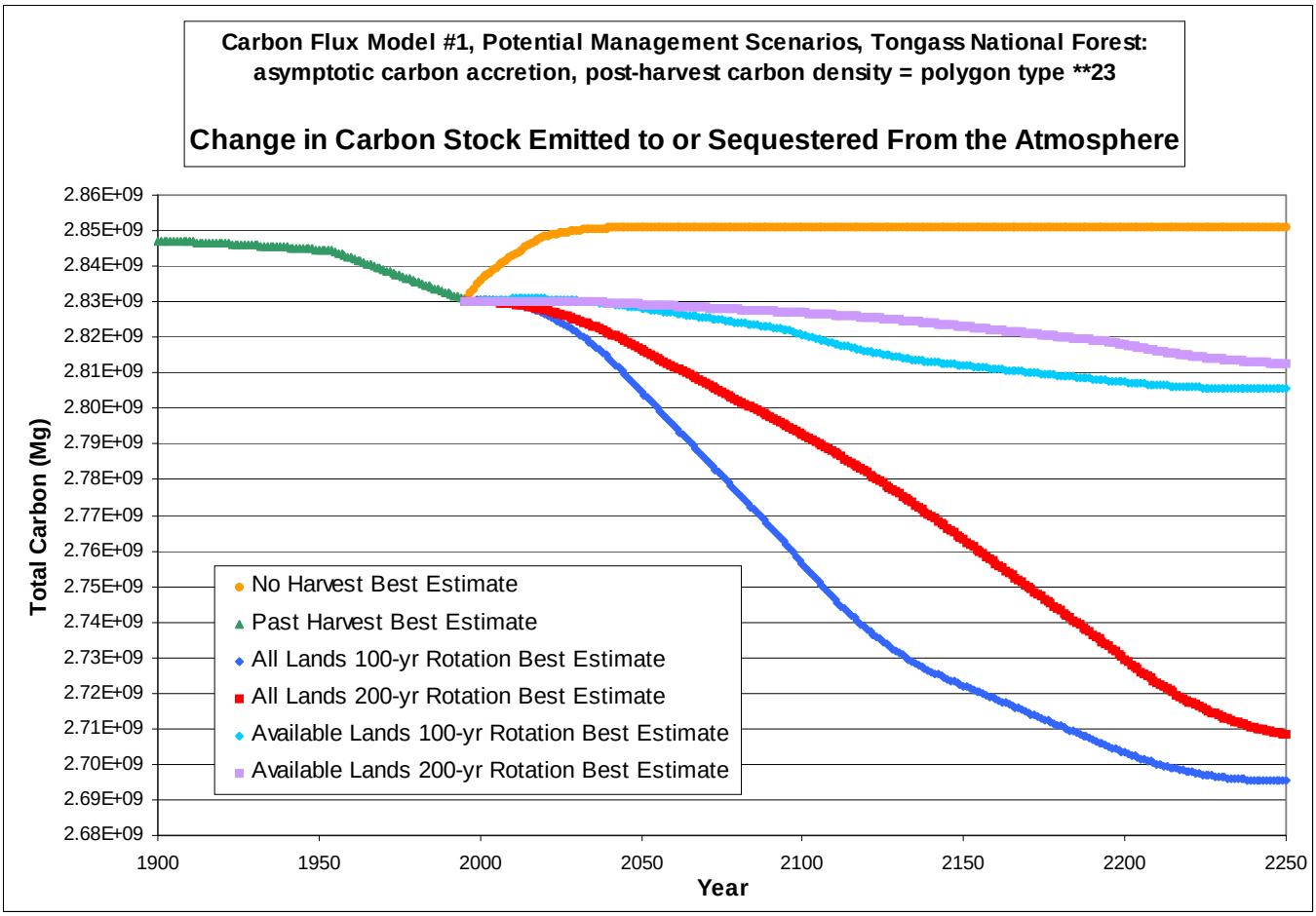

E (CD 1\excel models 5-5-01\final versions 1\ flux graph poly C2)

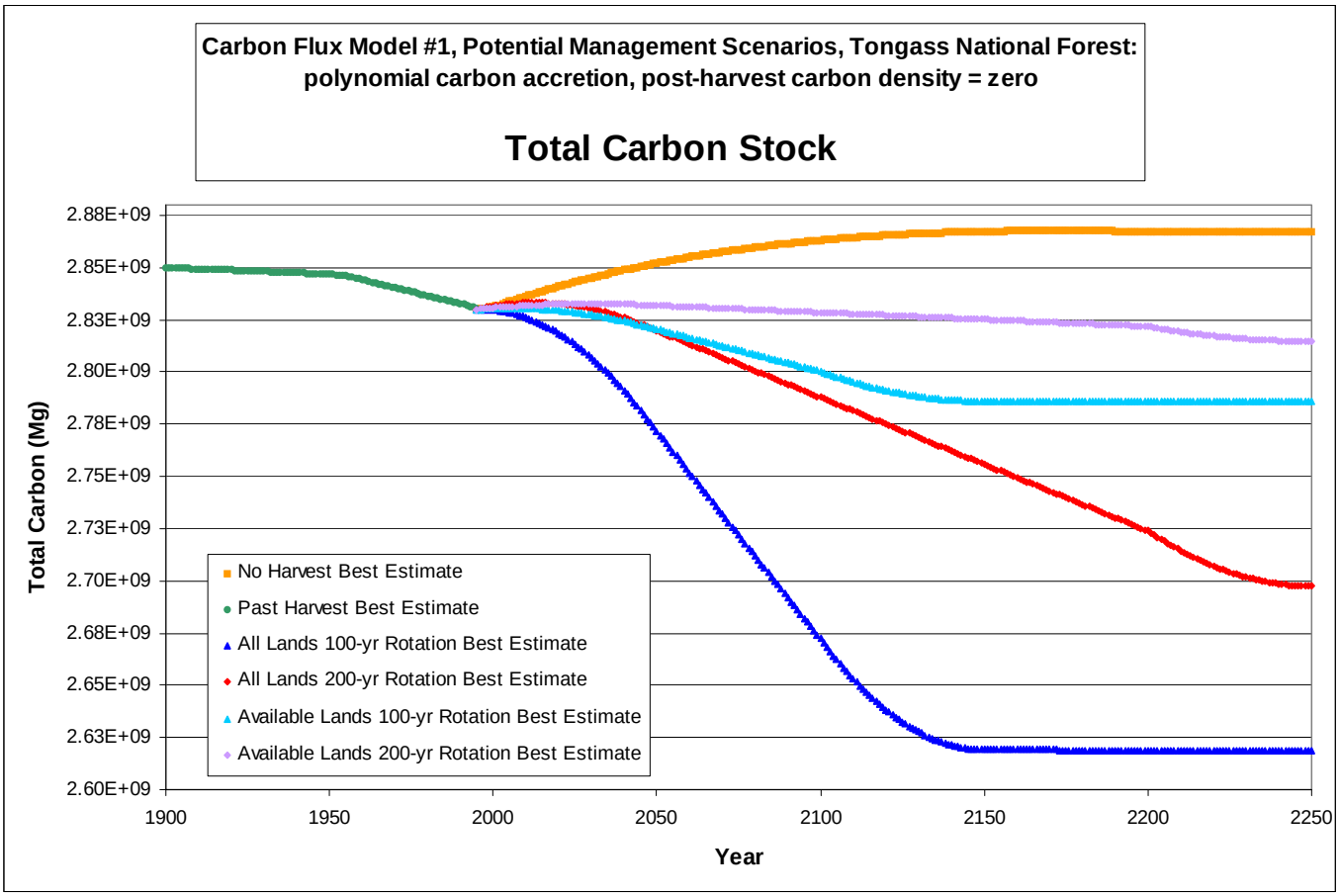

F (CD 1\excel models 5-5-01\final versions 1\ flux graph poly C2)

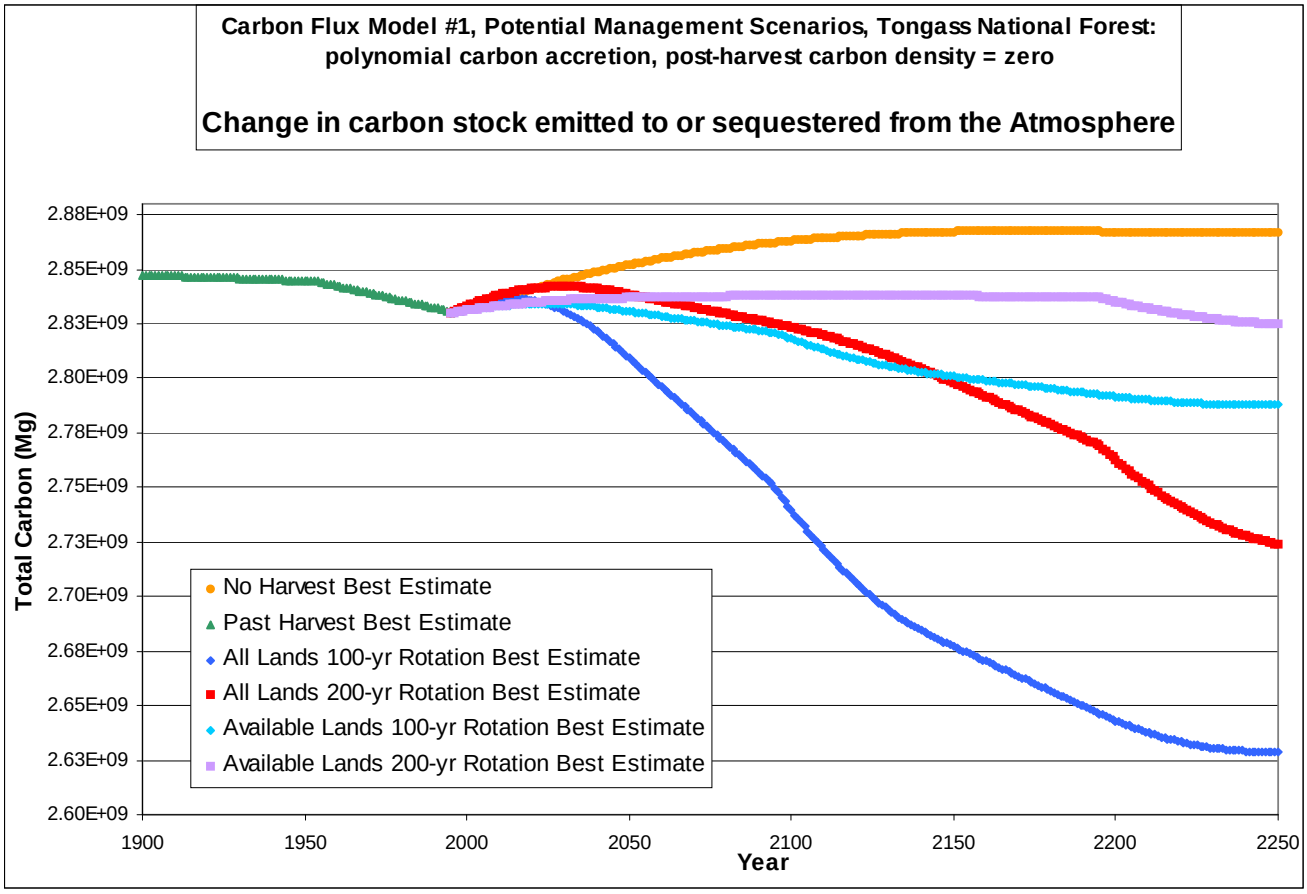

G (CD 1\excel models 5-5-01\final versions 1\flux graph asym C2)

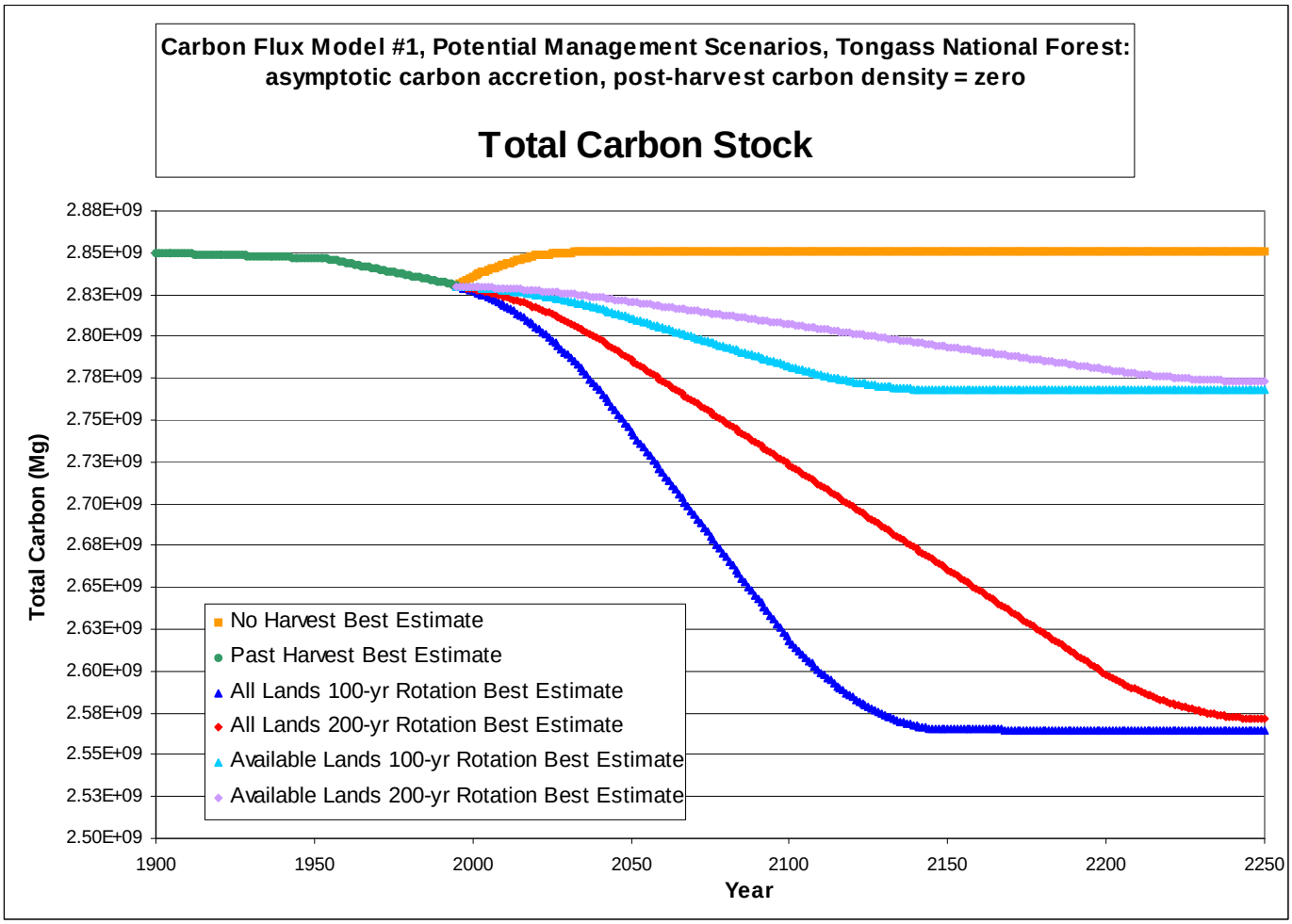

H (CD 1\excel models 5-5-01\final versions 1\flux graph asym C2)

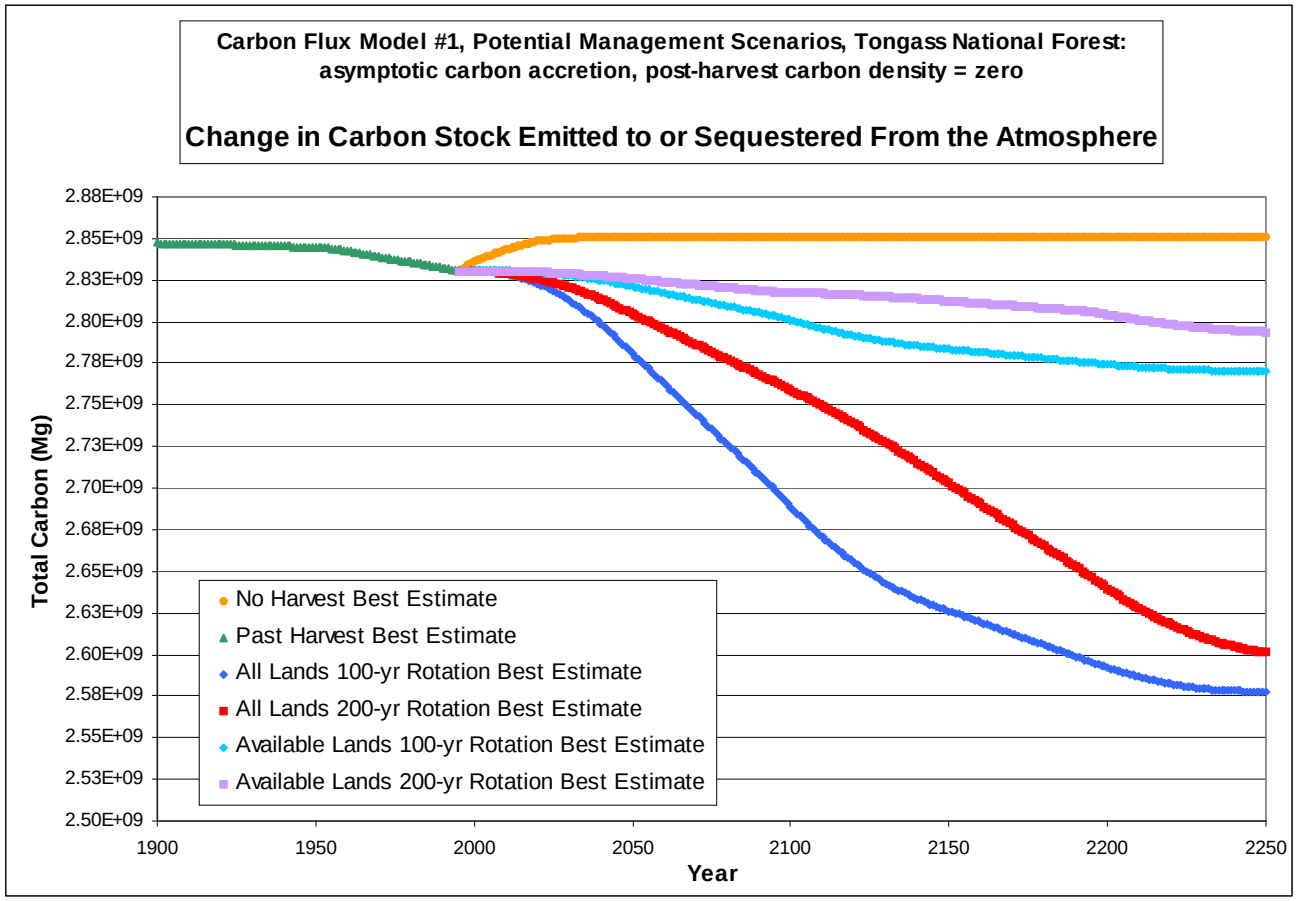

Average Annual Carbon Flux from the Tongass Forest							
(thousands of tons, annualized over 100 years)							
		C-density after harvest = polygon type **23			Carbon density after harvest = 0		
Management Scenario Modeled	Carbon Accretion Modeled	Upper bound	Best estimate	Lower bound	Upper bound	Best estimate	Lower bound
Cessation of	Polynomial Accretion	-404	-323	-221	-404	-323	-221
all harvest (#1)	Asymptotic Accretion	-288	-209	-107	-288	-209	-107
Past carbon	Polynomial Accretion	223	201	83	223	201	83
flux (#2)	Asymptotic Accretion	223	201	83	223	201	83
All forested lands managed	Polynomial Accretion	1025	542	143	1962	1479	1080
on a 100-yr rotation (#3)	Asymptotic Accretion	1678	1056	535	2615	1994	1472
All forested lands managed	Polynomial Accretion	67	-78	-193	535	390	276
on a 200-yr rotation (#4)	Asymptotic Accretion	847	536	276	1316	1005	744
Forested lands available for harvest	Polynomial Accretion	166	-1	-136	444	277	142
managed on a 100-yr rotation (#5)	Asymptotic Accretion	376	172	2	654	450	280
Forested lands available for harvest	Polynomial Accretion	-59	-127	-178	80	12	-39
managed on a 200-yr rotation (#6)	Asymptotic Accretion	188	75	-17	327	214	121

A

Average Annual Carbon Flux from the Tongass Forest							
(thousands of tons, annualized over 200 years)							
		C-density after harvest = polygon type **23			Carbon density after harvest = 0		
Management Scenario Modeled	Carbon Accretion Modeled	Upper bound	Best estimate	Lower bound	Upper bound	Best estimate	Lower bound
Cessation of	Polynomial Accretion	-232	-186	-130	-232	-186	-130
all harvest (#1)	Asymptotic Accretion	-144	-105	-53	-144	-105	-53
Past carbon	Polynomial Accretion	223	201	83	223	201	83
flux (#2)	Asymptotic Accretion	223	201	83	223	201	83
All forested lands managed	Polynomial Accretion	772	437	158	1390	1055	776
on a 100-yr rotation (#3)	Asymptotic Accretion	1115	707	364	1733	1325	982
All forested lands managed	Polynomial Accretion	170	-14	-162	698	515	366
on a 200-yr rotation (#4)	Asymptotic Accretion	950	600	306	1478	1129	835
Forested lands available for harvest	Polynomial Accretion	147	37	-54	331	220	129
managed on a 100-yr rotation (#5)	Asymptotic Accretion	258	128	18	441	311	201
Forested lands available for harvest	Polynomial Accretion	-38	-117	-178	119	39	-21
managed on a 200-yr rotation (#6)	Asymptotic Accretion	209	85	-17	365	242	139

B

Table 7:

Estimates of carbon flux to and from the Tongass associated with management scenarios were sensitive to the function chosen to represent carbon accretion in secondary growth (fig. 6), either polynomial or asymptotic. Carbon flux estimates were also sensitive to the carbon density in standing aboveground biomass used in each model run. Although the density in polygon type **23 (86 Mg/ ha) was the closest approximation available in polygon data, assuming a value of zero approximates the true value more closely. Upper and lower bounds incorporate the 95% confidence interval in carbon density estimates for each polygon type as well as the sensitivity

analyses performed for all major assumptions. Consequently, these bounds represent a generous confidence interval for the true value of carbon flux associated with each management policy. Negative numbers indicate carbon sequestration in the Tongass; positive numbers indicate carbon emissions from the Tongass. Carbon fluxes are in thousands of tons and were annualized over 100 years in panel A and 200 years in panel B.

Average Annual Carbon Flux to the Atmosphere (thousands of tons, annualized over 100 years)							
		C-density after harvest = polygon type **23			Carbon density after harvest = 0		
Management Scenario Modeled	Carbon Accretion Modeled	Upper bound	Best estimate	Lower bound	Upper bound	Best estimate	Lower bound
Cessation of	Polynomial Accretion	-404	-323	-221	-404	-323	-221
all harvest (#1)	Asymptotic Accretion	-288	-209	-107	-288	-209	-107
Past carbon	Polynomial Accretion	193	174	72	193	174	72
flux (#2)	Asymptotic Accretion	193	174	72	193	174	72
All forested lands managed	Polynomial Accretion	460	173	-58	1092	804	573
on a 100-yr rotation (#3)	Asymptotic Accretion	1107	682	330	1738	1314	962
All forested lands managed	Polynomial Accretion	-220	-266	-296	96	49	19
on a 200-yr rotation (#4)	Asymptotic Accretion	560	348	172	876	664	488
Forested lands available for harvest	Polynomial Accretion	17	-95	-180	204	92	7
managed on a 100-yr rotation (#5)	Asymptotic Accretion	227	78	-42	414	265	145
Forested lands available for harvest	Polynomial Accretion	-133	-174	-200	-40	-81	-107
managed on a 200-yr rotation (#6)	Asymptotic Accretion	113	28	-39	207	122	25

A

Average Annual Carbon Flux to the Atmosphere (thousands of tons, annualized over 200 years)							
		C-density after harvest = polygon type **23			Carbon density after harvest = 0		
Management Scenario Modeled	Carbon Accretion Modeled	Upper bound	Best estimate	Lower bound	Upper bound	Best estimate	Lower bound
Cessation of	Polynomial Accretion	-232	-186	-130	-232	-186	-130
all harvest (#1)	Asymptotic Accretion	-144	-105	-53	-144	-105	-53
Past carbon	Polynomial Accretion	193	174	72	193	174	72
flux (#2)	Asymptotic Accretion	193	174	72	193	174	72
All forested lands managed	Polynomial Accretion	663	370	126	1212	918	674
on a 100-yr rotation (#3)	Asymptotic Accretion	987	625	320	1535	1173	868
All forested lands managed	Polynomial Accretion	-8	-130	-226	426	304	208
on a 200-yr rotation (#4)	Asymptotic Accretion	773	484	242	1207	918	677
Forested lands available for harvest	Polynomial Accretion	123	24	-57	286	187	107
managed on a 100-yr rotation (#5)	Asymptotic Accretion	228	111	12	391	274	176
Forested lands available for harvest	Polynomial Accretion	-85	-147	-192	44	-35	-63
managed on a 200-yr rotation (#6)	Asymptotic Accretion	162	56	-31	291	120	83

B

Table 8:

Similar to table 7, decomposition of slash and stumps left on the harvest site and sawtimber products initially removed from the site were included to convert estimates of carbon flux from the forest to carbon flux to the atmosphere in management scenarios numbered 2-6 (fig. 7). Carbon fluxes are in thousands of tons and were annualized over 100 years in panel A and 200 years in panel B.

Average Annual Value of Carbon Flux to the Atmosphere (millions of dollars, annualized over 100 years)							
		C-density after harvest = polygon type **23			Carbon density after harvest = 0		
Management Scenario Modeled	Carbon Accretion Modeled	Upper bound	Best estimate	Lower bound	Upper bound	Best estimate	Lower bound
Cessation of	Polynomial Accretion	8.1	6.5	4.4	8.1	6.5	4.4
all harvest (#1)	Asymptotic Accretion	5.8	4.2	2.1	5.8	4.2	2.1
Past carbon	Polynomial Accretion	-3.9	-3.5	-1.4	-3.9	-3.5	-1.4
flux (#2)	Asymptotic Accretion	-3.9	-3.5	-1.4	-3.9	-3.5	-1.4
All forested lands managed	Polynomial Accretion	-9.2	-3.5	1.2	-21.8	-16.1	-11.5
on a 100-yr rotation (#3)	Asymptotic Accretion	-22.1	-13.6	-6.6	-34.8	-26.3	-19.2
All forested lands managed	Polynomial Accretion	4.4	5.3	5.9	-1.9	-1.0	-0.4
on a 200-yr rotation (#4)	Asymptotic Accretion	-11.2	-7.0	-3.4	-17.5	-13.3	-9.8
Forested lands available for harvest	Polynomial Accretion	-0.3	1.9	3.6	-4.1	-1.8	-0.1
managed on a 100-yr rotation (#5)	Asymptotic Accretion	-4.5	-1.6	0.8	-8.3	-5.3	-2.9
Forested lands available for harvest	Polynomial Accretion	2.7	3.5	4.0	0.8	1.6	2.1
managed on a 200-yr rotation (#6)	Asymptotic Accretion	-2.3	-0.6	0.8	-4.1	-2.4	-0.5

A

Average Annual Value of Carbon Flux to the Atmosphere (millions of dollars, annualized over 200 years)							
		C-density after harvest = polygon type **23			Carbon density after harvest = 0		
Management Scenario Modeled	Carbon Accretion Modeled	Upper bound	Best estimate	Lower bound	Upper bound	Best estimate	Lower bound
Cessation of	Polynomial Accretion	4.6	3.7	2.6	4.6	3.7	2.6
all harvest (#1)	Asymptotic Accretion	2.9	2.1	1.1	2.9	2.1	1.1
Past carbon	Polynomial Accretion	-3.9	-3.5	-1.4	-3.9	-3.5	-1.4
flux (#2)	Asymptotic Accretion	-3.9	-3.5	-1.4	-3.9	-3.5	-1.4
All forested lands managed	Polynomial Accretion	-13.3	-7.4	-2.5	-24.2	-18.4	-13.5
on a 100-yr rotation (#3)	Asymptotic Accretion	-19.7	-12.5	-6.4	-30.7	-23.5	-17.4
All forested lands managed	Polynomial Accretion	0.2	2.6	4.5	-8.5	-6.1	-4.2
on a 200-yr rotation (#4)	Asymptotic Accretion	-15.5	-9.7	-4.8	-24.1	-18.4	-13.5
Forested lands available for harvest	Polynomial Accretion	-2.5	-0.5	1.1	-5.7	-3.7	-2.1
managed on a 100-yr rotation (#5)	Asymptotic Accretion	-4.6	-2.2	-0.2	-7.8	-5.5	-3.5
Forested lands available for harvest	Polynomial Accretion	1.7	2.9	3.8	-0.9	0.7	1.3
managed on a 200-yr rotation (#6)	Asymptotic Accretion	-3.2	-1.1	0.6	-5.8	-2.4	-1.7

B

Table 9:

Carbon flux between the Tongass and the atmosphere (table 8) was converted to monetary units assuming a value of carbon equal to $20 per ton. Positive numbers represent potential revenue from the sale of carbon emission permits made possible by the carbon sequestration associated with the management policy modeled while negative numbers represent the cost of emission permit purchase for carbon emissions associated with the management policy modeled. The annual economic values of carbon fluxes are in millions of 1995 dollars and were annualized over 100 years in panel A and 200 years in panel B.

Polynomial Accretion:	Carbon density after harvest = polygon type **23	Carbon density after harvest = 0
Cessation of all Harvest =	$4.4 to $8.1 million	$4.4 to $8.1 million
100-year Rotation (all forested lands) =	$1.2 to -$9.2 million	-$11.5 to -$21.8 million
200-year Rotation (all forested lands) =	$5.9 to $4.4 million	-$0.4 to -$1.9 million
100-year Rotation (available forested lands) =	$3.6 to -$0.3 million	-$0.1 to -$4.1 million
200-year Rotation (available forested lands) =	$4.0 to $2.7 million	$2.1 to $0.8 million
Net annual carbon value for ceasing harvest =	-$1.5 to $17.3 million	**$2.3 to $29.9 million**

Asymptotic Accretion:	Carbon density after harvest = polygon type **23	Carbon density after harvest = 0
Cessation of all Harvest =	$2.1 to $5.8 million	$2.1 to $5.8 million
100-year Rotation (all forested lands) =	-$6.6 to -$22.1 million	-$19.2 to -$34.8 million
200-year Rotation (all forested lands) =	-$3.4 to -$11.2 million	-$9.8 to -$17.5 million
100-year Rotation (available forested lands) =	$0.8 to -$4.5 million	-$2.9 to -$8.3 million
200-year Rotation (available forested lands) =	$0.8 to -$2.3 million	-$0.5 to -$4.1 million
Net annual carbon value for ceasing harvest =	$1.3 to $27.9 million	**$2.6 to $40.6 million**

A: **annual value, 1995 - 2095**

Polynomial Accretion:	Carbon density after harvest = polygon type **23	Carbon density after harvest = 0
Cessation of all Harvest =	$2.6 to $4.6 million	$2.6 to $4.6 million
100-year Rotation (all forested lands) =	-$2.5 to -$13.3 million	-$13.5 to -$24.2 million
200-year Rotation (all forested lands) =	$4.5 to $0.2 million	-$4.2 to -$8.5 million
100-year Rotation (available forested lands) =	$1.1 to -$2.5 million	-$2.1 to -$5.7 million
200-year Rotation (available forested lands) =	$3.8 to $1.7 million	$1.3 to -$0.9 million
Net annual carbon value for ceasing harvest =	-$1.9 to $17.9 million	**$1.3 to $28.8 million**

Asymptotic Accretion:	Carbon density after harvest = polygon type **23	Carbon density after harvest = 0
Cessation of all Harvest =	$1.1 to $2.9 million	$1.1 to $2.9 million
100-year Rotation (all forested lands) =	-$6.4 to -$19.7 million	-$17.4 to -$30.7 million
200-year Rotation (all forested lands) =	-$4.8 to -$15.5 million	-$13.5 to -$24.1 million
100-year Rotation (available forested lands) =	-$0.2 to -$4.6 million	-$3.5 to -$7.8 million
200-year Rotation (available forested lands) =	$0.6 to -$3.2 million	-$1.7 to -$5.8 million
Net annual carbon value for ceasing harvest =	$0.5 to $22.6 million	**$2.8 to $33.6 million**

B: annual value, 1995 - 2195

Table 10:

The economic value of carbon flux associated with each potential management scenario modeled were calculated based on a value of carbon equal to $20 per ton. Although the density in polygon type **23 (86 Mg/ ha) was the closest approximation available in polygon data, assuming a value of zero approximates the true value more closely, as do estimates of the economic value of carbon flux calculated with this assumption. The range of economic value in carbon flux associated with each management scenario represents the upper and lower bounds in carbon flux estimates, which incorporate the 95% confidence interval in carbon density estimates for each polygon type as well as the sensitivity analyses performed for all major assumptions.

Consequently, these ranges in economic value represent generous confidence intervals for the true value of carbon flux associated with each management policy. Furthermore, the net annual value of carbon sequestered from ceasing harvest depends on which of the other scenarios is deemed "business-as-usual" in the allocation of Certified Emissions Reduction credits (CERs). Business-as-usual was defined so as to give the largest range in net annual value of carbon flux. The annual economic values of carbon fluxes are in millions of 1995 dollars and were annualized over 100 years in panel A and 200 years in panel B.

Average Annual Value of Carbon Flux to the Atmosphere (millions of dollars, annualized over 100 years)							
		C-density after harvest = polygon type **23			Carbon density after harvest = 0		
Management Scenario Modeled	Carbon Accretion Modeled	Upper bound	Best estimate	Lower bound	Upper bound	Best estimate	Lower bound
Cessation of	Polynomial Accretion	7.0	5.6	3.8	7.0	5.6	3.8
all harvest (#1)	Asymptotic Accretion	5.0	3.6	1.9	5.0	3.6	1.9
Past carbon	Polynomial Accretion	-3.9	-3.5	-1.4	-3.9	-3.5	-1.4
flux (#2)	Asymptotic Accretion	-3.9	-3.5	-1.4	-3.9	-3.5	-1.4
All forested lands managed	Polynomial Accretion	-9.2	-3.5	1.2	-21.8	-16.1	-11.5
on a 100-yr rotation (#3)	Asymptotic Accretion	-22.1	-13.6	-6.6	-34.8	-26.3	-19.2
All forested lands managed	Polynomial Accretion	4.4	5.3	5.9	-1.9	-1.0	-0.4
on a 200-yr rotation (#4)	Asymptotic Accretion	-11.2	-7.0	-3.4	-17.5	-13.3	-9.8
Forested lands available for harvest	Polynomial Accretion	-0.3	1.9	3.6	-4.1	-1.8	-0.1
managed on a 100-yr rotation (#5)	Asymptotic Accretion	-4.5	-1.6	0.8	-8.3	-5.3	-2.9
Forested lands available for harvest	Polynomial Accretion	2.7	3.5	4.0	0.8	1.6	2.1
managed on a 200-yr rotation (#6)	Asymptotic Accretion	-2.3	-0.6	0.8	-4.1	-2.4	-0.5

A

Average Annual Value of Carbon Flux to the Atmosphere (millions of dollars, annualized over 200 years)							
		C-density after harvest = polygon type **23			Carbon density after harvest = 0		
Management Scenario Modeled	Carbon Accretion Modeled	Upper bound	Best estimate	Lower bound	Upper bound	Best estimate	Lower bound
Cessation of	Polynomial Accretion	4.0	3.2	2.3	4.0	3.2	2.3
all harvest (#1)	Asymptotic Accretion	2.5	1.8	0.9	2.5	1.8	0.9
Past carbon	Polynomial Accretion	-3.9	-3.5	-1.4	-3.9	-3.5	-1.4
flux (#2)	Asymptotic Accretion	-3.9	-3.5	-1.4	-3.9	-3.5	-1.4
All forested lands managed	Polynomial Accretion	-13.3	-7.4	-2.5	-24.2	-18.4	-13.5
on a 100-yr rotation (#3)	Asymptotic Accretion	-19.7	-12.5	-6.4	-30.7	-23.5	-17.4
All forested lands managed	Polynomial Accretion	0.2	2.6	4.5	-8.5	-6.1	-4.2
on a 200-yr rotation (#4)	Asymptotic Accretion	-15.5	-9.7	-4.8	-24.1	-18.4	-13.5
Forested lands available for harvest	Polynomial Accretion	-2.5	-0.5	1.1	-5.7	-3.7	-2.1
managed on a 100-yr rotation (#5)	Asymptotic Accretion	-4.6	-2.2	-0.2	-7.8	-5.5	-3.5
Forested lands available for harvest	Polynomial Accretion	1.7	2.9	3.8	-0.9	0.7	1.3
managed on a 200-yr rotation (#6)	Asymptotic Accretion	-3.2	-1.1	0.6	-5.8	-2.4	-1.7

B

Table 11:

Similar to table 9, estimates of the monetary value of carbon sequestration with cessation of all harvest were calculated based on 87% of the total carbon sequestration to account for the potential reduction in Certified Emission Reduction credit (CER) allocation for this management policy due to leakage as a result of elimination of long-term carbon storage in forest products. The annual economic values of carbon fluxes are in millions of 1995 dollars and were annualized over 100 years in panel A and 200 years in panel B.

Polynomial Accretion:	Carbon density after harvest = polygon type **23	Carbon density after harvest = 0
Cessation of all Harvest =	$3.8 to $7.0 million	$3.8 to $7.0 million
100-year Rotation (all forested lands) =	$1.2 to -$9.2 million	-$11.5 to -$21.8 million
200-year Rotation (all forested lands) =	$5.9 to $4.4 million	-$0.4 to -$1.9 million
100-year Rotation (available forested lands) =	$3.6 to -$0.3 million	-$0.1 to -$4.1 million
200-year Rotation (available forested lands) =	$4.0 to $2.7 million	$2.1 to $0.8 million
Net annual carbon value for ceasing harvest =	-$2.1 to $16.2 million	**$1.7 to $28.8 million**

Asymptotic Accretion:	Carbon density after harvest = polygon type **23	Carbon density after harvest = 0
Cessation of all Harvest =	$1.9 to $5.0 million	$1.9 to $5.0 million
100-year Rotation (all forested lands) =	-$6.6 to -$22.1 million	-$19.2 to -$34.8 million
200-year Rotation (all forested lands) =	-$3.4 to -$11.2 million	-$9.8 to -$17.5 million
100-year Rotation (available forested lands) =	$0.8 to -$4.5 million	-$2.9 to -$8.3 million
200-year Rotation (available forested lands) =	$0.8 to -$2.3 million	-$0.5 to -$4.1 million
Net annual carbon value for ceasing harvest =	$1.1 to $27.1 million	**$2.4 to $39.8 million**

A: **annual value, 1995 - 2095**

Polynomial Accretion:	Carbon density after harvest = polygon type **23	Carbon density after harvest = 0
Cessation of all Harvest =	$2.3 to $4.0 million	$2.3 to $4.0 million
100-year Rotation (all forested lands) =	-$2.5 to -$13.3 million	-$13.5 to -$24.2 million
200-year Rotation (all forested lands) =	$4.5 to $0.2 million	-$4.2 to -$8.5 million
100-year Rotation (available forested lands) =	$1.1 to -$2.5 million	-$2.1 to -$5.7 million
200-year Rotation (available forested lands) =	$3.8 to $1.7 million	$1.3 to -$0.9 million
Net annual carbon value for ceasing harvest =	-$2.2 to $17.3 million	**$1.0 to $28.2 million**

Asymptotic Accretion:	Carbon density after harvest = polygon type **23	Carbon density after harvest = 0
Cessation of all Harvest =	$0.9 to $2.5 million	$0.9 to $2.5 million
100-year Rotation (all forested lands) =	-$6.4 to -$19.7 million	-$17.4 to -$30.7 million
200-year Rotation (all forested lands) =	-$4.8 to -$15.5 million	-$13.5 to -$24.1 million
100-year Rotation (available forested lands) =	-$0.2 to -$4.6 million	-$3.5 to -$7.8 million
200-year Rotation (available forested lands) =	$0.6 to -$3.2 million	-$1.7 to -$5.8 million
Net annual carbon value for ceasing harvest =	$0.3 to $22.2 million	**$2.6 to $33.2 million**

B: annual value, 1995 - 2195

Table 12:

Similar to table 10, this table shows the economic value of carbon flux associated with each potential management scenario modeled, calculated based on a value of carbon equal to $20 per ton. However, this table assumes a 13% reduction in carbon sequestration credited for cessation of all harvest in the allocation of Certified Emissions Reduction credits CERs due to leakage as a result of elimination of long-term storage in wood products. The annual economic values of carbon fluxes are in millions of 1995 dollars and were annualized over 100 years in panel A and 200 years in panel B.

Flux Model Two

Unique Assumptions:

5.) Carbon in pulpwood products is released to the atmosphere linearly over 50 years, either through decomposition or combustion
6.) Carbon in sawtimber products is released to the atmosphere through decomposition linearly over 50 years, beginning 50 years after harvest (average product lifespan = 75 years)
7.) Carbon in slash and stumps left on site after harvest is released to the atmosphere through decomposition linearly over 100 years
8.) Carbon in the extant downed woody debris pool prior to harvest decomposes to ½ of the original amount linearly over 50 years due to decreased input of material after harvest. This pool then increases to the original amount linearly over 200 years, beginning 50 years after harvest.

Figure 13:

Projections of carbon flux to and from the Tongass National Forest under six potential management scenarios are shown. The total carbon stock in the Tongass in 1995 was estimated to be 2.83 Pg. Carbon flux from decomposing slash and stumps left on site after harvest and from decomposition of sawtimber products from previous harvests are included to convert estimates of changes in the carbon stock in the Tongass to estimates of the change in Tongass carbon stock that is exchanged with the atmosphere. The assumption of whether polynomial or asymptotic secondary growth rates more accurately describe the Tongass significantly influences the carbon flux projections, as does the value for standing aboveground carbon density after harvest used in the model. Panels A, B, E, and F show the results of model runs assuming polynomial carbon accretion in secondary growth. Panels C, D, G, and H show the results of model runs assuming asymptotic carbon accretion in secondary growth. Panels A-D show the results of model runs assuming carbon density in standing aboveground biomass after harvest equal to that in polygon type **23 (seedlings and saplings). Panels E-H show the results of model runs assuming carbon density in standing aboveground biomass after harvest equal to zero.

A (CD 1\excel models 5-5-01\final versions 1\flux graph poly B2)

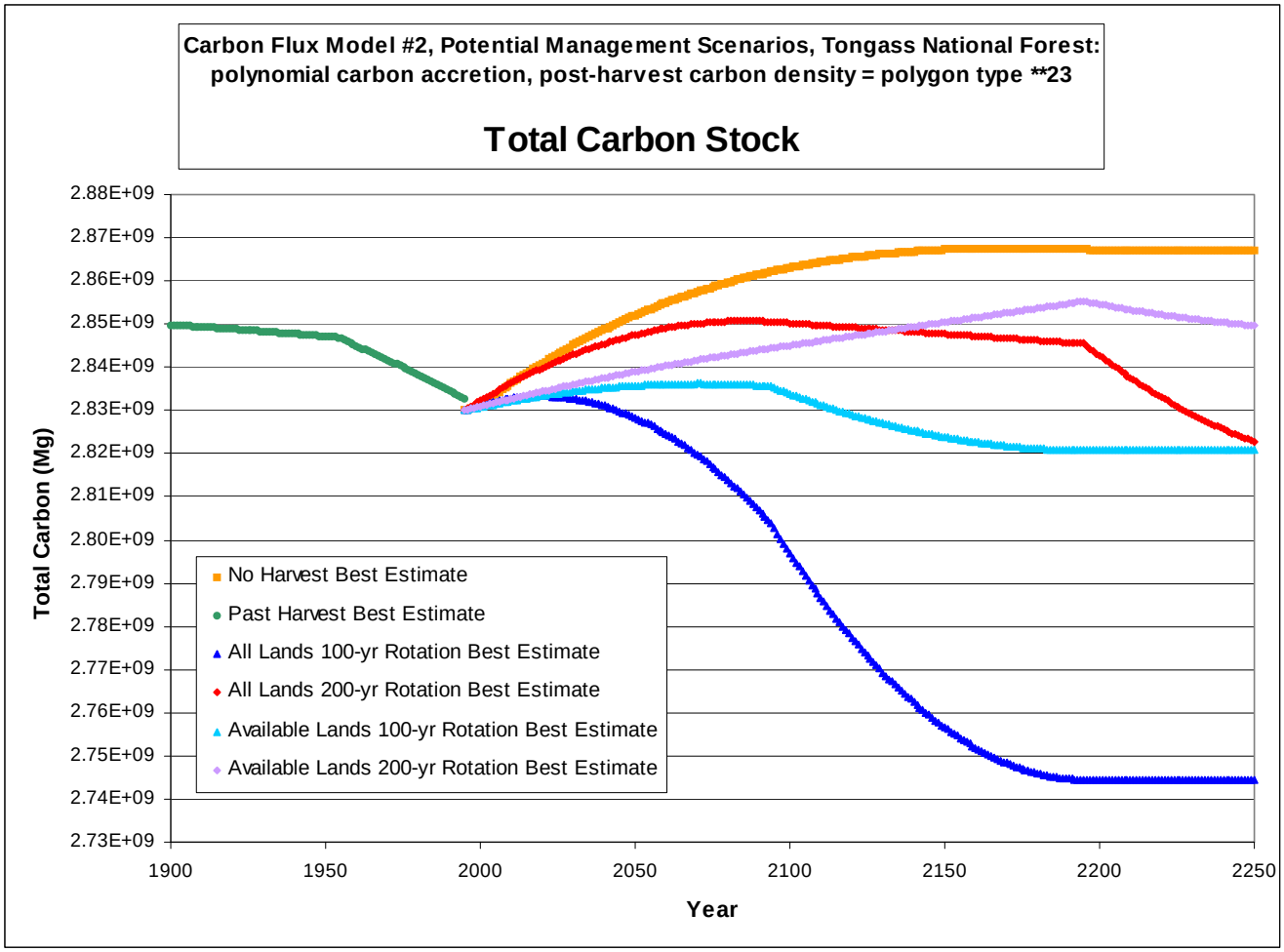

B (CD 1\excel models 5-5-01\final versions 1\flux graph poly B2)

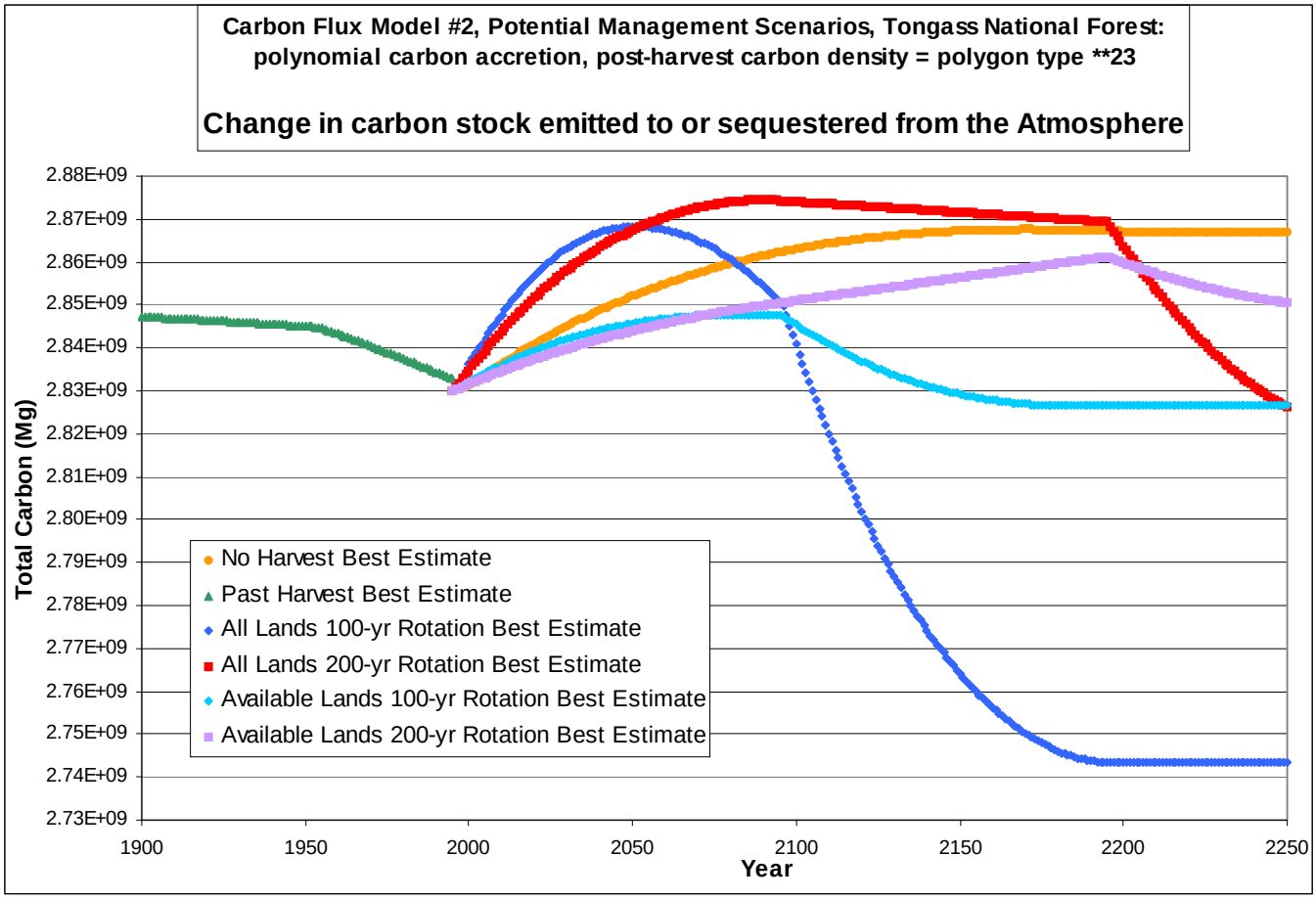

C (CD 1\excel models 5-5-01\final versions 1\ flux graph asym B2)

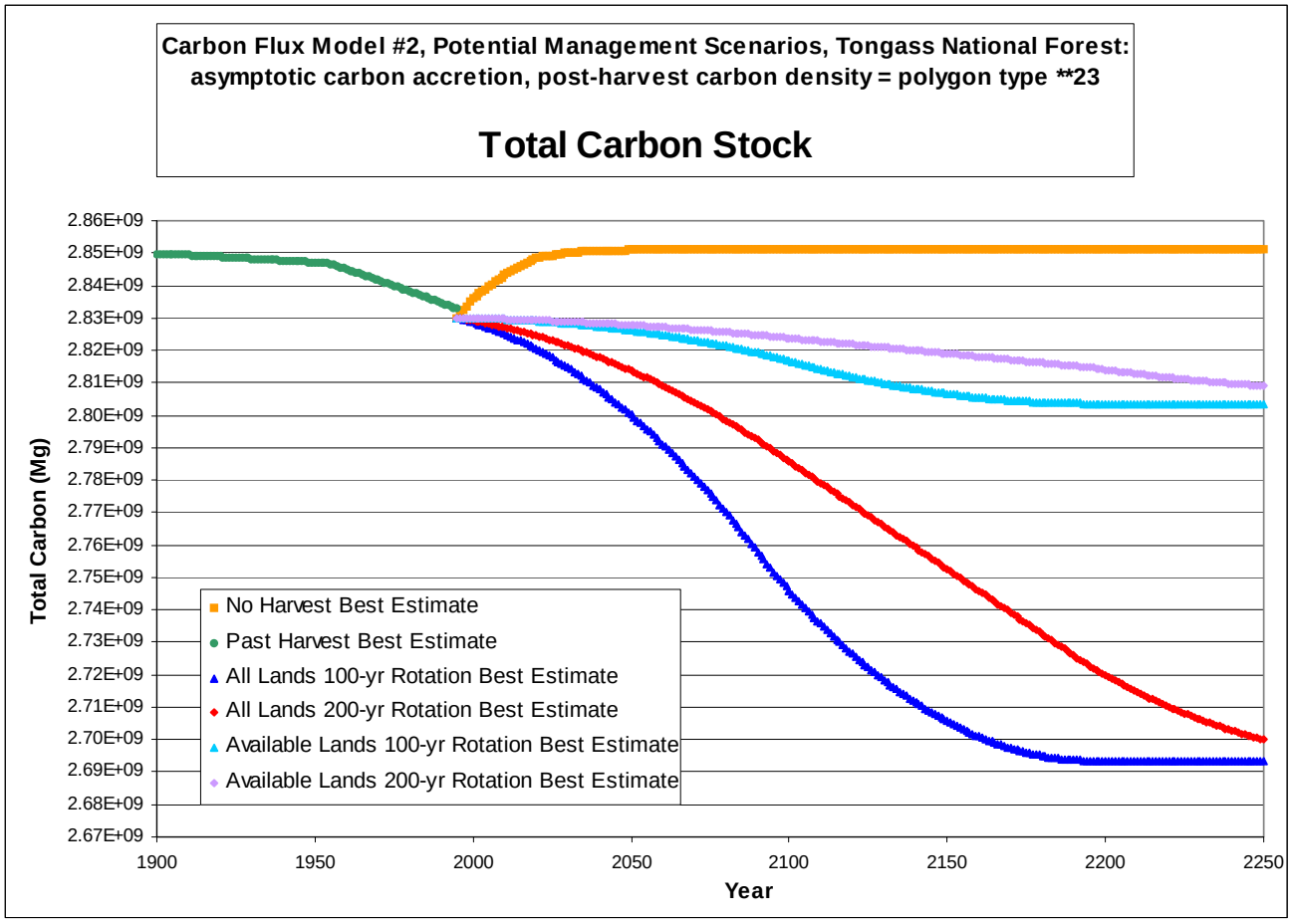

D (CD 1\excel models 5-5-01\final versions 1\ flux graph asym B2)

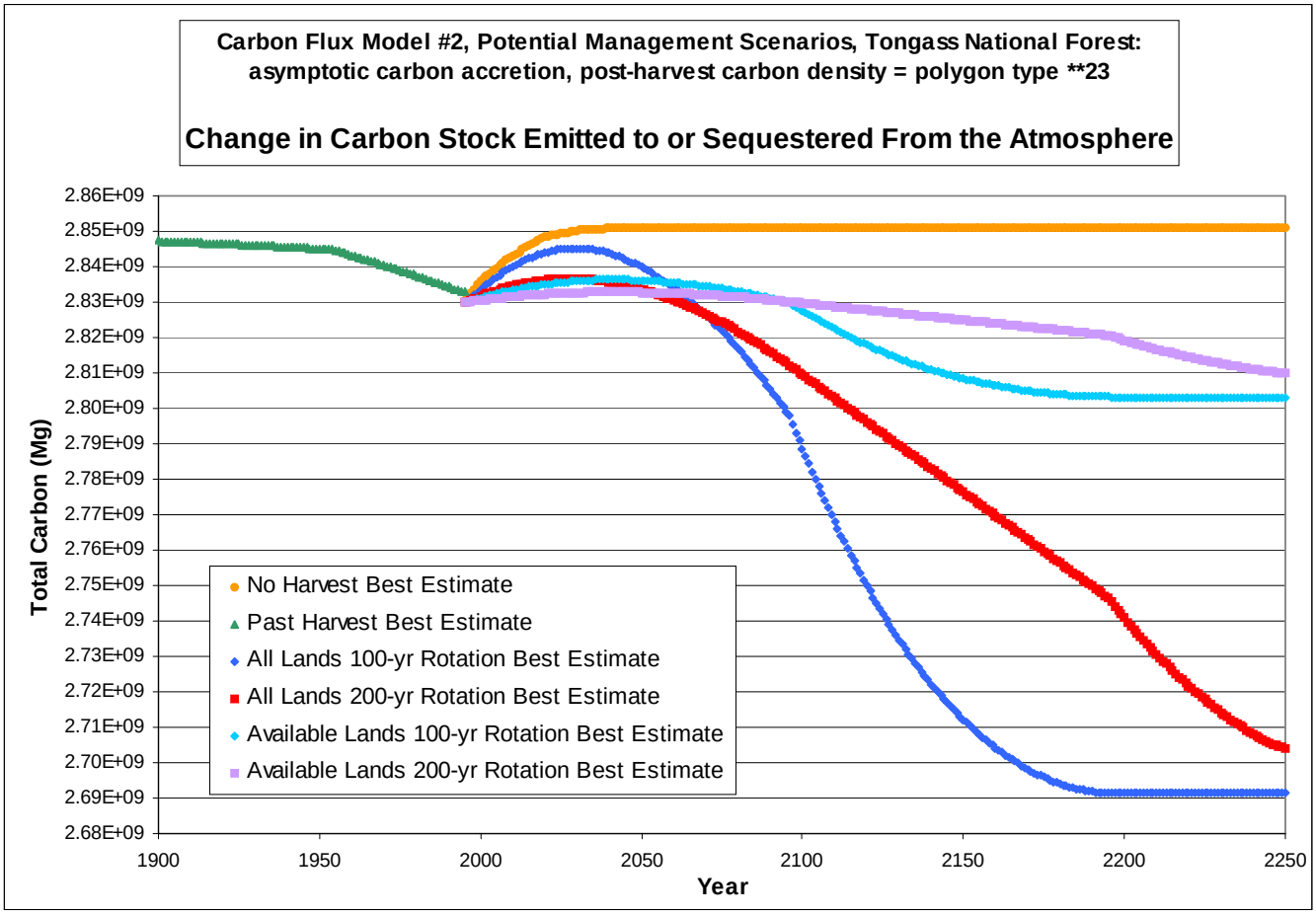

E (CD 1\excel models 5-5-01\final versions 1\ flux graph poly C2)

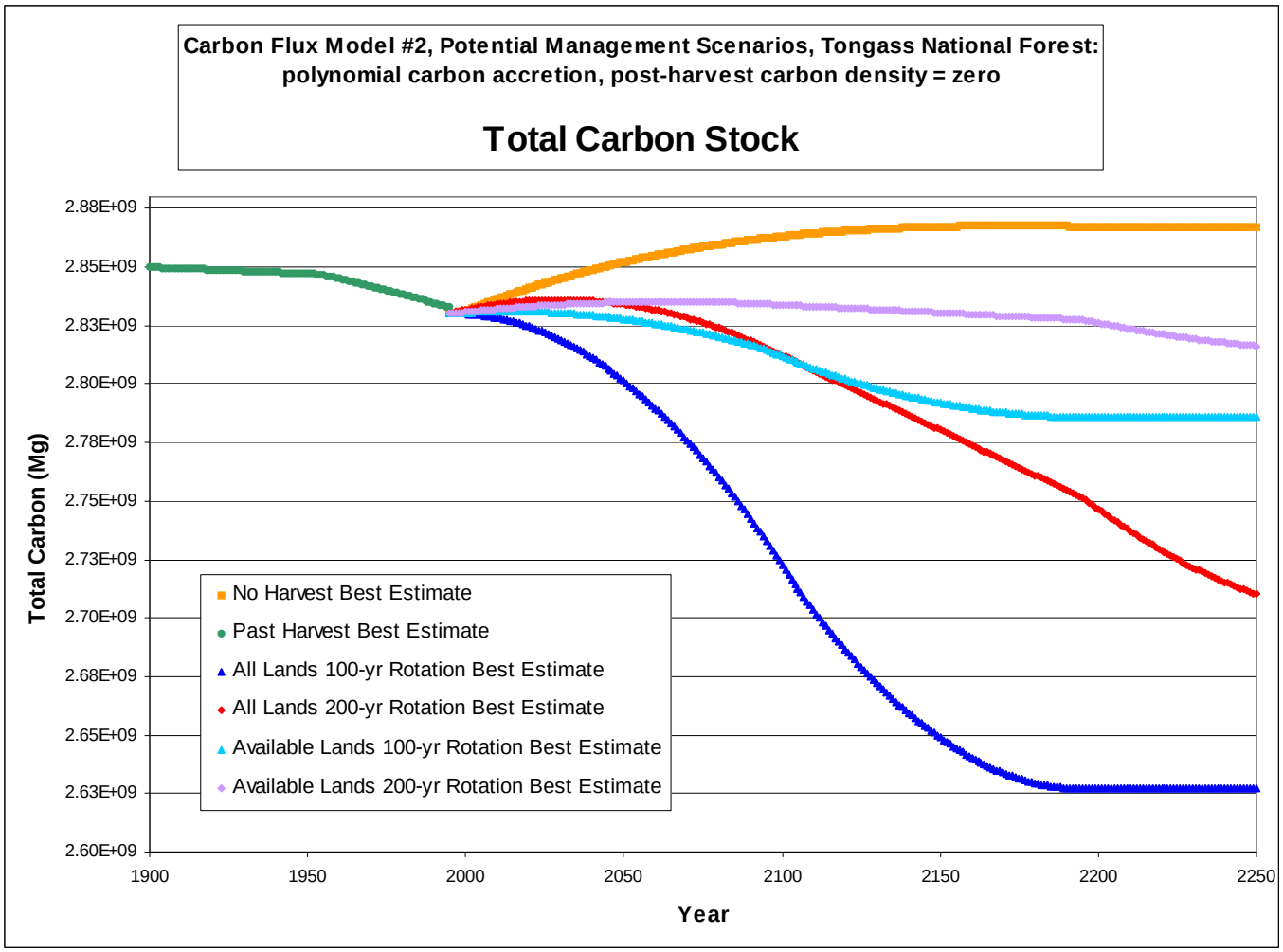

F (CD 1\excel models 5-5-01\final versions 1\ flux graph poly C2)

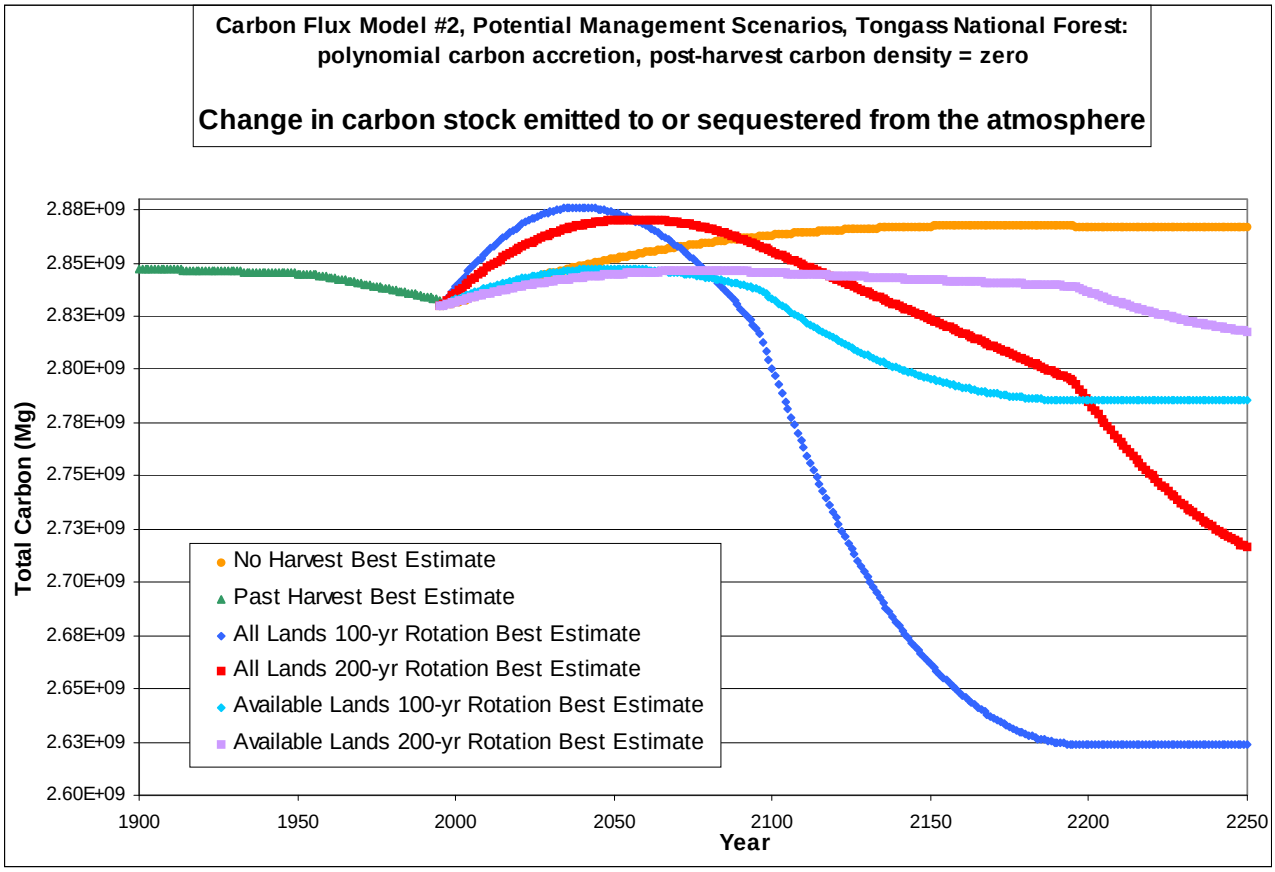

G (CD 1\excel models 5-5-01\final versions 1\flux graph asym C2)

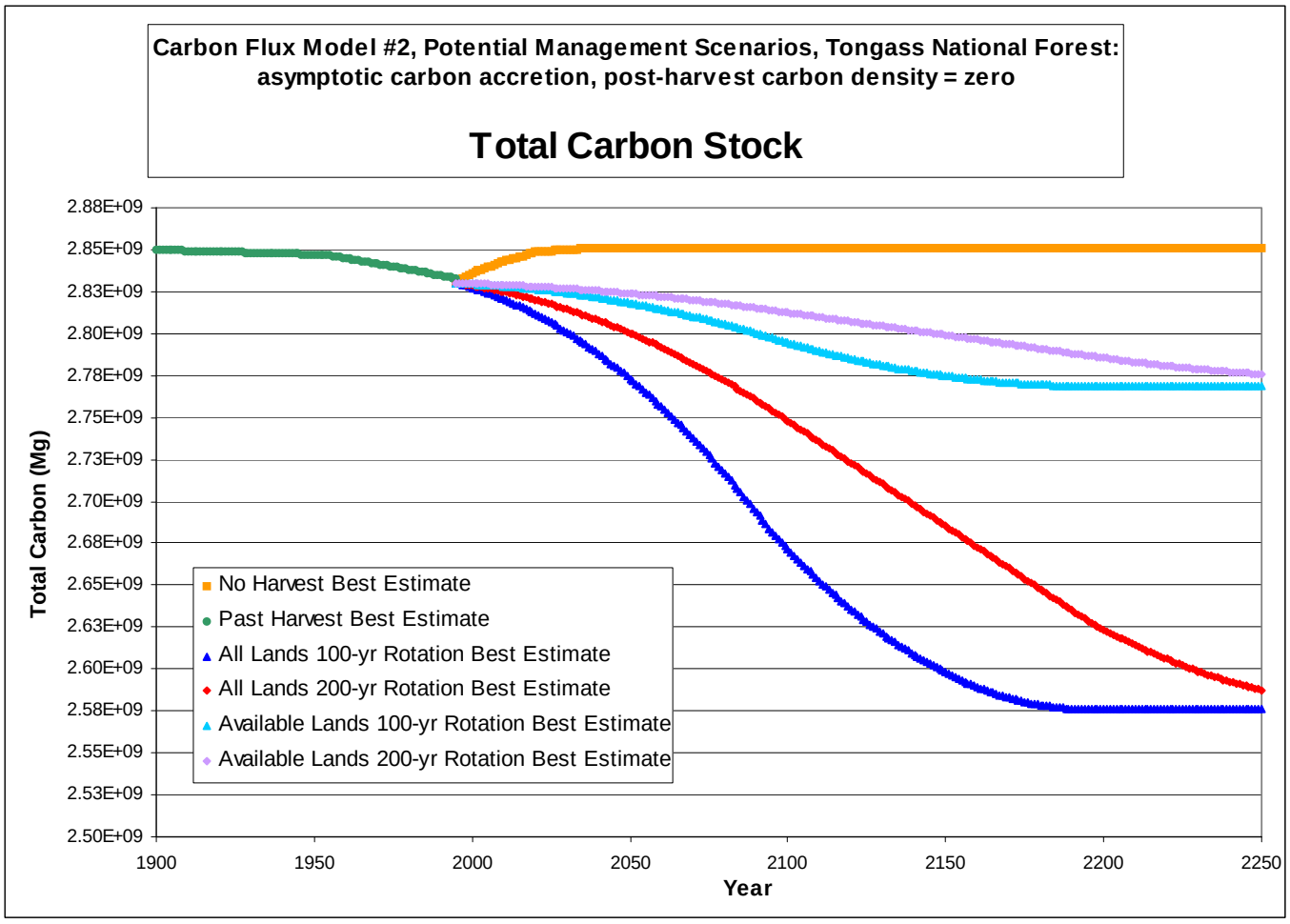

H (CD 1\excel models 5-5-01\final versions 1\flux graph asym C2)

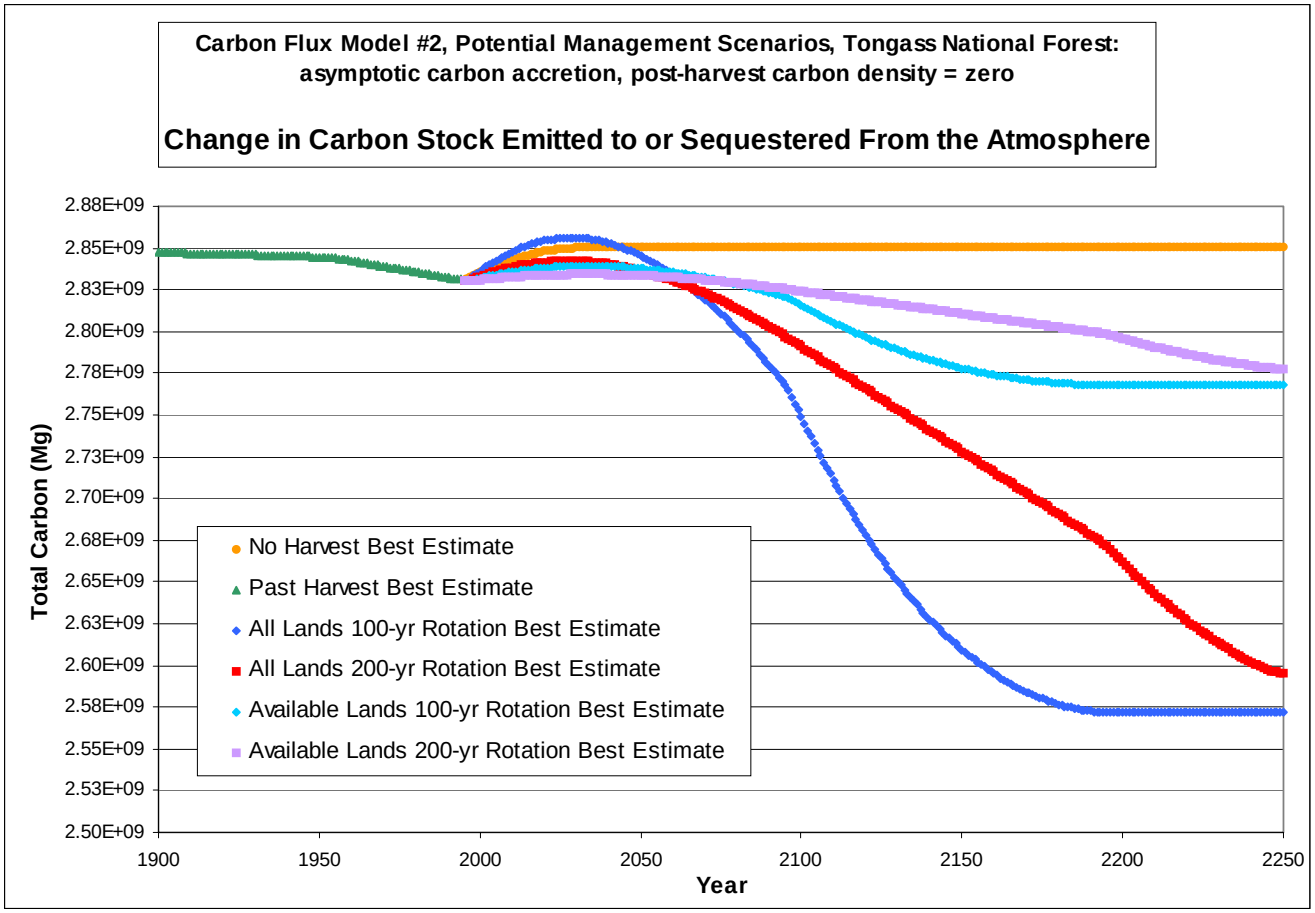

Average Annual Carbon Flux from the Tongass Forest							
(thousands of tons, annualized over 100 years)							
		C-density after harvest = polygon type **23			Carbon density after harvest = 0		
Management Scenario Modeled	Carbon Accretion Modeled	Upper bound	Best estimate	Lower bound	Upper bound	Best estimate	Lower bound
Cessation of	Polynomial Accretion	-404	-323	-221	-404	-323	-221
all harvest (#1)	Asymptotic Accretion	-288	-209	-107	-288	-209	-107
Past carbon	Polynomial Accretion	199	180	74	199	180	74
flux (#2)	Asymptotic Accretion	199	180	74	199	180	74
All forested lands managed	Polynomial Accretion	605	274	5	1304	973	705
on a 100-yr rotation (#3)	Asymptotic Accretion	1252	783	394	1951	1483	1093
All forested lands managed	Polynomial Accretion	-135	-205	-254	215	146	97
on a 200-yr rotation (#4)	Asymptotic Accretion	645	410	214	996	761	565
Forested lands available for harvest	Polynomial Accretion	71	-53	-149	279	154	58
managed on a 100-yr rotation (#5)	Asymptotic Accretion	279	119	-12	487	326	195
Forested lands available for harvest	Polynomial Accretion	-98	-145	-177	6	-41	-73
managed on a 200-yr rotation (#6)	Asymptotic Accretion	149	57	-16	253	161	88

A

Average Annual Carbon Flux from the Tongass Forest							
(thousands of tons, annualized over 200 years)							
		C-density after harvest = polygon type **23			Carbon density after harvest = 0		
Management Scenario Modeled	Carbon Accretion Modeled	Upper bound	Best estimate	Lower bound	Upper bound	Best estimate	Lower bound
Cessation of	Polynomial Accretion	-232	-186	-130	-232	-186	-130
all harvest (#1)	Asymptotic Accretion	-144	-105	-53	-144	-105	-53
Past carbon	Polynomial Accretion	199	180	74	199	180	74
flux (#2)	Asymptotic Accretion	199	180	74	199	180	74
All forested lands managed	Polynomial Accretion	746	427	161	1333	1015	749
on a 100-yr rotation (#3)	Asymptotic Accretion	1069	682	356	1657	1270	943
All forested lands managed	Polynomial Accretion	68	-77	-193	538	392	277
on a 200-yr rotation (#4)	Asymptotic Accretion	849	537	276	1318	1007	745
Forested lands available for harvest	Polynomial Accretion	151	46	-41	325	220	133
managed on a 100-yr rotation (#5)	Asymptotic Accretion	255	132	27	429	306	202
Forested lands available for harvest	Polynomial Accretion	-58	-126	-177	82	13	-38
managed on a 200-yr rotation (#6)	Asymptotic Accretion	189	76	-17	328	215	123

B

Table 7:

Estimates of carbon flux to and from the Tongass associated with management scenarios were sensitive to the function chosen to represent carbon accretion in secondary growth (fig. 6), either polynomial or asymptotic. Carbon flux estimates were also sensitive to the carbon density in standing aboveground biomass used in each model run. Although the density in polygon type **23 (86 Mg/ ha) was the closest approximation available in polygon data, assuming a value of zero approximates the true value more closely. Upper and lower bounds incorporate the 95% confidence interval in carbon

density estimates for each polygon type as well as the sensitivity analyses performed for all major assumptions. Consequently, these bounds represent a generous confidence interval for the true value of carbon flux associated with each management policy. Negative numbers indicate carbon sequestration in the Tongass; positive numbers indicate carbon emissions from the Tongass. Carbon fluxes are in thousands of tons and were annualized over 100 years in panel A and 200 years in panel B.

Average Annual Carbon Flux to the Atmosphere (thousands of tons, annualized over 100 years)							
		C-density after harvest = polygon type **23			Carbon density after harvest = 0		
Management Scenario Modeled	Carbon Accretion Modeled	Upper bound	Best estimate	Lower bound	Upper bound	Best estimate	Lower bound
Cessation of	Polynomial Accretion	-404	-323	-221	-404	-323	-221
all harvest (#1)	Asymptotic Accretion	-288	-209	-107	-288	-209	-107
Past carbon	Polynomial Accretion	169	153	63	169	153	63
flux (#2)	Asymptotic Accretion	169	153	63	193	174	72
All forested lands managed	Polynomial Accretion	-125	-206	-260	190	109	55
on a 100-yr rotation (#3)	Asymptotic Accretion	529	309	133	843	623	447
All forested lands managed	Polynomial Accretion	-499	-443	-385	-341	-285	-227
on a 200-yr rotation (#4)	Asymptotic Accretion	282	172	84	440	329	241
Forested lands available for harvest	Polynomial Accretion	-119	-174	-207	-26	-81	-114
managed on a 100-yr rotation (#5)	Asymptotic Accretion	91	0	-69	185	93	25
Forested lands available for harvest	Polynomial Accretion	-192	-205	-205	-145	-158	-157
managed on a 200-yr rotation (#6)	Asymptotic Accretion	55	-1	-43	102	45	3

A

Average Annual Carbon Flux to the Atmosphere (thousands of tons, annualized over 200 years)							
		C-density after harvest = polygon type **23			Carbon density after harvest = 0		
Management Scenario Modeled	Carbon Accretion Modeled	Upper bound	Best estimate	Lower bound	Upper bound	Best estimate	Lower bound
Cessation of	Polynomial Accretion	-232	-186	-130	-232	-186	-130
all harvest (#1)	Asymptotic Accretion	-144	-105	-53	-144	-105	-53
Past carbon	Polynomial Accretion	169	153	63	169	153	63
flux (#2)	Asymptotic Accretion	169	153	63	193	174	72
All forested lands managed	Polynomial Accretion	756	433	163	1353	1030	760
on a 100-yr rotation (#3)	Asymptotic Accretion	1086	693	361	1683	1290	958
All forested lands managed	Polynomial Accretion	-114	-197	-258	259	176	114
on a 200-yr rotation (#4)	Asymptotic Accretion	667	418	210	1039	790	583
Forested lands available for harvest	Polynomial Accretion	134	16	-80	330	223	135
managed on a 100-yr rotation (#5)	Asymptotic Accretion	259	134	28	436	311	205
Forested lands available for harvest	Polynomial Accretion	-105	-156	-191	6	-46	-81
managed on a 200-yr rotation (#6)	Asymptotic Accretion	142	47	-30	253	157	80

B

Table 8:

Similar to table 7, decomposition of slash and stumps left on the harvest site and sawtimber products initially removed from the site were included to convert estimates of carbon flux from the forest to carbon flux to the atmosphere in management scenarios numbered 2-6 (fig. 7). Carbon fluxes are in thousands of tons and were annualized over 100 years in panel A and 200 years in panel B.

Average Annual Value of Carbon Flux to the Atmosphere (millions of dollars, annualized over 100 years)							
		C-density after harvest = polygon type **23			Carbon density after harvest = 0		
Management Scenario Modeled	Carbon Accretion Modeled	Upper bound	Best estimate	Lower bound	Upper bound	Best estimate	Lower bound
Cessation of	Polynomial Accretion	8.1	6.5	4.4	8.1	6.5	4.4
all harvest (#1)	Asymptotic Accretion	5.8	4.2	2.1	5.8	4.2	2.1
Past carbon	Polynomial Accretion	-3.4	-3.1	-1.3	-3.4	-3.1	-1.3
flux (#2)	Asymptotic Accretion	-3.4	-3.1	-1.3	-3.9	-3.5	-1.4
All forested lands managed	Polynomial Accretion	2.5	4.1	5.2	-3.8	-2.2	-1.1
on a 100-yr rotation (#3)	Asymptotic Accretion	-10.6	-6.2	-2.7	-16.9	-12.5	-8.9
All forested lands managed	Polynomial Accretion	10.0	8.9	7.7	6.8	5.7	4.5
on a 200-yr rotation (#4)	Asymptotic Accretion	-5.6	-3.4	-1.7	-8.8	-6.6	-4.8
Forested lands available for harvest	Polynomial Accretion	2.4	3.5	4.1	0.5	1.6	2.3
managed on a 100-yr rotation (#5)	Asymptotic Accretion	-1.8	0.0	1.4	-3.7	-1.9	-0.5
Forested lands available for harvest	Polynomial Accretion	3.8	4.1	4.1	2.9	3.2	3.1
managed on a 200-yr rotation (#6)	Asymptotic Accretion	-1.1	0.0	0.9	-2.0	-0.9	-0.1

A

Average Annual Value of Carbon Flux to the Atmosphere (millions of dollars, annualized over 200 years)							
		C-density after harvest = polygon type **23			Carbon density after harvest = 0		
Management Scenario Modeled	Carbon Accretion Modeled	Upper bound	Best estimate	Lower bound	Upper bound	Best estimate	Lower bound
Cessation of	Polynomial Accretion	4.6	3.7	2.6	4.6	3.7	2.6
all harvest (#1)	Asymptotic Accretion	2.9	2.1	1.1	2.9	2.1	1.1
Past carbon	Polynomial Accretion	-3.4	-3.1	-1.3	-3.4	-3.1	-1.3
flux (#2)	Asymptotic Accretion	-3.4	-3.1	-1.3	-3.9	-3.5	-1.4
All forested lands managed	Polynomial Accretion	-15.1	-8.7	-3.3	-27.1	-20.6	-15.2
on a 100-yr rotation (#3)	Asymptotic Accretion	-21.7	-13.9	-7.2	-33.7	-25.8	-19.2
All forested lands managed	Polynomial Accretion	2.3	3.9	5.2	-5.2	-3.5	-2.3
on a 200-yr rotation (#4)	Asymptotic Accretion	-13.3	-8.4	-4.2	-20.8	-15.8	-11.7
Forested lands available for harvest	Polynomial Accretion	-2.7	-0.3	1.6	-6.6	-4.5	-2.7
managed on a 100-yr rotation (#5)	Asymptotic Accretion	-5.2	-2.7	-0.6	-8.7	-6.2	-4.1
Forested lands available for harvest	Polynomial Accretion	2.1	3.1	3.8	-0.1	0.9	1.6
managed on a 200-yr rotation (#6)	Asymptotic Accretion	-2.8	-0.9	0.6	-5.1	-3.1	-1.6

B

Table 9:

Carbon flux between the Tongass and the atmosphere (table 8) was converted to monetary units assuming a value of carbon equal to $20 per ton. Positive numbers represent potential revenue from the sale of carbon emission permits made possible by the carbon sequestration associated with the management policy modeled while negative numbers represent the cost of emission permit purchase for carbon emissions associated with the management policy modeled. The annual economic values of carbon fluxes are in millions of 1995 dollars and were annualized over 100 years in panel A and 200 years in panel B.

Polynomial Accretion:	Carbon density after harvest = polygon type **23	Carbon density after harvest = 0
Cessation of all Harvest =	$4.4 to $8.1 million	$4.4 to $8.1 million
100-year Rotation (all forested lands) =	$1.2 to -$9.2 million	-$1.1 to -$3.8 million
200-year Rotation (all forested lands) =	$5.9 to $4.4 million	$4.5 to $6.8 million
100-year Rotation (available forested lands) =	$3.6 to -$0.3 million	$2.3 to $0.5 million
200-year Rotation (available forested lands) =	$4.0 to $2.7 million	$3.1 to $2.9 million
Net annual carbon value for ceasing harvest =	-$1.5 to $17.3 million	**-$0.1 to $11.9 million**

Asymptotic Accretion:	Carbon density after harvest = polygon type **23	Carbon density after harvest = 0
Cessation of all Harvest =	$2.1 to $5.8 million	$2.1 to $5.8 million
100-year Rotation (all forested lands) =	-$6.6 to -$22.1 million	-$19.2 to -$34.8 million
200-year Rotation (all forested lands) =	-$3.4 to -$11.2 million	-$9.8 to -$17.5 million
100-year Rotation (available forested lands) =	$0.8 to -$4.5 million	-$2.9 to -$8.3 million
200-year Rotation (available forested lands) =	$0.8 to -$2.3 million	-$0.5 to -$4.1 million
Net annual carbon value for ceasing harvest =	$1.3 to $27.9 million	**$2.6 to $40.6 million**

A: **annual value, 1995 - 2095**

Polynomial Accretion:	Carbon density after harvest = polygon type **23	Carbon density after harvest = 0
Cessation of all Harvest =	$2.6 to $4.6 million	$2.6 to $4.6 million
100-year Rotation (all forested lands) =	-$2.5 to -$13.3 million	-$15.2 to -$27.1 million
200-year Rotation (all forested lands) =	$4.5 to $0.2 million	-$2.3 to -$5.2 million
100-year Rotation (available forested lands) =	$1.1 to -$2.5 million	-$2.7 to -$6.6 million
200-year Rotation (available forested lands) =	$3.8 to $1.7 million	$1.6 to -$0.1 million
Net annual carbon value for ceasing harvest =	-$1.9 to $17.9 million	**$1.0 to $31.7 million**

Asymptotic Accretion:	Carbon density after harvest = polygon type **23	Carbon density after harvest = 0
Cessation of all Harvest =	$1.1 to $2.9 million	$1.1 to $2.9 million
100-year Rotation (all forested lands) =	-$6.4 to -$19.7 million	-$17.4 to -$30.7 million
200-year Rotation (all forested lands) =	-$4.8 to -$15.5 million	-$13.5 to -$24.1 million
100-year Rotation (available forested lands) =	$-0.2 to -$4.6 million	-$3.5 to -$7.8 million
200-year Rotation (available forested lands) =	$0.6 to -$3.2 million	-$1.7 to -$5.8 million
Net annual carbon value for ceasing harvest =	$0.5 to $22.6 million	**$2.8 to $33.6 million**

B: annual value, 1995 - 2195

Table 10:

The economic value of carbon flux associated with each potential management scenario modeled were calculated based on a value of carbon equal to $20 per ton. Although the density in polygon type **23 (86 Mg/ ha) was the closest approximation available in polygon data, assuming a value of zero approximates the true value more closely, as do estimates of the economic value of carbon flux calculated with this assumption. The range of economic value in carbon flux associated with each management scenario represents the upper and lower bounds in carbon flux estimates, which incorporate the 95% confidence interval in carbon density estimates for each polygon type as well as the sensitivity analyses performed for all major assumptions.

Consequently, these ranges in economic value represent generous confidence intervals for the true value of carbon flux associated with each management policy. Furthermore, the net annual value of carbon sequestered from ceasing harvest depends on which of the other scenarios is deemed "business-as-usual" in the allocation of Certified Emissions Reduction credits (CERs). Business-as-usual was defined so as to give the largest range in net annual value of carbon flux. The annual economic values of carbon fluxes are in millions of 1995 dollars and were annualized over 100 years in panel A and 200 years in panel B.

Average Annual Value of Carbon Flux to the Atmosphere (millions of dollars, annualized over 100 years)							
		C-density after harvest = polygon type **23			Carbon density after harvest = 0		
Management Scenario Modeled	Carbon Accretion Modeled	Upper bound	Best estimate	Lower bound	Upper bound	Best estimate	Lower bound
Cessation of	Polynomial Accretion	7.0	5.6	3.8	7.0	5.6	3.8
all harvest (#1)	Asymptotic Accretion	5.0	3.6	1.9	5.0	3.6	1.9
Past carbon	Polynomial Accretion	-3.4	-3.1	-1.3	-3.4	-3.1	-1.3
flux (#2)	Asymptotic Accretion	-3.4	-3.1	-1.3	-3.9	-3.5	-1.4
All forested lands managed	Polynomial Accretion	2.5	4.1	5.2	-3.8	-2.2	-1.1
on a 100-yr rotation (#3)	Asymptotic Accretion	-10.6	-6.2	-2.7	-16.9	-12.5	-8.9
All forested lands managed	Polynomial Accretion	10.0	8.9	7.7	6.8	5.7	4.5
on a 200-yr rotation (#4)	Asymptotic Accretion	-5.6	-3.4	-1.7	-8.8	-6.6	-4.8
Forested lands available for harvest	Polynomial Accretion	2.4	3.5	4.1	0.5	1.6	2.3
managed on a 100-yr rotation (#5)	Asymptotic Accretion	-1.8	0.0	1.4	-3.7	-1.9	-0.5
Forested lands available for harvest	Polynomial Accretion	3.8	4.1	4.1	2.9	3.2	3.1
managed on a 200-yr rotation (#6)	Asymptotic Accretion	-1.1	0.0	0.9	-2.0	-0.9	-0.1

A

Average Annual Value of Carbon Flux to the Atmosphere (millions of dollars, annualized over 200 years)							
		C-density after harvest = polygon type **23			Carbon density after harvest = 0		
Management Scenario Modeled	Carbon Accretion Modeled	Upper bound	Best estimate	Lower bound	Upper bound	Best estimate	Lower bound
Cessation of	Polynomial Accretion	4.0	3.2	2.3	4.0	3.2	2.3
all harvest (#1)	Asymptotic Accretion	2.5	1.8	0.9	2.5	1.8	0.9
Past carbon	Polynomial Accretion	-3.4	-3.1	-1.3	-3.4	-3.1	-1.3
flux (#2)	Asymptotic Accretion	-3.4	-3.1	-1.3	-3.9	-3.5	-1.4
All forested lands managed	Polynomial Accretion	-15.1	-8.7	-3.3	-27.1	-20.6	-15.2
on a 100-yr rotation (#3)	Asymptotic Accretion	-21.7	-13.9	-7.2	-33.7	-25.8	-19.2
All forested lands managed	Polynomial Accretion	2.3	3.9	5.2	-5.2	-3.5	-2.3
on a 200-yr rotation (#4)	Asymptotic Accretion	-13.3	-8.4	-4.2	-20.8	-15.8	-11.7
Forested lands available for harvest	Polynomial Accretion	-2.7	-0.3	1.6	-6.6	-4.5	-2.7
managed on a 100-yr rotation (#5)	Asymptotic Accretion	-5.2	-2.7	-0.6	-8.7	-6.2	-4.1
Forested lands available for harvest	Polynomial Accretion	2.1	3.1	3.8	-0.1	0.9	1.6
managed on a 200-yr rotation (#6)	Asymptotic Accretion	-2.8	-0.9	0.6	-5.1	-3.1	-1.6

B

Table 11:

Similar to table 9, estimates of the monetary value of carbon sequestration with cessation of all harvest were calculated based on 87% of the total carbon sequestration to account for the potential reduction in Certified Emission Reduction credit (CER) allocation for this management policy due to leakage as a result of elimination of long-term carbon storage in forest products. The annual economic values of carbon fluxes are in millions of 1995 dollars and were annualized over 100 years in panel A and 200 years in panel B.

Polynomial Accretion:	Carbon density after harvest = polygon type **23	Carbon density after harvest = 0
Cessation of all Harvest =	$3.8 to $7.0 million	$3.8 to $7.0 million
100-year Rotation (all forested lands) =	$1.2 to -$9.2 million	-$1.1 to -$3.8 million
200-year Rotation (all forested lands) =	$5.9 to $4.4 million	$4.5 to $6.8 million
100-year Rotation (available forested lands) =	$3.6 to -$0.3 million	$2.3 to $0.5 million
200-year Rotation (available forested lands) =	$4.0 to $2.7 million	$3.1 to $2.9 million
Net annual carbon value for ceasing harvest =	-$2.1 to $16.2 million	**-$0.7 to $10.8 million**

Asymptotic Accretion:	Carbon density after harvest = polygon type **23	Carbon density after harvest = 0
Cessation of all Harvest =	$1.9 to $5.0 million	$1.9 to $5.0 million
100-year Rotation (all forested lands) =	-$6.6 to -$22.1 million	-$19.2 to -$34.8 million
200-year Rotation (all forested lands) =	-$3.4 to -$11.2 million	-$9.8 to -$17.5 million
100-year Rotation (available forested lands) =	$0.8 to -$4.5 million	-$2.9 to -$8.3 million
200-year Rotation (available forested lands) =	$0.8 to -$2.3 million	-$0.5 to -$4.1 million
Net annual carbon value for ceasing harvest =	$1.1 to $27.1 million	**$2.4 to $39.8 million**

A: **annual value, 1995 - 2095**

Polynomial Accretion:	Carbon density after harvest = polygon type **23	Carbon density after harvest = 0
Cessation of all Harvest =	$2.3 to $4.0 million	$2.3 to $4.0 million
100-year Rotation (all forested lands) =	$-2.5 to -$13.3 million	-$15.2 to -$27.1 million
200-year Rotation (all forested lands) =	$4.5 to $0.2 million	-$2.3 to -$5.2 million
100-year Rotation (available forested lands) =	$1.1 to -$2.5 million	-$2.7 to -$6.6 million
200-year Rotation (available forested lands) =	$3.8 to $1.7 million	$1.6 to -$0.1 million
Net annual carbon value for ceasing harvest =	-$2.2 to $17.3 million	**$0.7 to $31.1 million**

Asymptotic Accretion:	Carbon density after harvest = polygon type **23	Carbon density after harvest = 0
Cessation of all Harvest =	$0.9 to $2.5 million	$0.9 to $2.5 million
100-year Rotation (all forested lands) =	-$6.4 to -$19.7 million	-$17.4 to -$30.7 million
200-year Rotation (all forested lands) =	-$4.8 to -$15.5 million	-$13.5 to -$24.1 million
100-year Rotation (available forested lands) =	$-0.2 to -$4.6 million	-$3.5 to -$7.8 million
200-year Rotation (available forested lands) =	$0.6 to -$3.2 million	-$1.7 to -$5.8 million
Net annual carbon value for ceasing harvest =	$0.3 to $22.2 million	**$2.6 to $33.2 million**

B: annual value, 1995 - 2195

Table 12:

Similar to table 10, this table shows the economic value of carbon flux associated with each potential management scenario modeled, calculated based on a value of carbon equal to $20 per ton. However, this table assumes a 13% reduction in carbon sequestration credited for cessation of all harvest in the allocation of Certified Emissions Reduction credits CERs due to leakage as a result of elimination of long-term storage in wood products. The annual economic values of carbon fluxes are in millions of 1995 dollars and were annualized over 100 years in panel A and 200 years in panel B.

Appendices

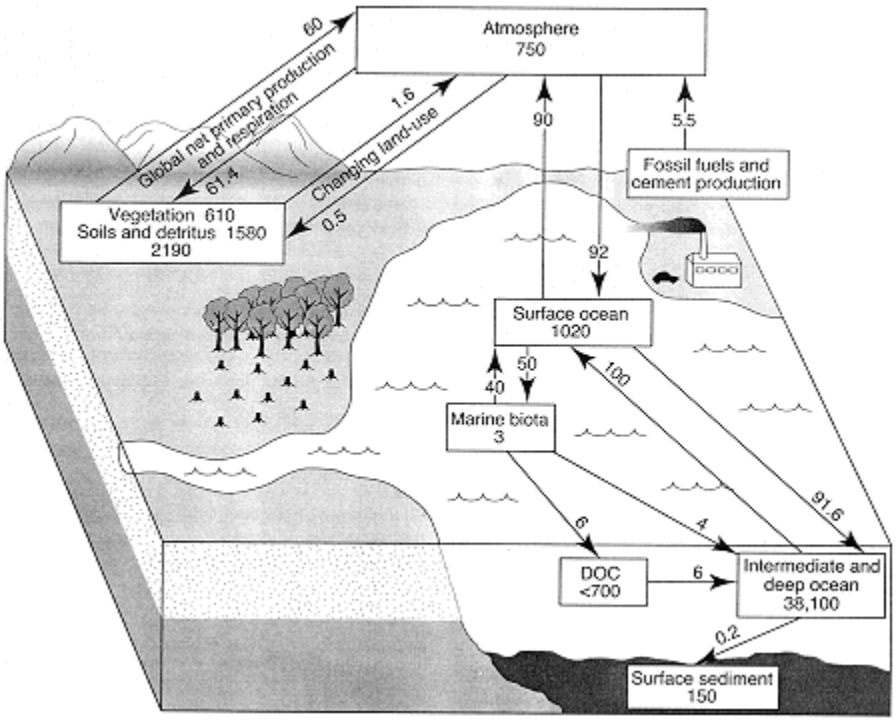

Appendix A:

Carbon cycles around the globe, moving between carbon sinks and changing forms. In forest carbon is in the form of organic material, both aboveground and belowground. In the atmosphere carbon is in the form of a gas, carbon dioxide (CO_2). Data is from Schimel et al, 1995, all numbers represent Pg of carbon, arrows represent annual fluxes.

Appendix C:

These photographs of Southeast Alaska illustrate the spatial heterogeneity of landscapes in the Tongass and myriad of forest structures considered in mapping carbon density in the Tongass.

The mouth of Glacier Bay in northern Southeast Alaska, with the Beardsley islands in the foreground. Glaciers filled Glacier Bay less than 200 years ago and some are still receding rapidly. 19 May 1965.

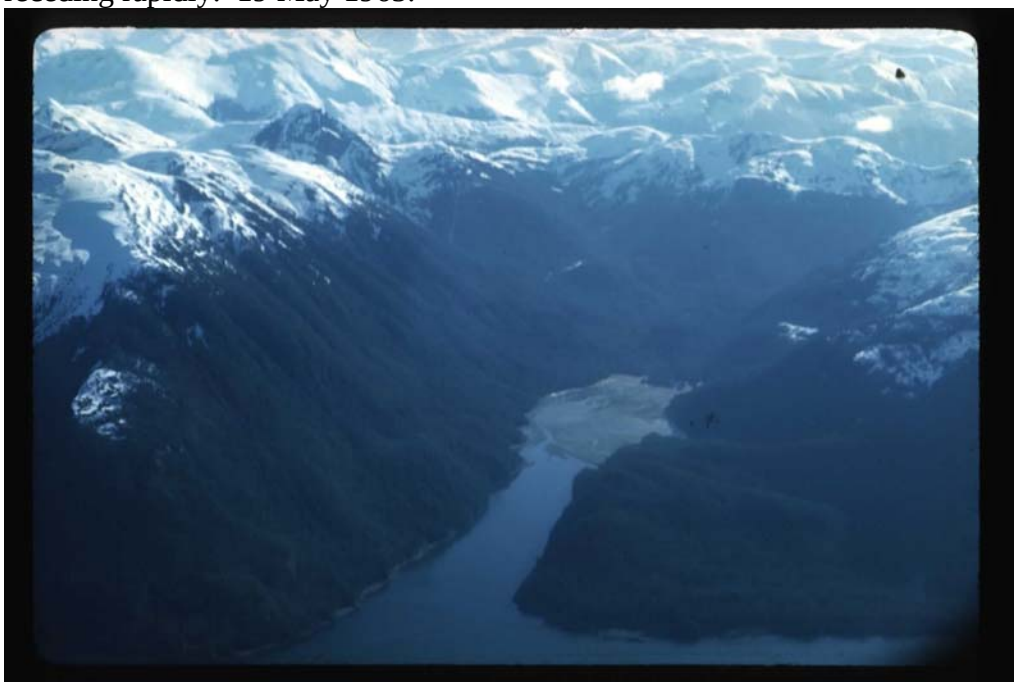

Limestone Inlet, south of Juneau, looking east over the mountains separating the coastlines of Southeast Alaska from the dry, inland climate of western Canada.

Rocky Pass in the Southern Tongass. 18 May 1977.

The hydroelectric development at Snettisham, south of Juneau, drawing water from an alpine lake.

Residuals left after harvest at Stancy Creek

Coco Harbor, 13 years after harvest, 1963

Spruce on well-drained soil bordering a stream

Forest transitioning into a large muskeg area with harvested areas in the upper left

Upper Game Creek, transition from alpine to lowland forest with avalanche chutes visible, 1979

Ketchikan Pulp Corporation, Ward Cove, 21 May 1974

Rear view of the Alaska Pulp Corporation mill near Sitka

Alpine muskeg in the Maybeso valley with a harvested mountainside in the background

Muskeg pond, 1982

Muskeg

Old-growth hemlock-spruce forest near Juneau

Old-growth forest, natural stand opening

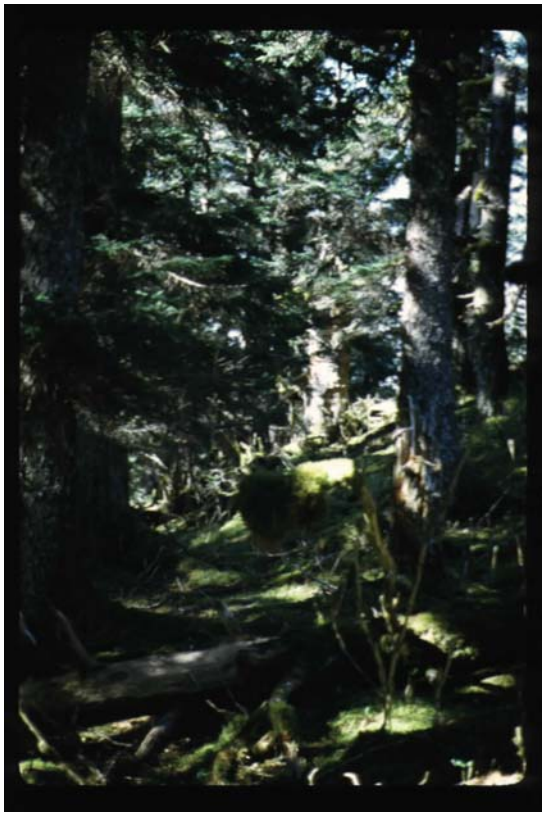

Old-growth forest, Danger Bay, 12 June 1973

Windthrow showing the shallow root system of spruce and hemlock trees

Blowdown, Chichagof Island, 1979

Logging road prior to harvest of high volume spruce-hemlock forest

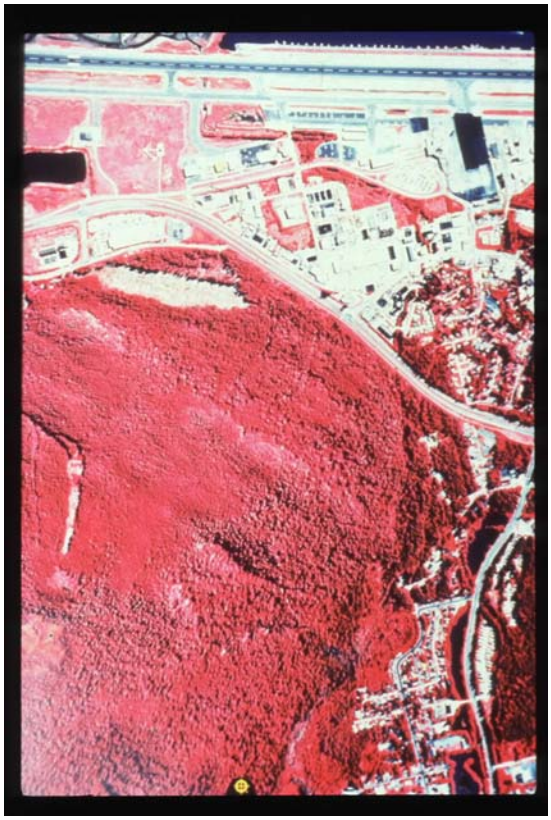

Heintzleman Ridge, Juneau, demonstrating the significance of southern exposure. The fine-textured slope is exposed to storms coming up the coast from the southeast. The rough-textured slope is in the lee of these storms, facing north. Slope aspect was one attribute included in mapping carbon density.

Peterson Creek, Juneau area, showing a patchwork of forest structures including muskeg (brown), rough-textured high volume forest, and smooth-textured low volume forest

Appendix D:

The files linked below contain the original 1995 FIA data used to calculate carbon density at sample locations. The data is saved in various formats, all of which originated from the Microsoft Access file "PPGVers1." Explanation of the collection methods for data contained in each file can be found in "Field Procedures for the Southeast Alaska Inventory 1995" (USDA Forest Service, 1995).

- FIA grid Access database: Original FIA data (.mbd format)
  - PPGVers1 (CD2\FIA data (various forms)\original FIA grid database)
- FIA grid .dbf exported: FIA data saved in .dbf format (CD2\FIA data (various forms)\FIA grid .dbf exported)
  - Downwood Dwnorepeats (sample locations duplicated in original data removed)
  - HVcomp1
  - HVcomp2
  - HVlayer
  - Location
  - Point
  - Polygon
  - Soil
  - Tree
- FIA grid excel spreadsheets: FIA data saved in .xls format (CD2\ FIA data (various forms)\ FIA grid excel spreadsheets)
  - Downwood1
  - Downwood2
  - Dwnorepeats
  - HV composition trunc1
  - HV composition trunc2
  - HV composition trunc2 sorted
  - HV comp trunc1
  - HV comp trunc1 sorted
  - HV layer
  - Location sorted
  - Location
  - Point
  - Polygon sorted
  - Polygon
  - Soil
  - Sorted tree
  - tree

Appendix E:

GPS instruments cease to work reliably within dense forest. Consequently, survey crews were forced to establish the location of a reference point at some distance from the sample location and then navigate their way to the sample location from this initial reference point. This navigation, often over demanding terrain, introduced discrepancy between the theoretical and actual location of the FIA sample. This error was corrected for a subset of locations, for which the estimated discrepancy ranged from 500 to 0.3 meters with an average error of 16.8 meters and standard deviation of 29.3 meters (fig E) (data is located in Excel file "location errors"). The significance of this error was estimated by locating the subset of corrected locations as well as the corresponding theoretical locations on the carbon density map to determine how many locations switched polygon type as a result of the spatial error. This exercise determined that none of the locations switched polygon type when spatial error was corrected, so this error was deemed inconsequential. The theoretical FIA locations are shown in the GIS coverage "tlmpoint" on CD 5. The corrected FIA locations are shown in the GIS "gpsfia" on CD 5. Data attributes in these coverages relevant for this study are listed below.

- Ptid – code identifying the FIA sample location
- Error – discrepancy between the theoretical sample location (tlmpoint) and actual location (gpsfia) in feet.
- Fngrpold – classification of carbon density polygons from a flawed mapping proceedure
- Fingroup – obsolete classification of carbon density polygons
- Fngrp2 – classification of carbon density polygons used in all subsequent analysis
- Some attributes in these coverages correspond to those used in carbon mapping. However, the attributes in tlmpoint and gpsfia were not used to identify FIA sample locations as representative of a particular polygon type. Rather, FIA sample coverages were overlaid on the carbon density polygon coverage and spatial correspondence was used to associate each sample location with a particular polygon type.

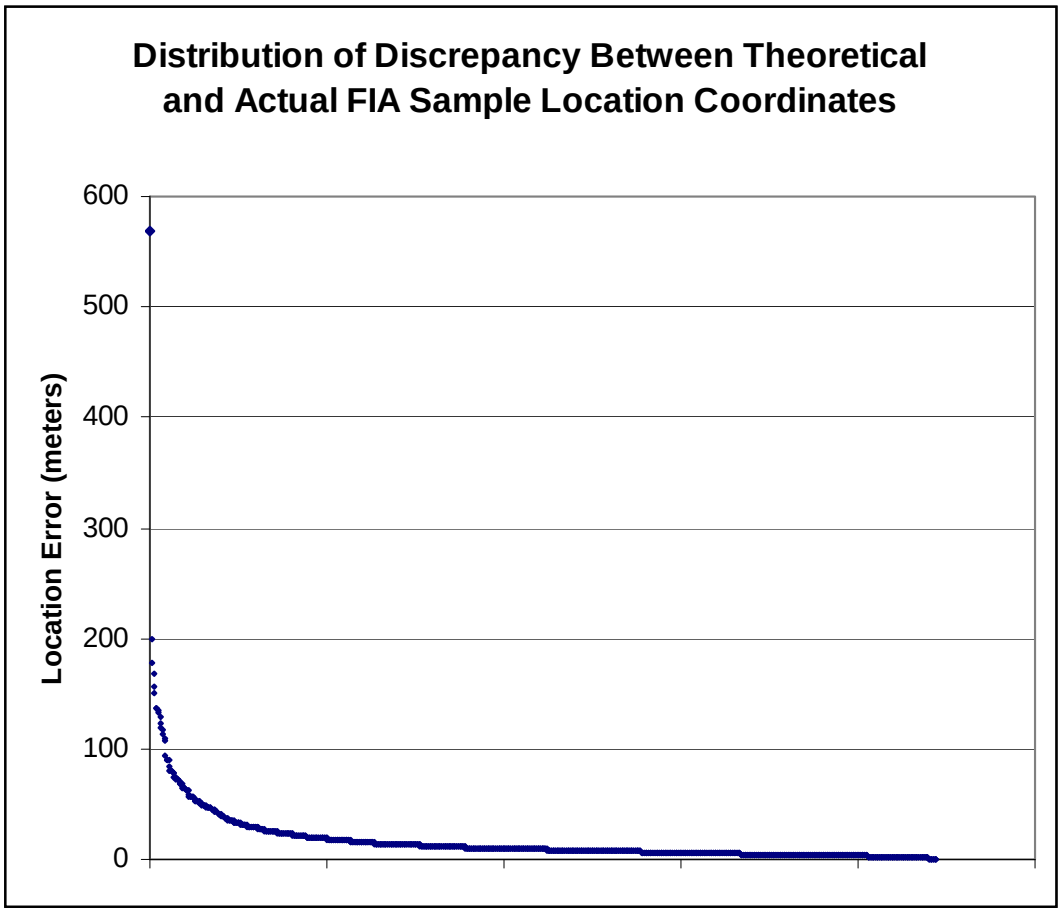

Figure E:
Distribution of discrepancy between theoretical and actual FIA sample location.

Appendix F:

The SAS program version 6.12 was used for calculation of carbon density estimates from FIA location data, map creation, and map manipulation. All the SAS programs are available on CD1. An index to these programs is presented below. Note that programs must be run in the order shown.

1. Carbon density calculation from FIA data:

- Programs employing low-end biomass equations (CDone\sasprograms\lowend)
  - aatreeimplow – imports FIA tree data from .dbf file
  - abtree6low – calculation of total carbon in each tree recorded in FIA data
  - actreesumbylow – aggregation of tree data by each point at a sample location
  - adtreeCphabyptlow – calculation of carbon density (kg/ ha) in trees at each point in a sample location
  - aetreeCphabyloclow – aggregation of sample points at each sample location to calculate carbon density (kg/ ha) in trees at each sample location
  - basoilimplow – imports FIA soil data from .dbf file
  - bbsoilcompletelow – calculation of soil carbon density (kg/ ha) at each sample location
  - caHVimplow – imports FIA understory data from .dbf file
  - cbHV2low – calculation of carbon density (kg/ ha) in understory vegetation at each sample location
  - daDWDimp2low – imports FIA downed woody debris data from .dbf file
  - dcDWDrevised2low – calculation of carbon density (kg/ ha) in downed woody debris at each sample location
  - eLCTlow
  - fFinalMerge2low – merges carbon densities calculated for all carbon pools into an estimate for total carbon density at each sample location
  - GpointsWpolygonslow – associates calculated carbon densities with the physical location of each FIA sample location given in the coverages “tlmpoint” and “gpsfia” using the attribute Ptid as the common identifier of each sample location
  - Gpsfiacarb2soilsdroppedlow – associates calculated carbon densities (excluding soils) with the physical location of each FIA sample location given in the coverage “gpsfia” using the attribute Ptid as the common identifier of each sample location
  - Htlmpcarb2soilsdroppedlow – associates calculated carbon densities (excluding soils) with the physical location of each FIA sample location given in the coverage “tlmpoint” using the attribute Ptid as the common identifier of each sample location
  - Itlmpcarbselectedforgpslow – identifies the FIA sample locations common to both “tlmpoint” and “gpsfia” for evaluation of the significance of discrepancy in physical location of sample locations in these two coverages.
  - Jtlmpgps2soilsdroppedlow – delineation of simplified carbon density polygon identifying codes
  - Kcleanuplow – cleaning out empty data records

Mcompleteprogramlow – compiled version of all the preceeding programs
Ntreeupdatelow

- Programs employing high-end biomass equations (CDone\sasprograms\highend)
  - aatreeimp – imports FIA tree data from .dbf file
  - abtree6 – calculation of total carbon in each tree recorded in FIA data
  - actreesumby – aggregation of tree data by each point at a sample location
  - adtreeCphabypt – calculation of carbon density (kg/ ha) in trees at each point in a sample location
  - aetreeCphabyloc – aggregation of sample points at each sample location to calculate carbon density (kg/ ha) in trees at each sample location
  - basoilimp – imports FIA soil data from .dbf file
  - bbsoilcomplete – calculation of soil carbon density (kg/ ha) at each sample location
  - caHVimp – imports FIA understory data from .dbf file
  - cbHV2 – calculation of carbon density (kg/ ha) in understory vegetation at each sample location
  - daDWDimp2 – imports FIA downed woody debris data from .dbf file
  - dcDWDrevised2 – calculation of carbon density (kg/ ha) in downed woody debris at each sample location
  - eLCT
  - fFinalMerge2 – merges carbon densities calculated for all carbon pools into an estimate for total carbon density at each sample location
  - gpointsWpolygons – associates calculated carbon densities with the physical location of each FIA sample location given in the coverages “tlmpoint” and “gpsfia” using the attribute Ptid as the common identifier of each sample location
  - gpsfiacarb2soilsdropped – associates calculated carbon densities (excluding soils) with the physical location of each FIA sample location given in the coverage “gpsfia” using the attribute Ptid as the common identifier of each sample location
  - htlmpcarb2soilsdropped – associates calculated carbon densities (excluding soils) with the physical location of each FIA sample location given in the coverage “tlmpoint” using the attribute Ptid as the common identifier of each sample location
  - itlmpcarbselectedforgps – identifies the FIA sample locations common to both “tlmpoint” and “gpsfia” for evaluation of the significance of discrepancy in physical location of sample locations in these two coverages.
  - jtlmpgps2soilsdropped – delineation of simplified carbon density polygon identifying codes
  - Kcleanup – cleaning out empty data records
  - Mcompleteprogram – compiled version of all the preceeding programs
  - Ntreeupdate
  - zBigdiamfinder – used to identify potential data entry errors by selecting trees with especially large diameter
  - zloctypecarbdensity – delineation of simplified carbon density polygon identifying codes

- Density calculations omitting willow and birch (CDone\sasprograms\nowillowbirch)
  Aatreeimp - imports FIA tree data from .dbf file
  Abtree6 - calculation of total carbon in each tree recorded in FIA data
  Actreesumby - aggregation of tree data by each point at a sample location
  AdtreeCphabypt - calculation of carbon density (kg/ ha) in trees at each point in a sample location
  AetreeCphabyloc - aggregation of sample points at each sample location to calculate carbon density (kg/ ha) in trees at each sample location
  Basoilimp - imports FIA soil data from .dbf file
  Bbsoilcomplete - calculation of soil carbon density (kg/ ha) at each sample location
  CaHVimp - imports FIA understory data from .dbf file
  CbHV2 - calculation of carbon density (kg/ ha) in understory vegetation at each sample location
  DaDWDimp2 - imports FIA downed woody debris data from .dbf file
  DcDWDrevised2 - calculation of carbon density (kg/ ha) in downed woody debris at each sample location
  ELCT
  FFinalMerge2 - merges carbon densities calculated for all carbon pools into an estimate for total carbon density at each sample location
    GpointsWpolygons - associates calculated carbon densities with the physical location of each FIA sample location given in the coverages "tlmpoint" and "gpsfia" using the attribute Ptid as the common identifier of each sample location
    Gpsfiacarb2soilsdropped - associates calculated carbon densities (excluding soils) with the physical location of each FIA sample location given in the coverage "gpsfia" using the attribute Ptid as the common identifier of each sample location
    Htlmpcarb2soilsdropped - associates calculated carbon densities (excluding soils) with the physical location of each FIA sample location given in the coverage "tlmpoint" using the attribute Ptid as the common identifier of each sample location
    Itlmpcarbselectedforgps - identifies the FIA sample locations common to both "tlmpoint" and "gpsfia" for evaluation of the significance of discrepancy in physical location of sample locations in these two coverages.
    Jtlmpgps2soilsdropped - delineation of simplified carbon density polygon identifying codes
  Kcleanup - cleaning out empty data records
  Mcompleteprogram - compiled version of all the preceeding programs
  Ntreeupdate

- Density calculations omitting trees outside verified size range for biomass equation (CDone\sasprograms\outofrange)
  aatreeimprange - imports FIA tree data from .dbf file
  abtree6range - calculation of total carbon in each tree recorded in FIA data
  actreesumbyrange - aggregation of tree data by each point at a sample location

adtreeCphabyptrange - calculation of carbon density (kg/ ha) in trees at each point in a sample location

aetreeCphabylocrange - aggregation of sample points at each sample location to calculate carbon density (kg/ ha) in trees at each sample location

basoilimprange - imports FIA soil data from .dbf file

bbsoilcompleterange - calculation of soil carbon density (kg/ ha) at each sample location

caHVimprange - imports FIA understory data from .dbf file

cbHV2range - calculation of carbon density (kg/ ha) in understory vegetation at each sample location

daDWDimp2range - imports FIA downed woody debris data from .dbf file

dcDWDrevised2range - calculation of carbon density (kg/ ha) in downed woody debris at each sample location

eLCTrange

fFinalMerge2range - merges carbon densities calculated for all carbon pools into an estimate for total carbon density at each sample location

gpointsWpolygonsrange - associates calculated carbon densities with the physical location of each FIA sample location given in the coverages "tlmpoint" and "gpsfia" using the attribute Ptid as the common identifier of each sample location

gpsfiacarb2soilsdroppedrange - associates calculated carbon densities (excluding soils) with the physical location of each FIA sample location given in the coverage "gpsfia" using the attribute Ptid as the common identifier of each sample location

htlmpcarb2soilsdroppedrange - associates calculated carbon densities (excluding soils) with the physical location of each FIA sample location given in the coverage "tlmpoint" using the attribute Ptid as the common identifier of each sample location

itlmpcarbselectedforgpsrange - identifies the FIA sample locations common to both "tlmpoint" and "gpsfia" for evaluation of the significance of discrepancy in physical location of sample locations in these two coverages.

Jtlmpgps2soilsdroppedrange - delineation of simplified carbon density polygon identifying codes

kcleanuprange - cleaning out empty data records

ntreeupdaterange

2. Map Creation

The challenge of incorporating multiple scales has always plagued map-making. A naturalist standing in the Tongass observes at many spatial and temporal scales simultaneously. She can see the trees surrounding her, can notice that she is standing on an alluvial fan that is at base of mountain slope facing south face. She may observe that this area was glaciated relatively recently, that deer has foraged here, and so on. Conversely, science must choose one spatial and one temporal scale. Thus we are left with an essential conflict: how to characterize the Tongass National Forest (specifically carbon) with only one scale.

The scale of data used for mapping carbon density was forest-wide GIS coverages based on aerial photo interpretation (coverages: TNFASPE, TNFCLU, TIMTYP,

UNITS95). John Caouette is using stand-level data to check the robustness of forest structure delineation based on forest-wide data.

The temporal scale of the carbon mapping undertaken in this project is somewhat confused. Data used in creation of the carbon density map may be as much as 20 years old while the FIA data used to quantify carbon densities is from the period 1995-2000. The raises the questions of what time period polygon types mapped represent and what time period total carbon estimates based on this map and FIA data represent. Furthermore, some GIS attributes used in mapping (e.g. Fprod, based on the productivity of an area (ft^3 / year growth)) are temporally ambiguous relative to other attributes. For example, a recent clear-cut and old-growth forest can both be "productive" in that they area capable of producing at least a minimal timber volume annually. With no means for resolution of these scale issues, it was assumed that estimates of total carbon represent the extant carbon stock in 1995. Furthermore, although the spatial quality of this carbon inventory is preserved and could be used to model carbon flux for management of specific areas in the Tongass, the model will likely break down as the scale becomes too small due to the scale of its basis in forest-wide data.

Lack of a quantifiable and agreed-upon classification system remains a sticking point of contention in forest structure stratification. For example, concurrence on a quantifiable definition of "old growth" or "productive forest" remains elusive. The method used for mapping carbon density largely avoids this by using mostly quantitative measures rather than arguably qualitative classifications (like old-growth and productive forest) to distinguish polygon types. However, the result is a forest stratification based these attributes, which begs the question of whether they the most relevant ones for carbon density. Quantification of carbon density in each polygon type from FIA data demonstrated significant differences in carbon density between polygon types. But, largely due to the limited number of FIA sample locations representing many polygon types, confidence intervals for carbon density were often of equal magnitude with differences in density between polygon types.

John Caouette has been studying the validity of forest structure stratification with quantifiable forest-wide data more rigorously. His first paper on the subject (Caouette et al, 2000) establishes the idea of stratification by forest structure and his second paper (Caouette, 2001) describes a process of mapping analogous to the one used in this research.

The traditional approach to mapping is to set up a classification system and then map areas according to it. Cartographers generally get 60-70% probability of accuracy for ecological variables with this approach. For example, if the classification system is that a certain mapped area (a "polygon type") has average mean tree diameter of 8-10 inches, and the Tongass is mapped based on this criteria, a surveyor will find an average mean tree diameter of 8-10 inches 70% of the time at any specific location within this polygon type. This is relatively poor accuracy, so consensus is that these maps aren't valuable for specific stand-scale investigations but are good at the landscape level.

Technically, the methods employed in this research stratified the Tongass by carbon density rather than mapping it. Rather than starting with a classification system and using it to map the forest, existing landscape level data was used to delineate polygon types. This is a stratification of the forest. To fit this in the box of mapping requires specification of a classification system and then checking it with specific locations to establish the probability of accuracy. This type of verification will probably find

approximately the same 70% level of accuracy (Caouette, personal communication). Like mapping, forest stratification may be of little value for stand-level investigations but of significant value at a landscape level. Fortunately, a landscape-level investigation was precisely the application of forest stratification in this research. The product of the GIS methods described below isn't a map but it is a landscape-level stratification perfectly suited to the landscape-level carbon estimation and flux modeling completed in this research.

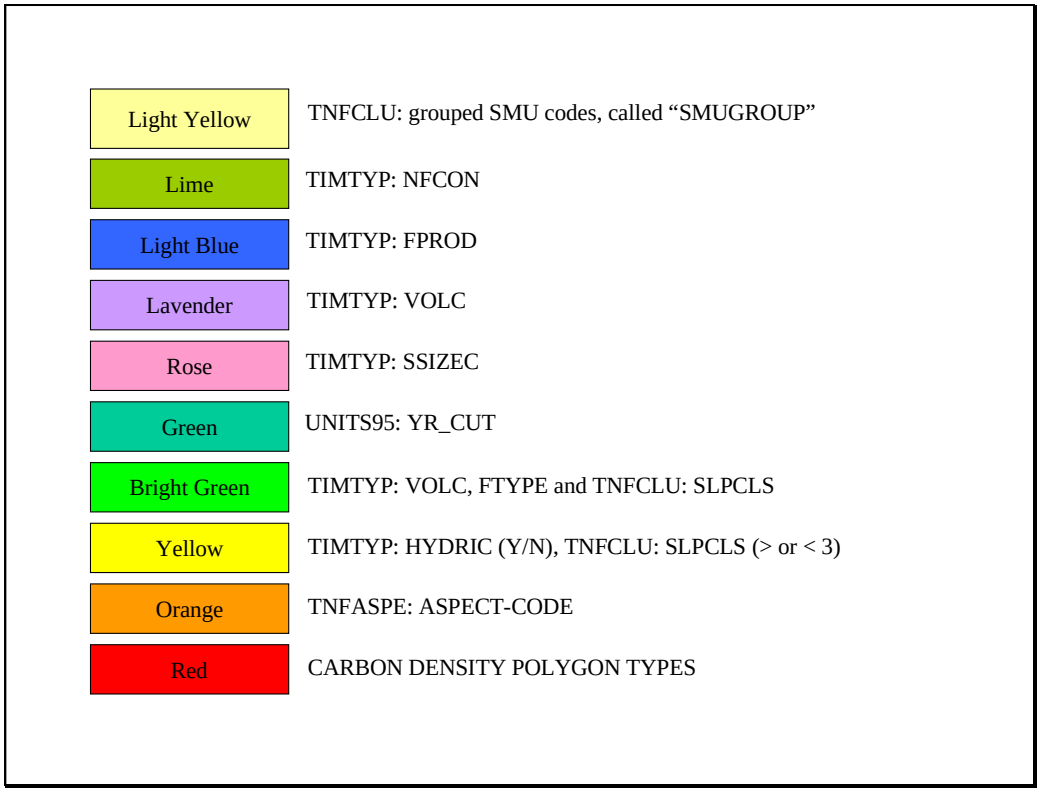

Figure F: index of GIS coverages (left of the colon) and attributes (right of colon) used in carbon stratification. Boxes are color-coded to correspond with the flow chart describing the stratification process in figure 4.

The existing GIS data described in figure F was synthesized as shown in figure 4 to stratify the Tongass by carbon density. All possible values for GIS coverage attributes indicated in figure E are listed below. Areas were dsitinguished by soil type first, then by whether forested or not, and then by whether productive or not. At this point there are three types of aboveground forest structures (nonforested, nonproductive forested, productive forested), times 11 soil types, to be further classified as indicated in figure 4.

Description of possible values of relevant GIS coverage attributes:

Ssizec: 1 Seedlings or Saplings; under 5" DBH
2 Poletimber; DBH 5" to 9"
3 Young-growth Sawtimber; 9"+ but LT 150 years
4 Old-growth Sawtimber; 9"+ and over 150 years
'' Nonforested lands

NFCON:	A	alder brush
	B	brush, other than alder
	C	census freshwater
	D	sand dunes
	F	river fill
	G	natural grassland
	H	alpine
	I	ice/ snowfield
	L	uplifted beach
	M	muskeg meadow
	N	noncensus freshwater
	O	other
	P	borrow pit
	R	rock
	S	slide zone
	T	willow
	U	urban
	W	mass wasting
	X	salt water
	‘’	NOT NONFORESTED
CT:	F	forested cover type
	N	nonforested cover type
	O	GT 40 acre polygon from Insertshore
CUT:	Y	harvested
	N	unharvested
FPROD:	2	productivity GT 20 CU FT/acre
	A	low productivity due to alder
	G	low productivity due to glacier
	H	low productivity due to high elevation
	L	low productivity due to low site index
	M	low productivity due to Muskeg
	R	low productivity due to rock cover
	S	low productivity in recurrent slide zone
	T	low productivity due to willow
FTYPE:	A	red alder
	B	birch
	C	cedar
	H	hemlock
	L	lodgepole pine
	M	black spruce
	P	black cottonwood
	Q	aspen
	S	spruce
	W	white spruce
	X	hemlock-spruce
	Z	cottonwood with Sitka spruce understory

VOLC: 3	0 to 8 MBF/acre	
4	8 to 20 MBF/acre	
5	20 to 30 MBF/acre	
6	30 to 50 MBF/acre	
7	greater than 50 MBF/acre	
‘’	0 to 8 MBF/acre	
YR_CUT:0	not harvested	
Year	date of harvest	
HYDRIC:Y	hydric conditions	
N	nonhydric conditions	
SLPCLS:1	slope less than 35%	
2	slope between 35% and 55%	
3	slope less than 55%	
ASPECT_C:	1	southern aspect
	-2	not southern aspect
	0	not southern aspect
	2	not southern aspect

SAS programs for map creation (CDone\sasprograms\mapcreation)

Unionedimp – imports data from the GIS coverage timclapu

Zunionedimp – imports data from the GIS coverage timclapu

Smucondense – groups Soil Management Unit (smu) codes into the soil types described by Alexander et al.

Smucondense2 – groups Soil Management Unit (smu) codes into the soil types described by Alexander et al.

Mapgrouping – creation of a new attribute delineating carbon density for each polygon area in the coverage timclapu, called fingroup, based on a flow chart similar to that shown in figure 4. This is the attribute on which timclapu was dissolved to create the coverage final. This coverage was flawed due to inadvertent classification of Fprod=’’ as nonproductive.

Leighty8fngrp2creation – creation of a new attribute delineating carbon density for each polygon area in the coverage timclapu, called fngrp2, based on the flow chart shown in figure 4. This is the attribute on which timclapu was dissolved to create the coverage leighty, from which leighty9 was created.

Mapgroupingnosoil – simplification of carbon density delineation by dropping polygon distinction by soil type. This was done to consolidate polygons into larger area for calculation of aboveground carbon density from FIA data.

Mapgroupsummary – summarizes the total area in each polygon type described by the attribute fingroup

Mapgroupexport – export of the newly created attribute fingroup for addition to the coverage timclapu

Some notes on details of attributes used in map creation deserve mention:

- The attribute “smugroup” was made from attributes “smu” and “for_smu” and represents to categorization of these attributes according to the soil types described by Alexander et al. For a complete listing of this categorization, see the file smucondensed4 on CDone.
- The attribute Fprod was separated into two categories: 2 and ‘’ (blank record), and everything else because blank records in Fprod were determined to indicate productive areas. Assumption of blank records indicating unproductive areas results in an unrealistic amount of area (>50%) classified as unproductive forested land.
- Blank records for the attribute Volc are defined as the same as a value of 3, but values of 1 and 2 are not defined, so they were assumed to also mean 0-8 MBF/acre and were lumped in with ‘’ and 3.
- Blank records do appear for the attribute Ftype when CT=F, Nfcon=’’, and Fprod=a letter. The blank record for Ftype is not defined. Fortunately, this is not a problem because the only distinction that matters is whether Ftype is S or X. Every other combination of attribute values is shunted away from high volume spruce and hemlock in the SAS program by whether the attribute fingroup has already been classified as high volume spruce and hemlock rather than by ftype codes.
- The value of Slpcls=0 was put in with Slpcls=1
- Values of Aspect_c=-9999 appear, but this is not a problem because 1 is south (the only distinction important for this stratification) and all other values are shunted to “not southern exposure” because the criteria set in the SAS program was aspect_c=1 or aspect_c ne 1.

3. Map Manipulation (CDone\sasprograms\mapmanipulation)
   areasum – summary of total area in each carbon density polygon type
   fingroupderivatives – various simplifications of complete carbon density delineation
   leighlud – identification of the land use designation for each carbon density polygon area, for flux scenarios 5 and 6.

4. Other SAS programs (CDone\sasprograms)
   Sliver ratio calculation – calculation of the ratio of perimeter to area for all polygons for elimination of slivers in the creation of Leighty9

Appendix G:

Selection of an allometric biomass equation for each species was often less than ideal. Therefor, the sensitivity to equation selection was tested (table 2). Equation selection for tamarack, red alder, and black cottonwood was simplified because only one equation for oven-dry biomass was found. Lack of species-specific volume equations often limited the choices to those biomass equations that did not include volume as a variable. For example, availability of volume equations only for douglas fir limited the choice of allometric equations for Pacific silver fir and for subalpine fir to those given by Standish (1983). Similarly, availability of volume equations only for Sitka spruce limited my choice of allometric equations for white spruce and black spruce to those given by Standish (1983). Equations given by Standish (1983) were used most frequently because this paper presented the most comprehensive group of tree species found in Southeast Alaska. This results in consistency of methods but may also lead to consistent under- or over-estimation of aboveground carbon. The model was run twice, with the high- and low-end extremes of biomass equations where more than one was available, to test the sensitivity of the model to biomass equation selection (table 2). This table also presents data on an analysis of the sensitivity of the model to the size restrictions of the biomass equations used. Mead (1998) was used to select biomass equations where more than one was available. For example, Mead suggested the equations given by Standish (1983) for Alaska yellow cedar and Sitka spruce. However, Mead's suggested equation was not used for several species because of inadequacies in the suggested equation. For example, Mead suggests Adamovich (1975) for lodgepole pine, but this equation yields estimates of green weight rather than oven-dry weight. The only other option was an equation for shore pine given by Standish (1983). The common names lodgepole pine and shore pine both refer to *Pinus contorta,* so this equation for shore pine was used when none for lodgepole pine was available. Two equations were available for each of these species: western red cedar (Standish (1983) or Shaw (1977) suggested by Mead), western hemlock (Standish (1983) or Shaw (1977) suggested by Mead), mountain hemlock (choices limited due to lack of volume equations, left with Standish (1983) or Krumlik (1974) suggested by Mead), and balsam poplar (Alemdag (1984) or Singh (1984)). Rather than simply follow Mead's suggestions for these species, they were grouped into low- and high-end groups based on three-dimensional plots of the biomass estimate returned for all possible combinations of diameter and height dimensions (Appendix H). The model was run with these low- and high-end groups to test its sensitivity to biomass equation selection. Results are presented in Table 2. The low-end model run was used for all subsequent calculations with the result of conservative estimates of the aboveground carbon pool and potential carbon fluxes. No equations for oven-dry biomass were available for paper birch or willow so equations for black cottonwood and quaking aspen were used respectively. These equations were chosen based on similarity between the two species in form, growth rate, and mature dimensions. The model was run once without these species and once using these equation substitutions to test the sensitivity to this assumption (table 2). No Pacific yew or quaking aspen were recorded in the FIA Grid Inventory.

Allometric biomass equations are shown in the Excel file "carbon equations6" and further justification for the selection of these equations is given in the file "justification for carbon equation selection".

Appendix H:

Three dimensional surface plots were created for all allometric biomass equations to look for irregularities outside the size range for which each equation had been verified and to establish which equation yielded the highest and lowest biomass estimates when more than one equation was available. Sensitivity of the total carbon estimation model to equation selection was tested with these "high-end" and "low-end" equations (table 1,2). No equation displayed erratic behavior outside verified size ranges, so the assumption was made that application of these equations to trees outside the range produced reasonable biomass estimates. Some of the surface plots are shown in the file "surface plots" on CD one.

Appendix I:

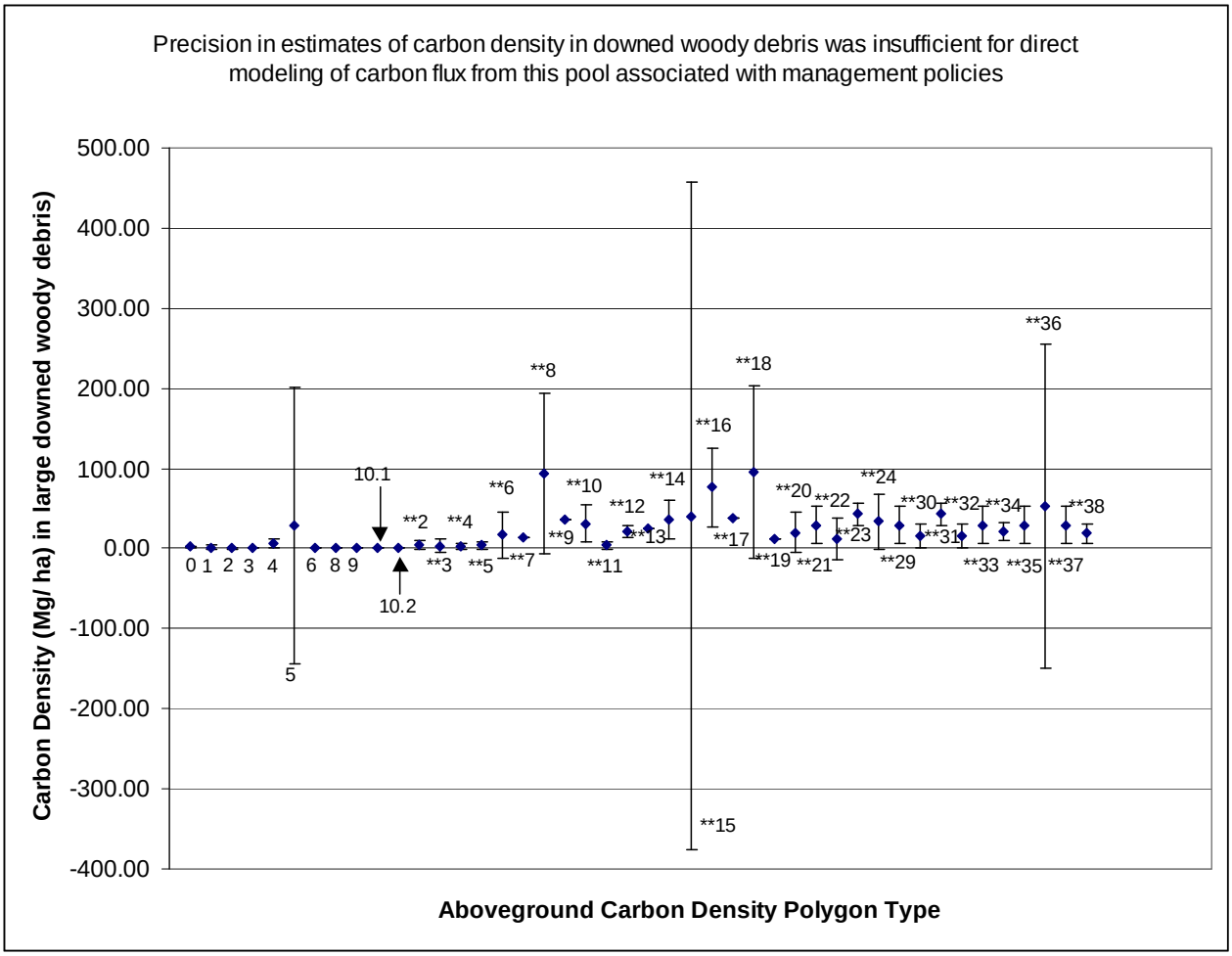
Precision in estimates of carbon density in downed woody debris was insufficient for direct modeling of carbon flux from this pool associated with management policies
Carbon Density (Mg/ ha) in large downed woody debris)
500.00
400.00
300.00
200.00
100.00
0.00
-100.00
-200.00
-300.00
-400.00
0 1 2 3 4 5 6 8 9 10.1 10.2 **2 **3 **4 **5 **6 **7 **8 **9 **10 **11 **12 **13 **14 **15 **16 **17 **18 **19 **20 **21 **22 **23 **24 **29 **30 **31 **32 **33 **34 **35 **36 **37 **38
Aboveground Carbon Density Polygon Type

Appendix J:

Assumptions and simplifications in calculation of the total carbon stock in the Tongass and the sensitivity analyses performed for some of these assumptions are explained below. Many assumptions involve calculation of total carbon in understory vegetation, which accounts for only 0.7% of the estimated total carbon in the Tongass. Explanation of these assumptions is provided for clarification of methods, but none of them significantly influenced the results of this research.

- Polygon types lacking representative FIA sample locations were assumed to contain the same aboveground carbon density as a similar polygon type.

Polygon type lacking data	Assumed C density of this polygon type:	Reasoning:
9	ZEROS	Don't include any Canadian carbon in this study
**11	**15	differs only in slope aspect
**21	**33	unknown sizeclass so is appropriate for a mid-range size class and is poly type for which have lots of data
**29	**33	unknown sizeclass so is appropriate for a mid-range size class and is poly type for which have lots of data
**30	**32	is only nonproductive poly type for which have data
**31	**23	conservative estimate for loggged forested muskeg - assume is more like 23 (seed/ sap) than 21 (poletimber)
**35	**33	Unknown sizeclass so is appropriate for a mid-range size class and is poly type for which have lots of data
**37	**33	Also unknown sizeclass – only difference is that is labeled productive which really does not influence what is there at the time of sampling

Table J: polygon types used as proxies for polygon types lacking representative FIA sample locations

However, this assumption impacted the estimate of total carbon in the Tongass very little due to the small area of these polygon types. Only 0.07% of the estimate of total carbon in the Tongass is contained in aboveground carbon in these polygon types. The level of certainty in these carbon density estimates was also assumed to be equal to that of the similar polygon type used as a proxy. The level of certainty in polygon types with insufficient FIA data to calculate a 95% confidence interval was calculated as a weighted average of the 95% confidence intervals of all other polygon types, weighted by total area (metadata worksheet in finalasym and finalpoly).

- Polygon types lacking GIS data on soil type were classified as “no soil data” and soil carbon density was calculated as a weighted average of the carbon densities in all the other soil categories described by Alexander et al, weighted by total area. With this assumption, 21.8% of the estimate of total carbon in the Tongass is contained in the soils of polygons lacking soil data. These areas are primarily large wilderness areas like Admiralty Island and Misty Fjords National Monument. The level of certainty in these carbon density estimates and in the estimates of carbon density in two soil categories lacking standard error information in Alexander et al (soil types 17 and 19)

was calculated as a weighted average of the 95% confidence intervals of all other soil types, weighted by total area.

- Allometric equations were used to calculate ovendry biomass. These were converted to estimates of carbon by assuming 50% of ovendry weight for woody fractions is carbon, 45% of ovendry weight for foliage and understory plants is carbon, and dead biomass is 70% of allometrically predicted biomass with 53% of that as carbon. (Hamburg et al 1997).

- For calculation of carbon in downed woody material, numbers for the specific gravity of Pacific yew could not be found. The wood is described as "hard, heavy, strong, durable, fine-grained, and resilient" (Elias, 1987). With this information, it was assumed that the specific gravity = 0.4, which is a conservative estimate because it is less than the average for softwoods found in Southeast Alaska.

- Also for calculation of carbon in downed woody material, the specific gravity of "unknown hardwood" was assumed to be the average of all hardwoods found in Southeast Alaska, which is 0.363. I was also assumed that the specific gravity of "unknown softwood" was equal to the average of all softwoods in Southeast Alaska, which is 0.401.

- Seedlings with diameter at breast height (dbh) less than 2.5cm were recorded as 0001 dbh in the FIA database. These seedlings were assumed to have an average dbh equal to 1 cm.

- For the downed wood transects, a "no tally" coding (999) in the FIA database means that there was no downed wood to be tallied on the transect.

- Some assumptions were made for classification of understory vegetation into the categories described by Yarie and Mead (1988):
    - Liverworts are phenotypically similar to mosses, assumed same equation
    - Aquatic species were lumped in with forbs
    - Horsetail is similar to grass, so the grass equation was used
    - Clubmoss is similar to liverwort and to moss; the moss equation was used
    - Ferns are similar to forbs, so the forb equation was used
    - Sedge is similar to grass, so the grass equation was used
    - Rush is similar to sedge, which is similar to grass, so the grass equation was used
    - Shrub trees are between a shrub and a tree, so the average of these equations was used
    - Basal vegetation was grouped with shrub trees
    - Mushrooms were grouped with forbs
    - Snags were grouped with shrub-tree. Snags account for only 1.6% of the observations

- The equations from Yarie and Mead (1988) only measure biomass in foliage and twigs less than 5mm in diameter because, "this is the approximate maximum sized twig that wildlife will browse." Consequently, these equations tend to underestimate carbon in shrub-tree and shrubs (which have stems etc larger than 5 mm diam.). However, these were the only equations available for understory vegetation. These equations are not appropriate for calculation of carbon in stumps recorded in the FIA HV data records, so a different approximation was developed.

- The method for calculating stump carbon developed is as follows:
  The total area of a plot is 100 m^2. Multiplying the data attribute cm11 by .01 yields the percentage of this area that is stump surface area, which can then be converted to the total surface area of stumps in the plot area in cm^2 by multiplying by 10,000. Stumps were assumed to have no bark and 80% of their original carbon content. The average of stump equations given by Singh (1984) was then used to calculate stump carbon (note, only used wood equations, omitting bark, to account for decomposition of stumps). Stump carbon was calculated as equal to $(-.49938+.73002*D+.00163*D^2+.0011*D^3)*.5*.7$, which yields kg of carbon per 100 m^2. This was multiplied by 100 to get kg C/ ha.

- Some overlap in data collection occurred in the FIA databases. For HV (understory) calculations downed wood was assigned a value of zero because it was assumed that downed wood had been accounted for in the downed wood data records. Similarly, it was assumed that residue was included in soil organic carbon and thus was excluded from HV calculations. HV calculations included mosses and other ground-level vegetation, but all the dead organic material in the forest floor mat was included in soil carbon calculations. Tree species in HV data are all acounted for in tree data with dbh coded as 0001 or 1 mm dbh, so trees recorded in the HV data records were left out of HV carbon calculations and adjusted for in tree carbon calculations.

- If moss-depth data was missing, it was assumed to be 2 cm (.2 dm) for HV calculations. This is a safe assumption because if there is no moss (ice, water, etc.) then there will be 0 percent cover and the 2 cm thickness will not matter. If there is some moss, the percent cover will reflect how dense it is and 2 cm is a reasonable estimate of thickness.

- 6,976 records in the HV database had species codes for which no definition was given in the FIA field manual. These errors were corrected by looking for a similar code. In many cases there was only one similar code, but for cases in which there was no clear match or no similar code at all, the average of the coefficients in all vegetation categories described by Yarie and Mead (1988) was used (6.66).

- A small number (102 out of 6267) of soil records returned negative values for carbon because the depth to a deeper layer was recorded as smaller than the depth to a shallower layer. In these cases I assumed that the field workers forgot to measure the depth from the bottom of the moss layer and measured thickness of the actual layer instead. With this method, 31 observations have more carbon (kg/ ha) than the

maximum possible with standard measuring procedures (50 cm of Oa sapric, with the highest carbon density of 360,000 kg/ ha). These locations are: DEN0016, DEN0016, PTA0142, PTB0157, PTB0157, PTB0367, PTB0367, BCA0044, KTK0211, BCA0211, JNU0265, PTB0052, PTB0310, SKY0167, STK0355, KTK0375, MTF0275, STK0123, STK0396, SKY0153, STK0277, CRG0118, STK0315, CRG0221, TAR0078, PTB0214, STK0048, CRG0221, KTK0321, CRG0196, STK0277. These locations were included in calculation of total soil carbon from FIA data, thus increasing the estimate, which further accentuates the fact that FIA data was insufficient for estimation of total soil carbon in the Tongass due to drastic underestimation from limited soil pit depth. Soil carbon was calculated from classification according to Alexander et al rather than with FIA data for the main body of this research.

- FIA sample points (4 at each sample location) that happened to lie on roads, in lakes, or other anomalies weren't distinguished as such because they were relatively few and, since sample location is random, they should give an accurate indication of the percent area of the polygon type that is anomalous. Thus, inclusion of data from these "anomalous" sample points should not bias the estimate of C/ ha for the polygon type. For example, 36 points fall on roads. This provides a good approximation of area of forested polygon types that is actually road and thus has essentially no carbon. However, inclusion of these anomalous sample points adds considerably to the 95% confidence interval for carbon density estimates, especially in polygon types with relatively few representative FIA sample locations. The only sample points that were eliminated from consideration were those that were inaccessible (LCT=0).

- Data with incomplete records were corrected as follows:
    - Point deleted if LCT=0 (inaccessible) – not measured
    - Point deleted if Mloc not equal to loc (means did not have a start and end date, indicating that it wasn't measured – applies to only one location).
    - All carbon pools that were .'s in SAS output were changed to 0 if LCT= 7 or 8 (barren land or barren water).
    - Tree carbon pools that were .'s in SAS output were changed to 0 if LCT=2 or 3 (shrub land or herbaceous).
    - HV and DWD records coded as .'s in SAS output were left in because HV and DWD measurements were only taken at the first two points of a Main Vegetation Type (MVT). Thus, only 2 of the 4 sample points should have HV and DWD records if the sample location is in a homogenous area. If left as .'s, the data then don't figure into the mean calculations when points are summarized by location.
    - Records with ALL pools coded as .'s in SAS output after the corrections stated above were then assumed to be all zeros.
    - Points with 'no trees' in polygon notes and .'s for tree carbon pools in SAS output were changed to zeros.
    - Records left .'s in the SAS output after all these corrections and 98 (disturbed or clearcut) in the MVT code were changed to zeros.

- 220 points were left with incomplete records after all the corrections outlined above were made. These records were left alone so carbon pools with numbers were figured into the C/ha estimate for the location and carbon pools with .'s were left out of these calculations (e.g. pool was added and then divided by 3 points instead of 4).
- Finally, FIA sample locations with total carbon coded as .'s in SAS output after aggregation by location were deleted because this indicated that they have had no records with data for at least on carbon pool. This was the case for 37 locations. Most of these lacked soil data and were in the JNU area.

- Approximately 1% (645/ 63833) for tree records were "non-tally" site, age, or site and age trees. These were deleted because the description as a non-tally tree means that it was not in the sample plot but was measured for the purpose of a site or age tree.

- Soils in Alaska are complex and over 800 Soil Management Unit (SMU) codes were collapsed into the 10 general soil categories described in Alexander et al for calculation of soil carbon (smucondensed4). In doing so, judgments about where to put complexes and associations of different soils were often necessary. These were made by trying to find the middle ground of total C/ ha of all the soil type names in the complex or association. Generally, the category contained at least one of the soil types named in the complex, thereby preventing the introduction of characteristics of some totally unrelated soil type that happened to have the middle-ground carbon density. When in doubt, judgments were made on the conservative side by putting the complex in a category with a lower rather than higher carbon density. Furthermore, soils described as "moderately deep" were mostly put into the appropriate "shallow" category rather than "deep" category (no "moderately deep" categories were described by Alexander et al but many SMU codes describe moderately deep soil complexes). SMU codes define "shallow" as less than 50cm, "deep" as more than 100 cm, and "moderately deep" as the middle ground (50-100 cm) (U.S. Department of Agriculture, Soil Survey Division Staff, 1993).

- One sample location was eliminated for calculation of carbon in downed woody debris due to probable error in the downed woody debris data (DWD outlier analysis). Approximate calculations suggest the improbability of the accuracy of this outlier. Data for this location indicates a carbon density of 6,922,160 kg carbon per hectare in large downed woody debris. This equates to 13,844,320 kg/ha or 1,384,432 g/m^2 of woody material. Assuming an average density of 0.5 g/cm^3, the conservative estimate of wood volume covering this area is 276.8 cm^3/cm^2, which equates to a layer of solid wood 2.76 meters deep. The improbability of this figure combined with the data point's position as an outlier justified its elimination from the data set. This action is further justified because it is on the side of a conservative estimate of total carbon and carbon flux. Examination of the data for this location revealed one tree 9 meters in diameter that was sampled repeatedly due to the radial transect method (USDA Forest Service, FIA field methods, 1995). The potential for duplicate

sampling is statistically valid when aggregated (Waddell, draft) but the 9-meter diameter suggests data entry error.

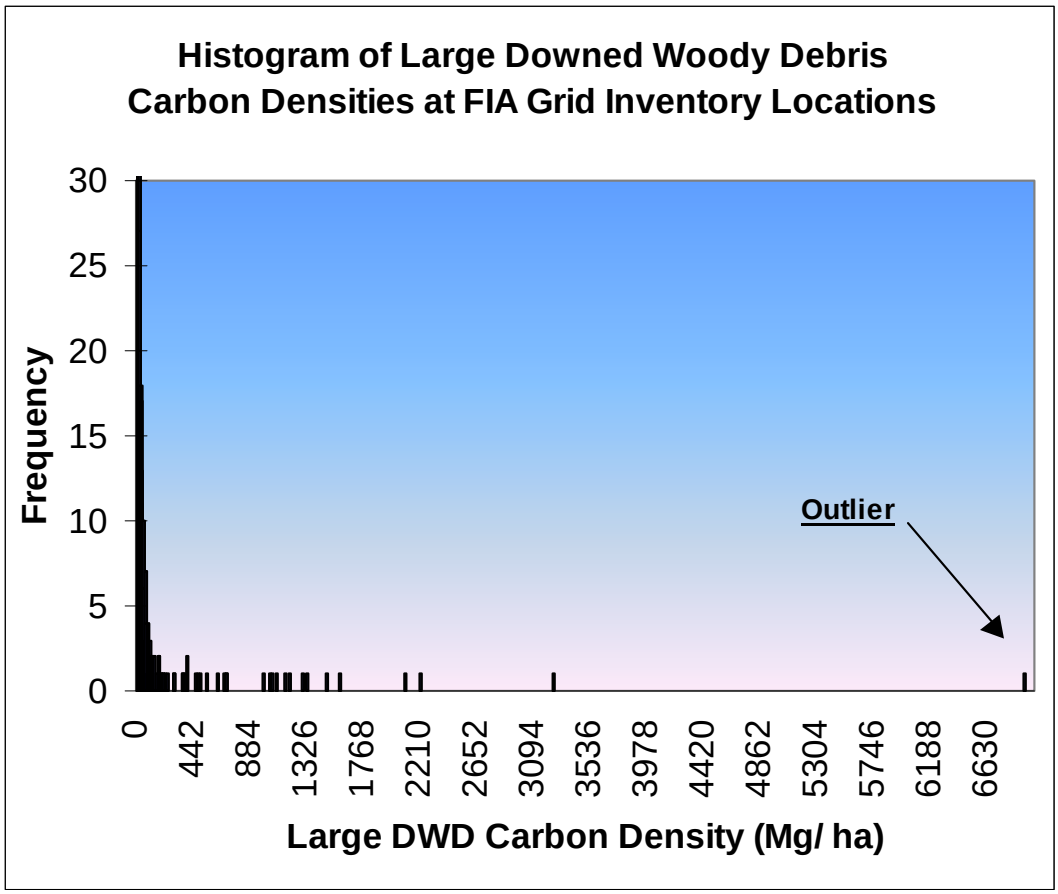

Figure J: histogram of carbon density in large downed woody debris, showing the position of one FIA sample location as a distinct outlier.

Appendix K:

The classification of SMU codes into the categories described by Alexander et al is shown in the file "SMUcondensed4" on CD one.

Appendix L: sorted SMU codes on CD one.

Appendix M:

The spreadsheet models for estimation of the total carbon in the Tongass and projection of carbon flux are listed below. The file "FinalFIAsoil" uses FIA data to calculate total soil carbon. Comparing this number to the total soil carbon in any of the other files, calculated with the soil categories described by Alexander et al, demonstrates the significant underestimation resulting from calculation using FIA data due to insufficient depth of FIA soil pits. The remaining four files are all formatted the same, with a page of metadata, a page of figures, several pages for carbon flux calculations (labeled scenario_), several pages of carbon density data by FIA location (labeled data_), and several pages of calculations for estimation of the total amount of carbon in the Tongass (labeled carb calc_). The file "FINALpoly" assumes the rate of carbon accretion with secondary growth given by the polynomial accretion curve while "FINALasym" assumes the rate given by the asymptotic accretion curve.

FinalFIAsoil (CD one)
FINALpoly (CD one)
FINALasym (CD one)

Appendix N: The GIS coverage Leighty9 is on CD 3a

Appendix O: The GIS coverage TIMCLAPU was too large to compress onto CD. Contact the author directly for this data.

Appendix P:

The coverage Leighty was the original coverage created by dissolving the coverage timclapu on the attribute fingroup. The coverage Leighty1 was created from Leighty by condensing all polygons with area < 0.01 acre into the largest neighboring polygon using the Eliminate command in ArcInfo. The coverage Leighty3 was created from Leighty by condensing all polygons with area < 5 acres into the neighboring polygon with largest perimeter. The coverage Leighty 4 was created from Leighty by condensing all polygons with area < 5 acres into the largest neighboring polygon. The coverage Leighty5 was created from Leighty1 by condensing all polygons with area < 1 acre and $\frac{perimeter}{area}$ ratio > 1 into the largest neighboring polygon. The coverage Leighty6 was created from Leighty1 by condensing all polygons with area < 0.1 acres into the largest neighboring polygon. Finally, the coverage Leighty7 was created from Leighty6 by condensing all polygons with area < 1 acre into the largest neighboring polygon. Leighty5 was created with the best method for identifying and removing slivers since only polygons with small area and large perimeter were condensed. This method also requires that the polygon be more elongated or sliver-like as the area increases. For example, a simple rectangular polygon with an area of 1 acre must have a length almost 10,000-times its width to be identified as a sliver while a rectangular polygon with an area of 0.01 acre must of a length slightly less than 100-times its width to be identified as a sliver. Since Leighty5 was made from Leighty1, the end result was that any polygon with area less than 0.01 acres was identified as a sliver and any polygon with area between 0.01 and 1 acres was subject to the perimeter-to-area ratio discussed above. Comparison of Leighty5 with Leighty1 and Leighty7 shows that the method employed for creation of Leighty5 did remove some slivers with area between 0.01 and 1 acres but was not such a crude instrument as in Leighty7. Leighty5 was tweaked a little, renamed Leighty9, and used for all subsequent calculations. The minimum resolution of the spatial soil data used to create timclapu was 4 acres and the minimum resolution of other coverages was not less than 1 acre. Although one would expect smaller polygons to result of intersecting these polygons, the coverages timclapu and Leighty contain greater resolution than any of the coverages used to create them. Thus, it is reasonable to condense slivers into large neighboring polygons and 1 acre was chosen as a reasonable maximum size for these slivers.

	# polygons	# arcs
Leighty	882013	2078538
Leighty1	762055	1956865
Leighty3	287043	1437592
Leighty4	287043	1398723
Leighty5	760577	1955065
Leighty6	666282	1858169
Leighty7	465774	1647197

The SAS program for calculation of perimeter-to-area ratios for polygon sliver elimination is stored as "sliver ratio calculation" on CD one\sasprograms.

Appendix Q: The AML programs used to locate FIA locations (both theoretical locations in the coverage tlmpoint and corrected locations in the coverage gpsfia) in polygon types are presented below. These programs created a new attribute in each FIA location coverage called fngrp2, which was assigned the value of the polygon type within which the sample location fell.

```
&echo &on
&do count = 0 &to 2138 &by 1

res leighty9 poly fngrp2 = %count%
res tlmpoint point OVERLAP leighty9 poly
calc tlmpoint point fngrp2 = %count%

clearselect
&end
&return
```

```
&echo &on
&do count = 0 &to 2138 &by 1

res leighty9 poly fngrp2 = %count%
res gpsfia point OVERLAP leighty9 poly
calc gpsfia point fngrp2 = %count%

clearselect
&end
&return
```

Appendix R_1: Please refer to the worksheets labeled "data" in the spreadsheet models FINALpoly and FINALasym on CD one.

Appendix R_2: Please refer to the worksheets labeled "metadata", "data" and "carb calc" in the spreadsheet models FINALpoly and FINALasym on CD one.

Appendix R_3: Please refer to the worksheets labeled "metadata" and "scenario" in the spreadsheet models FINALpoly and FINALasym on CD one\final interlinked spreadsheets. Scenarios marked "a" and "b" refer to analysis of the sensitivity of carbon flux projections to the assumption of re-growth progression. The endings "poly" and "asym" refer to analysis of the sensitivity of estimates to accretion curve selection.

Scenario	Description
1	Cessation of all harvest: secondary forest re-grows, all else assumed to be in equilibrium
2	Estimation of carbon flux since 1900
3	All forested lands managed on a 100-year rotation
4	All forested lands managed on a 200-year rotation
5	Lands currently available for harvest managed on a 100-year rotation
6	Lands currently available for harvest managed on a 200-year rotation

Carbon flux was modeled for six potential management scenarios. Lands currently available for harvest were mapped using the GIS coverage LUD99 (app. T) and 1997 Tongass National Forest Land and Resource Management Plan (CD 6).

Appendix S:

The original data for permanent sample locations, measured repeatedly over time, is saved in the file FARRDATA2 on CD two\cooperative stand density study.

Appendix T: The GIS coverage of land-use designations (LUD99) is saved on CD5. Descriptions of each designation are contained on CD6, which is a copy of the 1997 Tongass Land Management Plan (TLMP). Although I didn't directly consider the effect of former president Bill Clinton's roadless designations (which came after the land-use designation coverage used), the effect of these designations may have been to make some LUD99 areas designated as no harvest truly off-limits to harvest permanently. Consequently, these designations were modeled indirectly because LUD99 designation of no harvest were assumed to mean no harvest permanently. The excel spreadsheet LUD areas containes the area of each polygon type in each of the land use designations described in the LUD99 coverage. These areas were calculated using SAS program Leighlud.

Appendix U:

The harvest history of the Tongass and calculations of the total carbon flux and average annual carbon flux for the periods 1900-1954 and 1955-1995 are saved in the file "past timber harvest" on CD one.

Appendix V:

Flux projections are plotted the files saved on CD one\excel models 5-5-01\final versions and CD one\excel models 5-5-01\final versions1. The endings "poly" and "asym" refer to which carbon accretion curve (polynomial or asymptotic) was used in each model (fig 6a, b). The ending "B" indicates projections assuming carbon density in standing aboveground biomass equal to that in polygon type **23 and the ending "C" indicates projections assuming carbon density in standing aboveground biomass equal to zero.